LUND UNIVERSITY

Multiple scattering by a collection of randomly located obstacles Part III: Theory - slab geometry

Kristensson, Gerhard; Wellander, Niklas

2017

[Link to publication](#)

Total number of authors:
2

LUND UNIVERSITY

PO Box 117
221 00 Lund
+46 46-222 00 00

Multiple scattering by a collection of randomly located obstacles
Part III: Theory — slab geometry

Gerhard Kristensson and Niklas Wellander

Gerhard Kristensson
Gerhard.Kristensson@eit.lth.se

Department of Electrical and Information Technology
Electromagnetic Theory
Lund University
P.O. Box 118
SE-221 00 Lund
Sweden

Niklas Wellander
Niklas.Wellander@foi.se

Swedish Defence Research Agency, FOI
P.O. Box 1165
SE-581 11 Linköping
Sweden

Abstract

In this paper, scattering of electromagnetic waves by discrete, randomly distributed objects inside a (finite thickness or semi-infinite) slab is addressed. In general, the non-intersecting scattering objects can be of arbitrary form, material and shape with a number density of n_0 (number of scatterers per volume). The main aim of this paper is to calculate the coherent reflection and transmission characteristics for this configuration. Applications of the results are found at a wide range of frequencies (radar up to optics), such as attenuation of electromagnetic propagation in rain, fog, and clouds *etc*. The integral representation of the solution of the deterministic problem constitutes the underlying framework of the stochastic problem. Conditional averaging and the employment of the Quasi Crystalline Approximation lead to a system of integral equations in the unknown expansion coefficients. With a uniform distribution of scatterers the analysis simplifies to a system of integral equations in the depth variable. Explicit solutions for tenuous media and low frequency approximations can be obtained for spherical obstacles.

1 Introduction

Multiple scattering of electromagnetic waves by a discrete collection of scatterers is a well-studied subject, and many excellent papers are found in the journal literature, *e.g.*, [3, 5, 12, 23, 28, 29, 31, 34, 48, 51, 52, 56–60, 62, 64, 66] and in textbooks, *e.g.*, [15, 16, 30, 37, 53–55]. In some of these treatments, the Null-field approach (Waterman's method) has been employed to solve complex deterministic electromagnetic scattering problem, which serves as a starting point for the stochastic analysis of the problem. The Null-field approach is well-documented [63, 65], and a comprehensive database of the method has been collected [38–45, 67]. A simple introduction to the method is found in Ref. 25.

The geometry analyzed in this paper generalizes the scattering geometry of earlier analyses further, so that different background materials are now possible to analyze. The background material is practical for a controlled experimental verification of the result. The deterministic analysis of the scattering problem in this paper is an extension of the problems treated in [18–20, 22, 26, 27]. Moreover, the present analysis generalizes the established results in two previous papers [14, 23] to a geometry with a more general background material. The transmitted and reflected intensities are conveniently represented as a sum of two terms — the coherent and the incoherent contributions. In this paper we focus on the analysis of the coherent term.

The paper is organized as follows. In Section 2, the geometry of the multiple electromagnetic scattering problem and a representation of the incident field are given, and in Section 3 the main tool to solve the problem, the integral representation, is introduced. The integral representations are exploited in the various homogeneous regions of the problem in Section 4, and the expansions of the surface fields are introduced in Section 5. The final goal of the paper is to calculate the transmitted and reflected fields of the problem. This is done in Section 6. The stochastic description of the many-body problem in this paper is made in Section 7, and two natural and
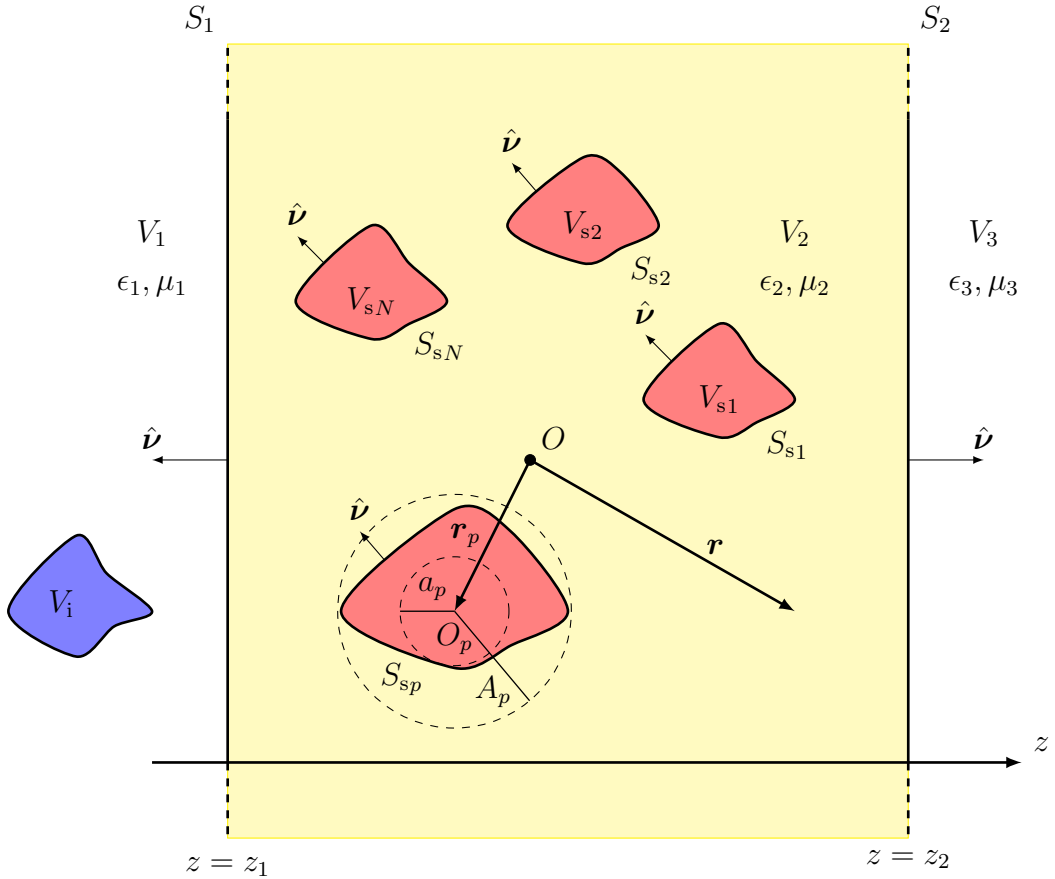
Figure 1: The geometry of a collection of the N scatterers and the region of prescribed sources V_i. The positions of the local origins are $\boldsymbol{r}_p$, $p = 1, \ldots, N$, and the radii of the maximum inscribed and the minimum circumscribed spheres of each local scatterer are a_p and A_p, respectively. The figure also shows the orientation of the unit normals of the surfaces, the global origin O, and the local origins O_p.

important approximations — the tenuous media and low-frequency approximations — are developed in Section 9. The paper ends with a short conclusion in Section 10 and several useful appendices. For convenience, a selection of the most important symbols is outlined in Appendix F.

2   Prerequisites

This section contains a description of the geometry of the problem and a description of the incident field with its sources in V_i.

2.1 The geometry

We study a collection of N different scatterers, where each scatterer is centered at the location $\boldsymbol{r}_p$, which defines the position of the local origin O_p, $p = 1, 2, \ldots, N$, relative the global origin O, see Figure 1. The volume of the individual scatterer is denoted $V_{\mathrm{s}p}$, bounded by the surface $S_{\mathrm{s}p}$, $p = 1, 2, \ldots, N$. The radii of the maximum inscribed and minimum circumscribed spheres, both centered at the local origin, of each scatterer are denoted a_p and A_p, $p = 1, 2, \ldots, N$, respectively. We assume that no minimum circumscribed spheres of the scatterers intersect. Each scatterer has its own material properties, which do not have to be the same for all scatterers.

All scatterers are located in a homogeneous, isotropic slab, volume V_2 — bounded by the planes $z = z_1$ and $z = z_2$ — with relative permittivity ϵ_2 and relative permeability μ_2, which can be lossless or lossy. No minimum circumscribed sphere of the scatterers is assumed to intersect with the planes $z = z_1$ and $z = z_2$. Notice that the volume V_2 is confined by the two planes, and excludes the finite scatterers $V_{\mathrm{s}p}$, $p = 1, 2, \ldots, N$, i.e., $V_2 = \{\boldsymbol{r} \in \mathbb{R}^3 : z_1 < z < z_2, \boldsymbol{r} \notin \overline{V_{\mathrm{s}p}}, p = 1, 2, \ldots, N\}$.

The half spaces to the left and to the right of the slab are denoted V_1 and V_3, respectively, and they are characterized by the lossless, homogeneous, isotropic (relative) material parameters ϵ_i and μ_i, $i = 1, 3$.

The prescribed sources of the configuration are located in the region V_{i}, which is located in V_1. These sources generate an electric field $\boldsymbol{E}_{\mathrm{i}}(\boldsymbol{r})$ and a magnetic field $\boldsymbol{H}_{\mathrm{i}}(\boldsymbol{r})$ everywhere outside V_{i}. Generalizations to other locations of the sources, such as in V_2, are possible, but not pursued in this paper.

With no loss of generality, we start with a collection of perfectly conducting obstacles in V_2, and then generalize to more complex scatterers below. The reason for this assumption is to make the derivation of the results more simple. The final result holds for a collection of scatterers with arbitrary materials and geometry, as long as the transition matrices of the scatterers are known.

In each domain, V_i, $i = 1, 2, 3$, the Maxwell equations are satisfied (the time conventions $\mathrm{e}^{-\mathrm{i}\omega t}$ is used throughout this paper, where ω is the angular frequency of the problem)

$$\begin{cases} \nabla \times \boldsymbol{E}(\boldsymbol{r}) = \mathrm{i}\omega\mu_0\mu_i\boldsymbol{H}(\boldsymbol{r}) = \mathrm{i}k_i\eta_0\eta_i\boldsymbol{H}(\boldsymbol{r}) \\ \nabla \times \boldsymbol{H}(\boldsymbol{r}) = -\mathrm{i}\omega\epsilon_0\epsilon_i\boldsymbol{E}(\boldsymbol{r}) = -\dfrac{\mathrm{i}k_i}{\eta_0\eta_i}\boldsymbol{E}(\boldsymbol{r}) \end{cases} \quad \boldsymbol{r} \in V_i, \quad i = 1, 2, 3$$

where the wave number $k_i = \omega(\epsilon_0\mu_0\epsilon_i\mu_i)^{1/2}$, and the wave impedances are given by $\eta_0 = (\mu_0/\epsilon_0)^{1/2}$ and $\eta_i = (\mu_i/\epsilon_i)^{1/2}$, $i = 1, 2, 3$, and ϵ_0 and μ_0 denote the permittivity and the permeability of vacuum, respectively.

Each scatterer is characterized by the boundary condition $\hat{\boldsymbol{\nu}} \times \boldsymbol{E} = \boldsymbol{0}$ on all $S_{\mathrm{s}p}$, $p = 1, 2, \ldots, N$. The boundary condition on the interfaces $z = z_1$ and $z = z_2$ are

$$\begin{cases} \hat{\boldsymbol{\nu}} \times \boldsymbol{E}_-(\boldsymbol{r}_{\mathrm{c}} + z_i\hat{\boldsymbol{z}}) = \hat{\boldsymbol{\nu}} \times \boldsymbol{E}_+(\boldsymbol{r}_{\mathrm{c}} + z_i\hat{\boldsymbol{z}}) \\ \hat{\boldsymbol{\nu}} \times \boldsymbol{H}_-(\boldsymbol{r}_{\mathrm{c}} + z_i\hat{\boldsymbol{z}}) = \hat{\boldsymbol{\nu}} \times \boldsymbol{H}_+(\boldsymbol{r}_{\mathrm{c}} + z_i\hat{\boldsymbol{z}}) \end{cases} \quad i = 1, 2$$

where the subscript $\pm$ denotes the limit values of the fields on the surface w.r.t. to the direction of the unit normal vector, and $\boldsymbol{r}_{\mathrm{c}} = x\hat{\boldsymbol{x}} + y\hat{\boldsymbol{y}}$.

3 Integral representation

The deterministic scattering problem, which is the first problem we address, is solved by the systematic employment of two main tools — the integral representation of the solution in a homogeneous domain and the decomposition of the Green dyadic for the electric field in free space [25].

Our starting point is the three integral representations of the electric field in the domains V_i, $i = 1, 2, 3$ [25, 50].

3.1 Integral representation in V_1

The appropriate integral representation in V_1 is ($V_1 = \{\boldsymbol{r} : z < z_1\}$)

$$
\begin{aligned}
&-\frac{1}{\mathrm{i}k_1}\nabla \times \left\{\nabla \times \iint_{S_1} \mathbf{G}_{\mathrm{e}}(k_1, |\boldsymbol{r} - \boldsymbol{r}'|) \cdot (\hat{\boldsymbol{\nu}} \times \eta_0\eta_1 \boldsymbol{H}(\boldsymbol{r}'))_+ \, \mathrm{d}S'\right\} \\
&+ \nabla \times \iint_{S_1} \mathbf{G}_{\mathrm{e}}(k_1, |\boldsymbol{r} - \boldsymbol{r}'|) \cdot (\hat{\boldsymbol{\nu}} \times \boldsymbol{E}(\boldsymbol{r}'))_+ \, \mathrm{d}S' = \begin{cases} \boldsymbol{E}_{\mathrm{r}}(\boldsymbol{r}), & \boldsymbol{r} \text{ inside } V_1 \\ -\boldsymbol{E}_{\mathrm{i}}(\boldsymbol{r}), & \boldsymbol{r} \text{ outside } V_1 \end{cases}
\end{aligned}
\tag{3.1}
$$

where the boundary values are taken as limits from the positive side of the surface S_1 w.r.t. the unit normal vector. The total fields in the left-hand side of the integral representation is the sum of the incident and reflected fields, *i.e.*, $\boldsymbol{E} = \boldsymbol{E}_{\mathrm{i}} + \boldsymbol{E}_{\mathrm{r}}$. To close the surface, we have added a half sphere in the left half space of V_1. This surface integral, due to radiation conditions, gives zero contribution. The Green dyadic for the electric field in free space $\mathbf{G}_{\mathrm{e}}(k, |\boldsymbol{r} - \boldsymbol{r}'|)$ is

$$
\mathbf{G}_{\mathrm{e}}(k, |\boldsymbol{r} - \boldsymbol{r}'|) = \left(\mathbf{I}_3 + \frac{1}{k^2}\nabla\nabla\right) g(k, |\boldsymbol{r} - \boldsymbol{r}'|)
$$

where the Green function $g(k, |\boldsymbol{r} - \boldsymbol{r}'|)$ in free space is

$$
g(k, |\boldsymbol{r} - \boldsymbol{r}'|) = \frac{\mathrm{e}^{\mathrm{i}k|\boldsymbol{r} - \boldsymbol{r}'|}}{4\pi|\boldsymbol{r} - \boldsymbol{r}'|}
$$

The top row in (3.1) holds for all points to the left of the dielectric slab. This field, the reflected field $\boldsymbol{E}_{\mathrm{r}}(\boldsymbol{r})$, is due to the slab and the inclusions in it. It satisfies appropriate radiation conditions at infinity.

3.2 Integral representation in V_2

The domain V_2 is bounded by the planes $z = z_1$ and $z = z_2$ and the domain excludes all scatterers V_{sp}, $p = 1, 2, \ldots, N$. The pertinent integral representation is

$$
-\frac{1}{ik_2} \nabla \times \left\{ \nabla \times \sum_{p=1}^{N} \iint_{S_{sp}} \mathbf{G}_e(k_2, |\boldsymbol{r} - \boldsymbol{r}'|) \cdot (\hat{\boldsymbol{\nu}} \times \eta_0 \eta_2 \boldsymbol{H}(\boldsymbol{r}'))_+ \, \mathrm{d}S' \right\}
$$

$$
+\frac{1}{ik_2} \nabla \times \left\{ \nabla \times \sum_{i=1}^{2} \iint_{S_i} \mathbf{G}_e(k_2, |\boldsymbol{r} - \boldsymbol{r}'|) \cdot (\hat{\boldsymbol{\nu}} \times \eta_0 \eta_2 \boldsymbol{H}(\boldsymbol{r}'))_- \, \mathrm{d}S' \right\} \qquad (3.2)
$$

$$
-\nabla \times \sum_{i=1}^{2} \iint_{S_i} \mathbf{G}_e(k_2, |\boldsymbol{r} - \boldsymbol{r}'|) \cdot (\hat{\boldsymbol{\nu}} \times \boldsymbol{E}(\boldsymbol{r}'))_- \, \mathrm{d}S' = \begin{cases} \boldsymbol{E}(\boldsymbol{r}), & \boldsymbol{r} \text{ inside } V_2 \\ \boldsymbol{0}, & \boldsymbol{r} \text{ outside } V_2 \end{cases}
$$

where the boundary condition $\hat{\boldsymbol{\nu}} \times \boldsymbol{E} = \boldsymbol{0}$ on each S_{sp}, $p = 1, 2, \ldots, N$, has been used. The boundary values on the planar surfaces are taken as limits from negative side of the surfaces w.r.t. to their unit normal vectors. In particular, the lower row in (3.2) holds for all points inside a particular scatterer bounded by S_{sp}.

3.3 Integral representation in V_3

The final integral representation of the domain $V_3 = \{\boldsymbol{r} : z > z_2\}$ is

$$
-\frac{1}{ik_3} \nabla \times \left\{ \nabla \times \iint_{S_2} \mathbf{G}_e(k_3, |\boldsymbol{r} - \boldsymbol{r}'|) \cdot (\hat{\boldsymbol{\nu}} \times \eta_0 \eta_3 \boldsymbol{H}(\boldsymbol{r}'))_+ \, \mathrm{d}S' \right\}
$$

$$
+\nabla \times \iint_{S_2} \mathbf{G}_e(k_3, |\boldsymbol{r} - \boldsymbol{r}'|) \cdot (\hat{\boldsymbol{\nu}} \times \boldsymbol{E}(\boldsymbol{r}'))_+ \, \mathrm{d}S' = \begin{cases} \boldsymbol{E}_t(\boldsymbol{r}), & \boldsymbol{r} \text{ inside } V_3 \\ \boldsymbol{0}, & \boldsymbol{r} \text{ outside } V_3 \end{cases} \qquad (3.3)
$$

where the boundary values are taken as limits from the right-hand side of the surface S_2.

The top row in (3.3) holds for all points to the right of the dielectric slab. This field, the transmitted field $\boldsymbol{E}_t(\boldsymbol{r})$, is due to the slab and the inclusions in it. It satisfies appropriate radiation conditions at infinity.

A simple count of the number of unknown surface fields gives four (two surface fields on S_1 and two surface fields on S_2) plus N unknown surface fields on the N scatterers in the slab. In this count, the boundary conditions on each interface have been used. The number of extinction parts (the number of different, distinct locations of the position vector $\boldsymbol{r}$ in the lower rows) in the integral representations is: one in (3.1), two plus N in (3.2), and one in (3.2). Consequently, the number of unknowns and equations matches. The top rows in the integral representations then give the fields in each specific volume. In particular, the reflected and transmitted fields, which are the main fields of interest in this paper.

4 Exploiting the integral representations

The position vector, $\boldsymbol{r}$, can take several principal positions. We exploit each of these cases to connect the fields in the three different regions to each other.

4.1 The volume V_1

Let the position vector $\boldsymbol{r}$ be located to the right of the surface $z = z_1$, i.e., $z > z_1$. The incident electric field has an expansion in terms of the planar vector waves $\boldsymbol{\varphi}_j^+(\boldsymbol{k}_t; k_1, \boldsymbol{r})$, see Appendix C for the definition, in the form

$$\boldsymbol{E}_i(\boldsymbol{r}) = \sum_{j=1,2} \iint_{\mathbb{R}^2} a_j(\boldsymbol{k}_t) \boldsymbol{\varphi}_j^+(\boldsymbol{k}_t; k_1, \boldsymbol{r}) \, dk_x \, dk_y, \quad z > z_1 \qquad (4.1)$$

where the expansion coefficients $a_j(\boldsymbol{k}_t)$, for a given incident field, are obtained by the use of (C.6) in Appendix C.2. These coefficients are the excitation of the scattering problem in this paper. If the incident is a plane wave, the form of the expansion functions is given in Section 7.2.2. The extinction part in integral representation (3.1) and the decomposition of the Green dyadic (D.2) imply that the expansion coefficients $a_j(\boldsymbol{k}_t)$ have the form

$$\begin{aligned}
a_j(\boldsymbol{k}_t) = &-\frac{2ik_1}{k_{1z}} \iint_{S_1} \boldsymbol{\varphi}_j^{-\dagger}(\boldsymbol{k}_t; k_1, \boldsymbol{r}') \cdot (\hat{\boldsymbol{\nu}} \times i\eta_0\eta_1 \boldsymbol{H}(\boldsymbol{r}'))_+ \, dS' \\
&-\frac{2ik_1}{k_{1z}} \iint_{S_1} \boldsymbol{\varphi}_{\bar{j}}^{-\dagger}(\boldsymbol{k}_t; k_1, \boldsymbol{r}') \cdot (\hat{\boldsymbol{\nu}} \times \boldsymbol{E}(\boldsymbol{r}'))_+ \, dS', \quad \boldsymbol{k}_t \in \mathbb{R}^2, \ j = 1, 2
\end{aligned} \qquad (4.2)$$

where $k_{1z} = (k_1^2 - k_t^2)^{1/2}$ and where $\bar{j}$ is the dual index of j, i.e., $\bar{1} = 2$ and $\bar{2} = 1$. Equation (4.1) is a representation of the incident field in the region $z > z_1$, given that the surface fields are known on surface S_1. The null field equation (4.2) is an equation for the unknown surface fields. The expansion functions of the incident field on the left-hand side drive the equation and the whole system, since the null-field equations are coupled via the boundary conditions on the surface S_1.

Similarly, expanding the reflected wave in planar vector waves for a position vector to the left of $z = z_1$, $z < z_1$, we have (using (3.1) and (D.2) and interchanging the order of integration)

$$\boldsymbol{E}_r(\boldsymbol{r}) = \sum_{j=1,2} \iint_{\mathbb{R}^2} r_j(\boldsymbol{k}_t) \boldsymbol{\varphi}_j^-(\boldsymbol{k}_t; k_1, \boldsymbol{r}) \, dk_x \, dk_y, \quad z < z_1 \qquad (4.3)$$

where the reflection coefficients are given by

$$\begin{aligned}
r_j(\boldsymbol{k}_t) = &\frac{2ik_1}{k_{1z}} \iint_{S_1} \boldsymbol{\varphi}_j^{+\dagger}(\boldsymbol{k}_t; k_1, \boldsymbol{r}') \cdot (\hat{\boldsymbol{\nu}} \times i\eta_0\eta_1 \boldsymbol{H}(\boldsymbol{r}'))_+ \, dS' \\
&+\frac{2ik_1}{k_{1z}} \iint_{S_1} \boldsymbol{\varphi}_{\bar{j}}^{+\dagger}(\boldsymbol{k}_t; k_1, \boldsymbol{r}') \cdot (\hat{\boldsymbol{\nu}} \times \boldsymbol{E}(\boldsymbol{r}'))_+ \, dS', \quad \boldsymbol{k}_t \in \mathbb{R}^2, \ j = 1, 2
\end{aligned} \qquad (4.4)$$

Hence, we need to know the two unknown tangential fields on S_1, $(\hat{\boldsymbol{\nu}} \times \boldsymbol{E})_+$ and $(\hat{\boldsymbol{\nu}} \times \mathrm{i}\eta_0\eta_1\boldsymbol{H})_+$, to compute the reflection expansion function $r_j(\boldsymbol{k}_{\mathrm{t}})$ for the inhomogeneous slab by evaluating (4.4). This is done by a system of equations, given by (4.2) and the extinction parts of equations (3.2) and (3.3). That is taking into account all interaction between the scatterers and the discontinuity surfaces S_1 and S_2, in combination with the standard boundary conditions at the interfaces. This is done in the following sections.

4.2 The volume V_2

The extinction part of the integral representation (3.2) has three principal regions, corresponding to the position vector $\boldsymbol{r}$ not in V_2, — 1) inside any of the scatterers, 2) to the left of $z = z_1$, and 3) to the right of $z = z_2$.

To prepare the analysis below, we decompose the Green dyadic, see (D.1). For an observation point inside the inscribed sphere of a particular scatterer, say the pth scatterer, we have $|\boldsymbol{r} - \boldsymbol{r}_p| < a_p$, where the vector $\boldsymbol{r}_p$ denotes the local origin depicted in Figure 1. The Green dyadic is then decomposed as

$$
\begin{aligned}
\mathbf{G}_{\mathrm{e}}(k_2, |\boldsymbol{r} - \boldsymbol{r}'|) &= \mathbf{G}_{\mathrm{e}}(k_2, |\boldsymbol{r} - \boldsymbol{r}_p - (\boldsymbol{r}' - \boldsymbol{r}_p)|) \\
&= \mathrm{i}k_2 \sum_n \boldsymbol{v}_n(k_2(\boldsymbol{r} - \boldsymbol{r}_p))\boldsymbol{u}_n(k_2(\boldsymbol{r}' - \boldsymbol{r}_p)), \quad \boldsymbol{r}' \in S_{\mathrm{s}p}
\end{aligned}
$$

for this particular scatterer. On all other scatterers, we have $|\boldsymbol{r} - \boldsymbol{r}_q| > |\boldsymbol{r}' - \boldsymbol{r}_q|$, where $\boldsymbol{r}$ is inside the inscribed sphere of $S_{\mathrm{s}p}$ and $\boldsymbol{r}' \in S_{\mathrm{s}q}$, $q = 1, 2, \ldots, N$, $q \neq p$. The Green dyadic is then decomposed as

$$
\begin{aligned}
\mathbf{G}_{\mathrm{e}}(k_2, |\boldsymbol{r} - \boldsymbol{r}'|) &= \mathbf{G}_{\mathrm{e}}(k_2, |\boldsymbol{r} - \boldsymbol{r}_q - (\boldsymbol{r}' - \boldsymbol{r}_q)|) \\
&= \mathrm{i}k_2 \sum_n \boldsymbol{u}_n(k_2(\boldsymbol{r} - \boldsymbol{r}_q))\boldsymbol{v}_n(k_2(\boldsymbol{r}' - \boldsymbol{r}_q)) \quad (4.5)
\end{aligned}
$$

where $\boldsymbol{r}' \in S_{\mathrm{s}q}$, $q = 1, 2, \ldots, N$, and $q \neq p$.

For this choice of position of $\boldsymbol{r}$, the integral representation in (3.2) implies with the two decomposition of the Green dyadic above, and the plane wave decomposition of the Green dyadic (D.2) ($p = 1, 2, \ldots, N$)

$$
\begin{aligned}
\boldsymbol{0} = &-\sum_n \alpha_n^p \boldsymbol{v}_n(k_2(\boldsymbol{r} - \boldsymbol{r}_p)) + \sum_{\substack{q=1 \\ q \neq p}}^N \sum_n f_n^q \boldsymbol{u}_n(k_2(\boldsymbol{r} - \boldsymbol{r}_q)) \\
&+ \sum_{j=1,2} \iint_{\mathbb{R}^2} \boldsymbol{\varphi}_j^+(\boldsymbol{k}_{\mathrm{t}}; k_2, \boldsymbol{r})\alpha_j^+(\boldsymbol{k}_{\mathrm{t}}) \, \mathrm{d}k_{\mathrm{x}} \, \mathrm{d}k_{\mathrm{y}} \\
&+ \sum_{j=1,2} \iint_{\mathbb{R}^2} \boldsymbol{\varphi}_j^-(\boldsymbol{k}_{\mathrm{t}}; k_2, \boldsymbol{r})\alpha_j^-(\boldsymbol{k}_{\mathrm{t}}) \, \mathrm{d}k_{\mathrm{x}} \, \mathrm{d}k_{\mathrm{y}}, \quad |\boldsymbol{r} - \boldsymbol{r}_p| < a_p \quad (4.6)
\end{aligned}
$$

where the expansion coefficients, α_n^p and f_n^p, are defined as

$$\alpha_n^p = k_2^2 \iint\limits_{S_{sp}} \boldsymbol{u}_n(k_2(\boldsymbol{r}' - \boldsymbol{r}_p)) \cdot (\hat{\boldsymbol{\nu}}(\boldsymbol{r}') \times \eta_0\eta_2\boldsymbol{H}(\boldsymbol{r}'))_+ \, \mathrm{d}S', \quad p = 1, 2, \dots, N \quad (4.7)$$

and

$$f_n^p = -k_2^2 \iint\limits_{S_{sp}} \boldsymbol{v}_n(k_2(\boldsymbol{r}' - \boldsymbol{r}_p)) \cdot (\hat{\boldsymbol{\nu}}(\boldsymbol{r}') \times \eta_0\eta_2\boldsymbol{H}(\boldsymbol{r}'))_+ \, \mathrm{d}S', \quad p = 1, 2, \dots, N \quad (4.8)$$

and where the expansion functions $\alpha_j^{\pm}(\boldsymbol{k}_t)$ are

$$\alpha_j^+(\boldsymbol{k}_t) = -\frac{2\mathrm{i}k_2}{k_{2z}} \iint\limits_{S_1} \boldsymbol{\varphi}_j^{-\dagger}(\boldsymbol{k}_t; k_2, \boldsymbol{r}') \cdot (\hat{\boldsymbol{\nu}} \times \mathrm{i}\eta_0\eta_2\boldsymbol{H}(\boldsymbol{r}'))_- \, \mathrm{d}S'$$
$$- \frac{2\mathrm{i}k_2}{k_{2z}} \iint\limits_{S_1} \boldsymbol{\varphi}_{\bar{j}}^{-\dagger}(\boldsymbol{k}_t; k_2, \boldsymbol{r}') \cdot (\hat{\boldsymbol{\nu}} \times \boldsymbol{E}(\boldsymbol{r}'))_- \, \mathrm{d}S', \quad \boldsymbol{k}_t \in \mathbb{R}^2, \ j = 1, 2 \quad (4.9)$$

and

$$\alpha_j^-(\boldsymbol{k}_t) = -\frac{2\mathrm{i}k_2}{k_{2z}} \iint\limits_{S_2} \boldsymbol{\varphi}_j^{+\dagger}(\boldsymbol{k}_t; k_2, \boldsymbol{r}') \cdot (\hat{\boldsymbol{\nu}} \times \mathrm{i}\eta_0\eta_2\boldsymbol{H}(\boldsymbol{r}'))_- \, \mathrm{d}S'$$
$$- \frac{2\mathrm{i}k_2}{k_{2z}} \iint\limits_{S_2} \boldsymbol{\varphi}_{\bar{j}}^{+\dagger}(\boldsymbol{k}_t; k_2, \boldsymbol{r}') \cdot (\hat{\boldsymbol{\nu}} \times \boldsymbol{E}(\boldsymbol{r}'))_- \, \mathrm{d}S', \quad \boldsymbol{k}_t \in \mathbb{R}^2, \ j = 1, 2 \quad (4.10)$$

Equation (4.6) can be written as

$$\boldsymbol{E}_{\mathrm{exc}p}(\boldsymbol{r}) \overset{\mathrm{def}}{=} \sum_n \alpha_n^p \boldsymbol{v}_n(k_2(\boldsymbol{r} - \boldsymbol{r}_p)) = \sum_{\substack{q=1 \\ q \neq p}}^N \sum_n f_n^q \boldsymbol{u}_n(k_2(\boldsymbol{r} - \boldsymbol{r}_q))$$
$$+ \sum_{j=1,2} \iint\limits_{\mathbb{R}^2} \boldsymbol{\varphi}_j^+(\boldsymbol{k}_t; k_2, \boldsymbol{r})\alpha_j^+(\boldsymbol{k}_t) \, \mathrm{d}k_x \, \mathrm{d}k_y$$
$$+ \sum_{j=1,2} \iint\limits_{\mathbb{R}^2} \boldsymbol{\varphi}_j^-(\boldsymbol{k}_t; k_2, \boldsymbol{r})\alpha_j^-(\boldsymbol{k}_t) \, \mathrm{d}k_x \, \mathrm{d}k_y, \quad |\boldsymbol{r} - \boldsymbol{r}_p| < a_p \quad (4.11)$$

where $\boldsymbol{E}_{\mathrm{exc}p}(\boldsymbol{r})$ is the exciting field at the position of the scatterer located at $\boldsymbol{r}_p$. This field consists of the contributions from the two planar surfaces S_1 and S_2 plus the scattered fields from all scatterers except the contribution from the pth scatterer itself.

The transition matrix of the pth scatterer, $T_{nn'}^p$, connects the expansion coefficients α_n^p in (4.7) and f_n^p in (4.8) to each other, $viz.$,

$$f_n^p = \sum_{n'} T_{nn'}^p \alpha_{n'}^p, \quad p = 1, 2, \dots, N \quad (4.12)$$

The transition matrix $T_{nn'}^p$ is the linear relation between the expansion coefficients of the scattered field, f_n^p, in terms of outgoing spherical vector waves, $\boldsymbol{u}_n(k_2(\boldsymbol{r}-\boldsymbol{r}_p))$, at the local origin $\boldsymbol{r}_p$, and the expansion coefficients, α_n^p, of the local excitation in terms of the regular spherical vector waves, $\boldsymbol{v}_n(k_2(\boldsymbol{r} - \boldsymbol{r}_p))$, at the local origin $\boldsymbol{r}_p$, see (4.11).

To proceed, expand the unknown surface field on the pth scatterer, $\mathrm{i}\hat{\boldsymbol{\nu}}\times\eta_0\eta_2\boldsymbol{H}$, in the tangential regular spherical vector waves. This set is a complete set of expansion functions in the space of square integrable tangential functions [1]. We have

$$\mathrm{i}\eta_0\eta_2\,\hat{\boldsymbol{\nu}}(\boldsymbol{r}) \times \boldsymbol{H}(\boldsymbol{r})|_+ = \sum_n \beta_n \hat{\boldsymbol{\nu}}(\boldsymbol{r}) \times \boldsymbol{v}_{\overline{n}}(k_2(\boldsymbol{r} - \boldsymbol{r}_p)), \quad \boldsymbol{r} \in S_p, \ p = 1, 2, \ldots, N$$

where $\overline{n}$ denotes the index set $\{\overline{\tau}, \sigma, m, l\}$, and where $\overline{\tau}$ is the dual index of τ, $i.e.$, $\overline{1} = 2$ and $\overline{2} = 1$. Introduce the two matrices

$$R_{nn'}^p = -\mathrm{i}k_2^2 \iint\limits_{S_{\mathrm{s}p}} \boldsymbol{v}_n(k_2(\boldsymbol{r} - \boldsymbol{r}_p)) \cdot (\hat{\boldsymbol{\nu}}(\boldsymbol{r}) \times \boldsymbol{v}_{\overline{n'}}(k_2(\boldsymbol{r} - \boldsymbol{r}_p))) \ \mathrm{d}S$$

and

$$Q_{nn'}^p = -\mathrm{i}k_2^2 \iint\limits_{S_{\mathrm{s}p}} \boldsymbol{u}_n(k_2(\boldsymbol{r} - \boldsymbol{r}_p)) \cdot (\hat{\boldsymbol{\nu}}(\boldsymbol{r}) \times \boldsymbol{v}_{\overline{n'}}(k_2(\boldsymbol{r} - \boldsymbol{r}_p))) \ \mathrm{d}S$$

Then, from (4.7) and (4.8)

$$f_n^p = -\sum_{n'} R_{nn'}^p \beta_{n'}^p, \quad \alpha_n^p = \sum_{n'} Q_{nn'}^p \beta_{n'}^p, \quad p = 1, 2, \ldots, N$$

and formal elimination of the expansion coefficients β_n^p gives

$$T_{nn'}^p = -\sum_{n''} R_{nn''}^p (Q^p)_{n''n'}^{-1} \tag{4.13}$$

This is the classic construction of the transition matrix by means of the Null-field approach (Waterman's method). The mathematical justification of the Null-field approach has been the subject of intensive research. Some of the efforts are reported in the literature [8–10, 21, 49]. Next, rewrite (4.11) by translating the planar vector waves to the local origin O_p, $i.e.$,

$$\sum_n \alpha_n^p \boldsymbol{v}_n(k_2(\boldsymbol{r} - \boldsymbol{r}_p)) = \sum_{\substack{q=1 \\ q \neq p}}^N \sum_n f_n^q \boldsymbol{u}_n(k_2(\boldsymbol{r} - \boldsymbol{r}_q))$$

$$+ \sum_{j=1,2} \iint\limits_{\mathbb{R}^2} \boldsymbol{\varphi}_j^+(\boldsymbol{k}_{\mathrm{t}}; k_2, \boldsymbol{r} - \boldsymbol{r}_p) \mathrm{e}^{\mathrm{i}\boldsymbol{k}_2^+ \cdot \boldsymbol{r}_p} \alpha_j^+(\boldsymbol{k}_{\mathrm{t}}) \ \mathrm{d}k_x \, \mathrm{d}k_y$$

$$+ \sum_{j=1,2} \iint\limits_{\mathbb{R}^2} \boldsymbol{\varphi}_j^-(\boldsymbol{k}_{\mathrm{t}}; k_2, \boldsymbol{r} - \boldsymbol{r}_p) \mathrm{e}^{\mathrm{i}\boldsymbol{k}_2^- \cdot \boldsymbol{r}_p} \alpha_j^-(\boldsymbol{k}_{\mathrm{t}}) \ \mathrm{d}k_x \, \mathrm{d}k_y, \quad |\boldsymbol{r} - \boldsymbol{r}_p| < a_p$$

where $\boldsymbol{k}_2^{\pm} = \boldsymbol{k}_{\mathrm{t}} \pm k_{2\mathrm{z}}\hat{\boldsymbol{z}}$. We now use the translation properties of the spherical vector waves, see Appendix B and [25]

$$\boldsymbol{u}_n(k_2(\boldsymbol{r} - \boldsymbol{r}_q)) = \sum_{n'} \mathcal{P}_{nn'}(k_2(\boldsymbol{r}_p - \boldsymbol{r}_q))\boldsymbol{v}_{n'}(k_2(\boldsymbol{r} - \boldsymbol{r}_p)), \quad |\boldsymbol{r} - \boldsymbol{r}_p| < |\boldsymbol{r}_p - \boldsymbol{r}_q|$$

and (D.5), *i.e.*,

$$\boldsymbol{\varphi}_j^{\pm}(\boldsymbol{k}_{\mathrm{t}}; k_2, \boldsymbol{r} - \boldsymbol{r}_p) = \sum_n B_{nj}^{\pm\,\dagger}(\boldsymbol{k}_{\mathrm{t}})\boldsymbol{v}_n(k_2(\boldsymbol{r} - \boldsymbol{r}_p))$$

We get

$$\sum_n \alpha_n^p \boldsymbol{v}_n(k_2(\boldsymbol{r} - \boldsymbol{r}_p)) = \sum_{\substack{q=1 \\ q \neq p}}^{N} \sum_{nn'} f_n^q \mathcal{P}_{nn'}(k_2(\boldsymbol{r}_p - \boldsymbol{r}_q))\boldsymbol{v}_{n'}(k_2(\boldsymbol{r} - \boldsymbol{r}_p))$$

$$+ \sum_n \sum_{j=1,2} \iint_{\mathbb{R}^2} B_{nj}^{+\,\dagger}(\boldsymbol{k}_{\mathrm{t}})\boldsymbol{v}_n(k_2(\boldsymbol{r} - \boldsymbol{r}_p))\mathrm{e}^{\mathrm{i}\boldsymbol{k}_2^+ \cdot \boldsymbol{r}_p}\alpha_j^+(\boldsymbol{k}_{\mathrm{t}})\;\mathrm{d}k_{\mathrm{x}}\,\mathrm{d}k_{\mathrm{y}}$$

$$+ \sum_n \sum_{j=1,2} \iint_{\mathbb{R}^2} B_{nj}^{-\,\dagger}(\boldsymbol{k}_{\mathrm{t}})\boldsymbol{v}_n(k_2(\boldsymbol{r} - \boldsymbol{r}_p))\mathrm{e}^{\mathrm{i}\boldsymbol{k}_2^- \cdot \boldsymbol{r}_p}\alpha_j^-(\boldsymbol{k}_{\mathrm{t}})\;\mathrm{d}k_{\mathrm{x}}\,\mathrm{d}k_{\mathrm{y}}, \quad |\boldsymbol{r} - \boldsymbol{r}_p| < a_p$$

The orthogonality of the regular spherical vector waves on a spherical surface implies

$$\alpha_n^p = \sum_{\substack{q=1 \\ q \neq p}}^{N} \sum_{n'} f_{n'}^q \mathcal{P}_{n'n}(k_2(\boldsymbol{r}_p - \boldsymbol{r}_q)) + \sum_{j=1,2} \iint_{\mathbb{R}^2} B_{nj}^{+\,\dagger}(\boldsymbol{k}_{\mathrm{t}})\mathrm{e}^{\mathrm{i}\boldsymbol{k}_2^+ \cdot \boldsymbol{r}_p}\alpha_j^+(\boldsymbol{k}_{\mathrm{t}})\;\mathrm{d}k_{\mathrm{x}}\,\mathrm{d}k_{\mathrm{y}}$$

$$+ \sum_{j=1,2} \iint_{\mathbb{R}^2} B_{nj}^{-\,\dagger}(\boldsymbol{k}_{\mathrm{t}})\mathrm{e}^{\mathrm{i}\boldsymbol{k}_2^- \cdot \boldsymbol{r}_p}\alpha_j^-(\boldsymbol{k}_{\mathrm{t}})\;\mathrm{d}k_{\mathrm{x}}\,\mathrm{d}k_{\mathrm{y}}, \quad p = 1, 2, \ldots, N \quad (4.14)$$

Equations (4.12) and (4.13) will be used in (4.14), when we in Section 5.3 derive the final system of equations for the deterministic system for a finite number of scatterers in the slab.

For a position vector to the left of $z = z_1$, $z < z_1$ (the global origin O is located in V_2, see Figure 1), we are using (4.5) for the expansion of the Green dyadic on all $S_{\mathrm{s}p}$ in combination with (D.3), and (D.2) on S_i, $i = 1, 2$, in the extinction part of the integral representation (3.2). The orthogonality of the plane waves $\boldsymbol{\varphi}_j^-$ on a planar surface yields

$$0 = \frac{2\mathrm{i}k_2}{k_{2\mathrm{z}}} \sum_n B_{nj}^-(\boldsymbol{k}_{\mathrm{t}}) \sum_{p=1}^{N} \mathrm{e}^{-\mathrm{i}\boldsymbol{k}_2^- \cdot \boldsymbol{r}_p} \iint_{S_{\mathrm{s}p}} \boldsymbol{v}_n(k_2(\boldsymbol{r}' - \boldsymbol{r}_p)) \cdot (\hat{\boldsymbol{\nu}}(\boldsymbol{r}') \times \mathrm{i}\eta_0\eta_2\boldsymbol{H}(\boldsymbol{r}'))_+ \;\mathrm{d}S'$$

$$- \frac{2\mathrm{i}k_2}{k_{2\mathrm{z}}} \sum_{i=1}^{2} \iint_{S_i} \boldsymbol{\varphi}_j^{+\,\dagger}(\boldsymbol{k}_{\mathrm{t}}; k_2, \boldsymbol{r}') \cdot (\hat{\boldsymbol{\nu}} \times \mathrm{i}\eta_0\eta_2\boldsymbol{H}(\boldsymbol{r}'))_- \;\mathrm{d}S'$$

$$- \frac{2\mathrm{i}k_2}{k_{2\mathrm{z}}} \sum_{i=1}^{2} \iint_{S_i} \boldsymbol{\varphi}_j^{+\,\dagger}(\boldsymbol{k}_{\mathrm{t}}; k_2, \boldsymbol{r}') \cdot (\hat{\boldsymbol{\nu}} \times \boldsymbol{E}(\boldsymbol{r}'))_- \;\mathrm{d}S', \quad \boldsymbol{k}_{\mathrm{t}} \in \mathbb{R}^2, \; j = 1, 2$$

where $\boldsymbol{k}_2^- = \boldsymbol{k}_t - k_{2z}\hat{\boldsymbol{z}}$, and where $k_{2z} = (k_2^2 - k_t^2)^{1/2}$. The surface fields on S_i, $i = 1, 2$, are taken from the inside of the slab.

For a position vector to the right of $z = z_2$, $z > z_2$, we get similarly

$$
\begin{aligned}
0 = & \frac{2\mathrm{i}k_2}{k_{2z}} \sum_n B_{nj}^+(\boldsymbol{k}_t) \sum_{p=1}^N \mathrm{e}^{-\mathrm{i}\boldsymbol{k}_2^+ \cdot \boldsymbol{r}_p} \iint_{S_{sp}} \boldsymbol{v}_n(k_2(\boldsymbol{r}' - \boldsymbol{r}_p)) \cdot (\hat{\boldsymbol{\nu}}(\boldsymbol{r}') \times \mathrm{i}\eta_0\eta_2 \boldsymbol{H}(\boldsymbol{r}'))_+ \, \mathrm{d}S' \\
& - \frac{2\mathrm{i}k_2}{k_{2z}} \sum_{i=1}^2 \iint_{S_i} \boldsymbol{\varphi}_j^{-\dagger}(\boldsymbol{k}_t; k_2, \boldsymbol{r}') \cdot (\hat{\boldsymbol{\nu}} \times \mathrm{i}\eta_0\eta_2 \boldsymbol{H}(\boldsymbol{r}'))_- \, \mathrm{d}S' \\
& - \frac{2\mathrm{i}k_2}{k_{2z}} \sum_{i=1}^2 \iint_{S_i} \boldsymbol{\varphi}_{\bar{j}}^{-\dagger}(\boldsymbol{k}_t; k_2, \boldsymbol{r}') \cdot (\hat{\boldsymbol{\nu}} \times \boldsymbol{E}(\boldsymbol{r}'))_- \, \mathrm{d}S', \quad \boldsymbol{k}_t \in \mathbb{R}^2, \; j = 1, 2
\end{aligned}
$$

where $\boldsymbol{k}_2^+ = \boldsymbol{k}_t + k_{2z}\hat{\boldsymbol{z}}$. The surface fields on S_i, $i = 1, 2$, are taken from the inside of the slab. These last two relations are not explicitly used in the paper, but serve as consistency checks. However, these relations play a role in the elimination of the unknown surface fields if a different set of expansion functions than the expansions (5.1) and (5.2) are used.

Finally, we let the position vector $\boldsymbol{r}$ be located in V_2. Moreover, assume that the observation point lies outside all minimum circumscribed spheres of the scatterers, *i.e.*, the position vector $\boldsymbol{r}$ satisfies $|\boldsymbol{r} - \boldsymbol{r}_p| > A_p$ for all $p = 1, 2, \ldots, N$, and the Green dyadic is decomposed as in (4.5).

Outside all circumscribed spheres, we get, using (4.5) in the upper row in (3.2) and using (D.2) in the integrals over S_1 and S_2 in (3.2)

$$
\begin{aligned}
\boldsymbol{E}(\boldsymbol{r}) = & \sum_n \sum_{p=1}^N f_n^p \boldsymbol{u}_n(k_2(\boldsymbol{r} - \boldsymbol{r}_p)) + \sum_{j=1,2} \iint_{\mathbb{R}^2} \boldsymbol{\varphi}_j^+(\boldsymbol{k}_t; k_2, \boldsymbol{r}) \alpha_j^+(\boldsymbol{k}_t) \, \mathrm{d}k_x \, \mathrm{d}k_y \\
& + \sum_{j=1,2} \iint_{\mathbb{R}^2} \boldsymbol{\varphi}_j^-(\boldsymbol{k}_t; k_2, \boldsymbol{r}) \alpha_j^-(\boldsymbol{k}_t) \, \mathrm{d}k_x \, \mathrm{d}k_y, \\
& \qquad\qquad \boldsymbol{r} \in V_2 \text{ and } |\boldsymbol{r} - \boldsymbol{r}_p| > A_p \text{ for all } p = 1, 2, \ldots, N \quad (4.15)
\end{aligned}
$$

where f_n^p and $a_j^\pm(\boldsymbol{k}_t)$ are given in (4.8), (4.9) and (4.10), respectively. This expression gives the field inside the slab provided the unknowns, f_n^p and $\alpha_j^\pm(\boldsymbol{k}_t)$, can be found.

4.3 The volume V_3

Let the position vector $\boldsymbol{r}$ be located to the left of $z = z_2$, $z < z_2$. The integral representation (3.3), the decomposition of the Green dyadic (D.2) imply

$$
\begin{aligned}
0 = & \frac{2\mathrm{i}k_3}{k_{3z}} \iint_{S_2} \boldsymbol{\varphi}_j^{+\dagger}(\boldsymbol{k}_t; k_3, \boldsymbol{r}') \cdot (\hat{\boldsymbol{\nu}} \times \mathrm{i}\eta_0\eta_3 \boldsymbol{H}(\boldsymbol{r}'))_+ \, \mathrm{d}S' \\
& + \frac{2\mathrm{i}k_3}{k_{3z}} \iint_{S_2} \boldsymbol{\varphi}_{\bar{j}}^{+\dagger}(\boldsymbol{k}_t; k_3, \boldsymbol{r}') \cdot (\hat{\boldsymbol{\nu}} \times \boldsymbol{E}(\boldsymbol{r}'))_+ \, \mathrm{d}S', \quad \boldsymbol{k}_t \in \mathbb{R}^2, \; j = 1, 2
\end{aligned}
\qquad (4.16)
$$

where $k_{3z} = (k_3^2 - k_t^2)^{1/2}$.

Similarly, for a position vector to the right of the surface $z = z_2$, $z > z_2$, we get a representation of the transmitted fields in planar vector waves. Analogously to the analysis above, we obtain

$$\boldsymbol{E}_t(\boldsymbol{r}) = \sum_{j=1,2} \iint_{\mathbb{R}^2} t_j(\boldsymbol{k}_t) \boldsymbol{\varphi}_j^+(\boldsymbol{k}_t; k_3, \boldsymbol{r}) \, \mathrm{d}k_x \, \mathrm{d}k_y, \quad z > z_2 \qquad (4.17)$$

where the transmission coefficients are given by

$$t_j(\boldsymbol{k}_t) = \frac{2\mathrm{i}k_3}{k_{3z}} \iint_{S_2} \boldsymbol{\varphi}_j^{-\dagger}(\boldsymbol{k}_t; k_3, \boldsymbol{r}') \cdot (\hat{\boldsymbol{\nu}} \times \mathrm{i}\eta_0 \eta_3 \boldsymbol{H}(\boldsymbol{r}'))_+ \, \mathrm{d}S'$$
$$+ \frac{2\mathrm{i}k_3}{k_{3z}} \iint_{S_2} \boldsymbol{\varphi}_j^{-\dagger}(\boldsymbol{k}_t; k_3, \boldsymbol{r}') \cdot (\hat{\boldsymbol{\nu}} \times \boldsymbol{E}(\boldsymbol{r}'))_+ \, \mathrm{d}S', \quad \boldsymbol{k}_t \in \mathbb{R}^2, \; j = 1, 2 \qquad (4.18)$$

5 Expansions of surface fields

To solve the reflection and transmission problem, we need to eliminate the unknown surface fields $\hat{\boldsymbol{\nu}} \times \boldsymbol{E}(\boldsymbol{r})|_-$ and the corresponding tangential magnetic fields on S_1 and S_2. We also have to eliminate the tangential magnetic fields on the finite scatterers S_{s_p}, which in (4.14) are contained in the unknown coefficients α_n^p and f_n^p for the regular and radiating spherical vector waves that are used in the expression for the exciting field (4.11) at each scatterer. One of these sets of coefficients, α_n^p, are eliminated by the use of the transition matrix (4.13) used in (4.12).

In fact, if the scatterers are not perfectly conducting conductors, as assumed above, the results above still hold. The main reason for the assumption of perfectly conducting scatterers was to simplify the theoretical work. If a more general scatterer is present, replace the transition matrix of the scatterer with the appropriate one. Therefore, the results above hold for any set of scatterers — single or multiple, transparent or not, homogeneous or not — only the individual transition matrices of the scatterers (non-intersecting minimum circumscribed spheres) are known.

5.1 Expansions on the surfaces $z = z_1$ and $z = z_2$

The electric field close to the surface $z = z_1$ has an expansion given by (4.15). This expansion is assumed valid in the domain $z \geq z_1$ and $z < \min_p\{\hat{\boldsymbol{z}} \cdot \boldsymbol{r}_p - A_p\}$, i.e., we assume no minimum circumscribed spheres of the scatterers intersect the surface S_1. Similarly, the electric field close to the surface $z = z_2$ is also assumed to be given by (4.15) in the domain $z \leq z_2$ and $z > \max_p\{\hat{\boldsymbol{z}} \cdot \boldsymbol{r}_p + A_p\}$.

Representation (4.15) gives us an expression of the traces (limit values) of the

tangential electric fields on $z = z_1$ and $z = z_2$, *i.e.*,

$$\hat{\boldsymbol{\nu}} \times \boldsymbol{E}(\boldsymbol{r})|_- = \sum_n \sum_{p=1}^N f_n^p \hat{\boldsymbol{\nu}} \times \boldsymbol{u}_n(k_2(\boldsymbol{r} - \boldsymbol{r}_p))$$
$$+ \sum_{j=1,2} \iint_{\mathbb{R}^2} \alpha_j^+(\boldsymbol{k}_{\mathrm{t}}) \hat{\boldsymbol{\nu}} \times \boldsymbol{\varphi}_j^+(\boldsymbol{k}_{\mathrm{t}}; k_2, \boldsymbol{r}) \, \mathrm{d}k_{\mathrm{x}} \, \mathrm{d}k_{\mathrm{y}}$$
$$+ \sum_{j=1,2} \iint_{\mathbb{R}^2} \alpha_j^-(\boldsymbol{k}_{\mathrm{t}}) \hat{\boldsymbol{\nu}} \times \boldsymbol{\varphi}_j^-(\boldsymbol{k}_{\mathrm{t}}; k_2, \boldsymbol{r}) \, \mathrm{d}k_{\mathrm{x}} \, \mathrm{d}k_{\mathrm{y}}, \quad z = z_1 \quad (5.1)$$

and

$$\hat{\boldsymbol{\nu}} \times \boldsymbol{E}(\boldsymbol{r})|_- = \sum_n \sum_{p=1}^N f_n^p \hat{\boldsymbol{\nu}} \times \boldsymbol{u}_n(k_2(\boldsymbol{r} - \boldsymbol{r}_p))$$
$$+ \sum_{j=1,2} \iint_{\mathbb{R}^2} \alpha_j^+(\boldsymbol{k}_{\mathrm{t}}) \hat{\boldsymbol{\nu}} \times \boldsymbol{\varphi}_j^+(\boldsymbol{k}_{\mathrm{t}}; k_2, \boldsymbol{r}) \, \mathrm{d}k_{\mathrm{x}} \, \mathrm{d}k_{\mathrm{y}}$$
$$+ \sum_{j=1,2} \iint_{\mathbb{R}^2} \alpha_j^-(\boldsymbol{k}_{\mathrm{t}}) \hat{\boldsymbol{\nu}} \times \boldsymbol{\varphi}_j^-(\boldsymbol{k}_{\mathrm{t}}; k_2, \boldsymbol{r}) \, \mathrm{d}k_{\mathrm{x}} \, \mathrm{d}k_{\mathrm{y}}, \quad z = z_2 \quad (5.2)$$

respectively. Note the similarities between these expressions of the tangential fields. Only the values of z vary.

It is convenient to introduce a new notation that contains the unknown f_n^p. We define

$$F_j^\pm(\boldsymbol{k}_{\mathrm{t}}) = \frac{2}{k_2 k_{2\mathrm{z}}} \sum_n \sum_{p=1}^N f_n^p B_{nj}^\pm(\boldsymbol{k}_{\mathrm{t}}) \mathrm{e}^{-\mathrm{i}\boldsymbol{k}_2^\pm \cdot \boldsymbol{r}_p} \quad (5.3)$$

With the use of (D.3) and this notation, we rewrite (5.1)

$$\hat{\boldsymbol{\nu}} \times \boldsymbol{E}(\boldsymbol{r})|_- = \sum_{j=1,2} \iint_{\mathbb{R}^2} \alpha_j^+(\boldsymbol{k}_{\mathrm{t}}) \hat{\boldsymbol{\nu}} \times \boldsymbol{\varphi}_j^+(\boldsymbol{k}_{\mathrm{t}}; k_2, \boldsymbol{r}) \, \mathrm{d}k_{\mathrm{x}} \, \mathrm{d}k_{\mathrm{y}}$$
$$+ \sum_{j=1,2} \iint_{\mathbb{R}^2} \left(F_j^-(\boldsymbol{k}_{\mathrm{t}}) + \alpha_j^-(\boldsymbol{k}_{\mathrm{t}}) \right) \hat{\boldsymbol{\nu}} \times \boldsymbol{\varphi}_j^-(\boldsymbol{k}_{\mathrm{t}}; k_2, \boldsymbol{r}) \, \mathrm{d}k_{\mathrm{x}} \, \mathrm{d}k_{\mathrm{y}}, \quad z = z_1 \quad (5.4)$$

In this relation $\hat{\boldsymbol{\nu}} = -\hat{\boldsymbol{z}}$. Similarly, we obtain from (5.2)

$$\hat{\boldsymbol{\nu}} \times \boldsymbol{E}(\boldsymbol{r})|_- = \sum_{j=1,2} \iint_{\mathbb{R}^2} \left(F_j^+(\boldsymbol{k}_{\mathrm{t}}) + \alpha_j^+(\boldsymbol{k}_{\mathrm{t}}) \right) \hat{\boldsymbol{\nu}} \times \boldsymbol{\varphi}_j^+(\boldsymbol{k}_{\mathrm{t}}; k_2, \boldsymbol{r}) \, \mathrm{d}k_{\mathrm{x}} \, \mathrm{d}k_{\mathrm{y}}$$
$$+ \sum_{j=1,2} \iint_{\mathbb{R}^2} \alpha_j^-(\boldsymbol{k}_{\mathrm{t}}) \hat{\boldsymbol{\nu}} \times \boldsymbol{\varphi}_j^-(\boldsymbol{k}_{\mathrm{t}}; k_2, \boldsymbol{r}) \, \mathrm{d}k_{\mathrm{x}} \, \mathrm{d}k_{\mathrm{y}}, \quad z = z_2 \quad (5.5)$$

where, in this relation, $\hat{\boldsymbol{\nu}} = \hat{\boldsymbol{z}}$.

We also obtain the corresponding tangential magnetic fields. The use of the Maxwell equations and the representation (4.15) imply

$$
\mathrm{i}\eta_0\eta_2 \, \hat{\boldsymbol{\nu}} \times \boldsymbol{H}(\boldsymbol{r})\big|_- = \sum_{j=1,2} \iint_{\mathbb{R}^2} \alpha_j^+(\boldsymbol{k}_\mathrm{t}) \hat{\boldsymbol{\nu}} \times \boldsymbol{\varphi}_{\bar{j}}^+(\boldsymbol{k}_\mathrm{t}; k_2, \boldsymbol{r}) \, \mathrm{d}k_\mathrm{x} \, \mathrm{d}k_\mathrm{y}
$$

$$
+ \sum_{j=1,2} \iint_{\mathbb{R}^2} \left(F_j^-(\boldsymbol{k}_\mathrm{t}) + \alpha_j^-(\boldsymbol{k}_\mathrm{t}) \right) \hat{\boldsymbol{\nu}} \times \boldsymbol{\varphi}_{\bar{j}}^-(\boldsymbol{k}_\mathrm{t}; k_2, \boldsymbol{r}) \, \mathrm{d}k_\mathrm{x} \, \mathrm{d}k_\mathrm{y}, \quad z = z_1 \quad (5.6)
$$

where $\hat{\boldsymbol{\nu}} = -\hat{\boldsymbol{z}}$, and

$$
\mathrm{i}\eta_0\eta_2 \, \hat{\boldsymbol{\nu}} \times \boldsymbol{H}(r)\big|_- = \sum_{j=1,2} \iint_{\mathbb{R}^2} \left(F_j^+(\boldsymbol{k}_\mathrm{t}) + \alpha_j^+(\boldsymbol{k}_\mathrm{t}) \right) \hat{\boldsymbol{\nu}} \times \boldsymbol{\varphi}_{\bar{j}}^+(\boldsymbol{k}_\mathrm{t}; k_2, \boldsymbol{r}) \, \mathrm{d}k_\mathrm{x} \, \mathrm{d}k_\mathrm{y}
$$

$$
+ \sum_{j=1,2} \iint_{\mathbb{R}^2} \alpha_j^-(\boldsymbol{k}_\mathrm{t}) \hat{\boldsymbol{\nu}} \times \boldsymbol{\varphi}_{\bar{j}}^-(\boldsymbol{k}_\mathrm{t}; k_2, \boldsymbol{r}) \, \mathrm{d}k_\mathrm{x} \, \mathrm{d}k_\mathrm{y}, \quad z = z_2 \quad (5.7)
$$

where $\hat{\boldsymbol{\nu}} = \hat{\boldsymbol{z}}$.

5.2 Elimination of the surface fields

We have several unknown coefficients that we have to eliminate and express in the expansion coefficients for the incident field, $a_j(\boldsymbol{k}_\mathrm{t})$, which are assumed to be given in the direct, deterministic scattering problem.

The unknowns in the scattering problem are $\alpha_j^\pm(\boldsymbol{k}_\mathrm{t})$, f_n^p and α_n^p. The aim is to eliminate the expansion coefficients $\alpha_j^\pm(\boldsymbol{k}_\mathrm{t})$, f_n^p and α_n^p, and express them in the known coefficients $a_j(\boldsymbol{k}_\mathrm{t})$. The coefficients $r_j(\boldsymbol{k}_\mathrm{t})$ and $t_j(\boldsymbol{k}_\mathrm{t})$ can then be expressed in $a_j(\boldsymbol{k}_\mathrm{t})$, which solves the deterministic reflection and transmission problems. This elimination is accomplished by the use of the equations (4.2), (4.12), (4.14), and (4.16).

We start the elimination of the unknown quantities with (4.2), the boundary conditions $\hat{\boldsymbol{\nu}} \times \boldsymbol{E}\big|_- = \hat{\boldsymbol{\nu}} \times \boldsymbol{E}\big|_+$ and $\hat{\boldsymbol{\nu}} \times \boldsymbol{H}\big|_- = \hat{\boldsymbol{\nu}} \times \boldsymbol{H}\big|_+$ on S_1, and insert the surface expansions (5.4) and (5.6). Changing the order of integration and the use of

the orthogonality in (C.3) imply

$$
\begin{aligned}
a_j(\boldsymbol{k}_\mathrm{t}) &= -\frac{2\mathrm{i}k_1}{k_{1\mathrm{z}}}\frac{\eta_1}{\eta_2}\iint\limits_{S_1} \boldsymbol{\varphi}_j^{-\dagger}(\boldsymbol{k}_\mathrm{t};k_1,\boldsymbol{r}')\cdot(\hat{\boldsymbol{\nu}}\times \mathrm{i}\eta_0\eta_2\boldsymbol{H}(\boldsymbol{r}'))_-\ \mathrm{d}S' \\
&\quad -\frac{2\mathrm{i}k_1}{k_{1\mathrm{z}}}\iint\limits_{S_1} \boldsymbol{\varphi}_{\bar{j}}^{-\dagger}(\boldsymbol{k}_\mathrm{t};k_1,\boldsymbol{r}')\cdot(\hat{\boldsymbol{\nu}}\times \boldsymbol{E}(\boldsymbol{r}'))_-\ \mathrm{d}S' \\
&= \frac{k_1\mathrm{e}^{-\mathrm{i}k_{1\mathrm{z}}z_1}}{2k_{1\mathrm{z}}}\frac{\eta_1}{\eta_2}\frac{k_{\bar{j}\mathrm{z}}}{k_{\bar{j}}}\left(\alpha_j^+(\boldsymbol{k}_\mathrm{t})\mathrm{e}^{\mathrm{i}k_{2\mathrm{z}}z_1}+(-1)^j\left(F_j^-(\boldsymbol{k}_\mathrm{t})+\alpha_j^-(\boldsymbol{k}_\mathrm{t})\right)\mathrm{e}^{-\mathrm{i}k_{2\mathrm{z}}z_1}\right) \\
&\quad +\frac{k_1\mathrm{e}^{-\mathrm{i}k_{1\mathrm{z}}z_1}}{2k_{1\mathrm{z}}}\frac{k_{j\mathrm{z}}}{k_j}\left(\alpha_j^+(\boldsymbol{k}_\mathrm{t})\mathrm{e}^{\mathrm{i}k_{2\mathrm{z}}z_1}+(-1)^{\bar{j}}\left(F_j^-(\boldsymbol{k}_\mathrm{t})+\alpha_j^-(\boldsymbol{k}_\mathrm{t})\right)\mathrm{e}^{-\mathrm{i}k_{2\mathrm{z}}z_1}\right) \\
&= \frac{k_1\mathrm{e}^{-\mathrm{i}k_{1\mathrm{z}}z_1}\mathrm{e}^{\mathrm{i}k_{2\mathrm{z}}z_1}}{2k_{1\mathrm{z}}}\left(\frac{\eta_1}{\eta_2}\frac{k_{\bar{j}\mathrm{z}}}{k_{\bar{j}}}+\frac{k_{j\mathrm{z}}}{k_j}\right)\alpha_j^+(\boldsymbol{k}_\mathrm{t}) \\
&\quad +\frac{k_1\mathrm{e}^{-\mathrm{i}k_{1\mathrm{z}}z_1}\mathrm{e}^{-\mathrm{i}k_{2\mathrm{z}}z_1}}{2k_{1\mathrm{z}}}(-1)^j\left(\frac{\eta_1}{\eta_2}\frac{k_{\bar{j}\mathrm{z}}}{k_{\bar{j}}}-\frac{k_{j\mathrm{z}}}{k_j}\right)\left(F_j^-(\boldsymbol{k}_\mathrm{t})+\alpha_j^-(\boldsymbol{k}_\mathrm{t})\right), \\
&\qquad \boldsymbol{k}_\mathrm{t}\in\mathbb{R}^2,\ j=1,2
\end{aligned}
\tag{5.8}
$$

where again we make frequent use of the dual index $\bar{j}$, *i.e.*, $\bar{1}=2$ and $\bar{2}=1$.

To simplify the expressions, we identify the numerator N_j^1 and the denominator D_j^1 in the reflection and transmission coefficients of the surface $z=z_1$ (the Fresnel reflection coefficients). The explicit expressions are [25, Sec. 10.6.1.2] or [17, Sec. 7.3]

$$
N_j^1(\boldsymbol{k}_\mathrm{t}) = -(-1)^j\begin{cases}\eta_2 k_2 k_{1\mathrm{z}}-\eta_1 k_1 k_{2\mathrm{z}}, & j=1 \\ \eta_2 k_1 k_{2\mathrm{z}}-\eta_1 k_2 k_{1\mathrm{z}}, & j=2\end{cases} = -(-1)^j\eta_1 k_1 k_2\left(\frac{\eta_2}{\eta_1}\frac{k_{j\mathrm{z}}}{k_j}-\frac{k_{\bar{j}\mathrm{z}}}{k_{\bar{j}}}\right)
\tag{5.9}
$$

and

$$
D_j^1(\boldsymbol{k}_\mathrm{t}) = \begin{cases}\eta_2 k_2 k_{1\mathrm{z}}+\eta_1 k_1 k_{2\mathrm{z}}, & j=1 \\ \eta_2 k_1 k_{2\mathrm{z}}+\eta_1 k_2 k_{1\mathrm{z}}, & j=2\end{cases} = \eta_1 k_1 k_2\left(\frac{\eta_2}{\eta_1}\frac{k_{j\mathrm{z}}}{k_j}+\frac{k_{\bar{j}\mathrm{z}}}{k_{\bar{j}}}\right)
\tag{5.10}
$$

The Fresnel reflection and transmission coefficients for the surface $z=z_1$ (reflection from the left side of S_1 and transmission from left to right) are

$$
\begin{cases}
R_j^1(\boldsymbol{k}_\mathrm{t}) = \dfrac{N_j^1(\boldsymbol{k}_\mathrm{t})}{D_j^1(\boldsymbol{k}_\mathrm{t})}\mathrm{e}^{2\mathrm{i}k_{1\mathrm{z}}z_1} \\[2mm]
T_j^1(\boldsymbol{k}_\mathrm{t}) = 2\eta_2 k_1 k_2\dfrac{k_{j\mathrm{z}}}{D_j^1(\boldsymbol{k}_\mathrm{t})k_j}\dfrac{k_j k_{1\mathrm{z}}}{k_1 k_{j\mathrm{z}}}\mathrm{e}^{\mathrm{i}k_{1\mathrm{z}}z_1}\mathrm{e}^{-\mathrm{i}k_{2\mathrm{z}}z_1} \quad \boldsymbol{k}_\mathrm{t}\in\mathbb{R}^2,\ j=1,2 \\[2mm]
\qquad = \dfrac{2\eta_2 k_2 k_{1\mathrm{z}}}{D_j^1(\boldsymbol{k}_\mathrm{t})}\mathrm{e}^{\mathrm{i}k_{1\mathrm{z}}z_1}\mathrm{e}^{-\mathrm{i}k_{2\mathrm{z}}z_1}
\end{cases}
\tag{5.11}
$$

respectively, where the exponential factors are due to phase corrections, since the surface S_1 is not located at $z=0$. Note the extra minus sign for $j=2$ in the reflection coefficient due to the change of sign in the definition of the plane waves

in (C.1), and the last factor in the definition of the transmission coefficient, which adds an extra factor for the $j = 2$ polarization.

Similarly, the reflection coefficient from the right side of S_1 and the transmission coefficient from right to left are

$$
\begin{cases}
\mathcal{R}_j^1(\boldsymbol{k}_{\mathrm{t}}) = -\dfrac{N_j^1(\boldsymbol{k}_{\mathrm{t}})}{D_j^1(\boldsymbol{k}_{\mathrm{t}})}\mathrm{e}^{-2\mathrm{i}k_{2\mathrm{z}}z_1} \\[2ex]
\mathcal{T}_j^1(\boldsymbol{k}_{\mathrm{t}}) = 2\eta_1 k_1 k_2 \dfrac{k_{\bar{j}\mathrm{z}}^{-}}{D_j^1(\boldsymbol{k}_{\mathrm{t}})k_{\bar{j}}^{-}}\dfrac{k_{\bar{j}}^{-}k_{2\mathrm{z}}}{k_2 k_{\bar{j}\mathrm{z}}^{-}}\mathrm{e}^{-\mathrm{i}k_{2\mathrm{z}}z_1}\mathrm{e}^{\mathrm{i}k_{1\mathrm{z}}z_1} \quad \boldsymbol{k}_{\mathrm{t}} \in \mathbb{R}^2,\ j = 1,2 \qquad (5.12) \\[2ex]
\hphantom{\mathcal{T}_j^1(\boldsymbol{k}_{\mathrm{t}})} = \dfrac{2\eta_1 k_1 k_{2\mathrm{z}}}{D_j^1(\boldsymbol{k}_{\mathrm{t}})}\mathrm{e}^{-\mathrm{i}k_{2\mathrm{z}}z_1}\mathrm{e}^{\mathrm{i}k_{1\mathrm{z}}z_1}
\end{cases}
$$

The reflection and transmission coefficients in (5.11) and (5.12) give in (5.8)

$$
T_j^1(\boldsymbol{k}_{\mathrm{t}})a_j(\boldsymbol{k}_{\mathrm{t}}) = \alpha_j^+(\boldsymbol{k}_{\mathrm{t}}) - \mathcal{R}_j^1(\boldsymbol{k}_{\mathrm{t}})\left(F_j^-(\boldsymbol{k}_{\mathrm{t}}) + \alpha_j^-(\boldsymbol{k}_{\mathrm{t}})\right), \quad \boldsymbol{k}_{\mathrm{t}} \in \mathbb{R}^2,\ j = 1,2 \quad (5.13)
$$

We proceed with (4.16). Using the boundary conditions, $\hat{\boldsymbol{\nu}} \times \boldsymbol{E}|_{-} = \hat{\boldsymbol{\nu}} \times \boldsymbol{E}|_{+}$ and $\hat{\boldsymbol{\nu}} \times \boldsymbol{H}|_{-} = \hat{\boldsymbol{\nu}} \times \boldsymbol{H}|_{+}$ on S_2, and insert the surface expansions (5.5) and (5.7), we get

$$
\begin{aligned}
0 &= \frac{\eta_3}{\eta_2}\iint\limits_{S_2} \boldsymbol{\varphi}_j^{+\dagger}(\boldsymbol{k}_{\mathrm{t}};k_3,\boldsymbol{r}') \cdot (\hat{\boldsymbol{z}} \times \mathrm{i}\eta_0\eta_2\boldsymbol{H}(\boldsymbol{r}'))_{-}\ \mathrm{d}S' \\
&\quad + \iint\limits_{S_2} \boldsymbol{\varphi}_{\bar{j}}^{+\dagger}(\boldsymbol{k}_{\mathrm{t}};k_3,\boldsymbol{r}') \cdot (\hat{\boldsymbol{z}} \times \boldsymbol{E}(\boldsymbol{r}'))_{-}\ \mathrm{d}S' \\
&= -\frac{\mathrm{e}^{\mathrm{i}k_{3\mathrm{z}}z_2}\mathrm{e}^{\mathrm{i}k_{2\mathrm{z}}z_2}}{4\mathrm{i}}(-1)^j\left(\frac{\eta_3}{\eta_2}\frac{k_{j+1\mathrm{z}}}{k_{j+1}} - \frac{k_{\bar{j}+1\mathrm{z}}}{k_{\bar{j}+1}}\right)\left(F_j^+(\boldsymbol{k}_{\mathrm{t}}) + \alpha_j^+(\boldsymbol{k}_{\mathrm{t}})\right) \\
&\quad - \frac{\mathrm{e}^{\mathrm{i}k_{3\mathrm{z}}z_2}\mathrm{e}^{-\mathrm{i}k_{2\mathrm{z}}z_2}}{4\mathrm{i}}\left(\frac{\eta_3}{\eta_2}\frac{k_{j+1\mathrm{z}}}{k_{j+1}} + \frac{k_{\bar{j}+1\mathrm{z}}}{k_{\bar{j}+1}}\right)\alpha_j^-(\boldsymbol{k}_{\mathrm{t}}) \\
&= \frac{\mathrm{e}^{\mathrm{i}k_{3\mathrm{z}}z_2}\mathrm{e}^{\mathrm{i}k_{2\mathrm{z}}z_2}}{4\mathrm{i}\eta_2 k_2 k_3}N_j^2(\boldsymbol{k}_{\mathrm{t}})\left(F_j^+(\boldsymbol{k}_{\mathrm{t}}) + \alpha_j^+(\boldsymbol{k}_{\mathrm{t}})\right) \\
&\quad - \frac{\mathrm{e}^{\mathrm{i}k_{3\mathrm{z}}z_2}\mathrm{e}^{-\mathrm{i}k_{2\mathrm{z}}z_2}}{4\mathrm{i}\eta_2 k_2 k_3}D_j^2(\boldsymbol{k}_{\mathrm{t}})\alpha_j^-(\boldsymbol{k}_{\mathrm{t}}), \quad \boldsymbol{k}_{\mathrm{t}} \in \mathbb{R}^2,\ j = 1,2
\end{aligned}
\tag{5.14}
$$

where we also used the orthogonality relation (C.4), and the numerator N_j^2 and the denominator D_j^2 in the reflection and transmission coefficients of the surface $z = z_2$ (Fresnel reflection coefficients), *viz.*,

$$
N_j^2(\boldsymbol{k}_{\mathrm{t}}) = -(-1)^j \begin{cases} \eta_3 k_3 k_{2\mathrm{z}} - \eta_2 k_2 k_{3\mathrm{z}}, & j = 1 \\ \eta_3 k_2 k_{3\mathrm{z}} - \eta_2 k_3 k_{2\mathrm{z}}, & j = 2 \end{cases} = -(-1)^j \eta_2 k_2 k_3 \left(\frac{\eta_3}{\eta_2}\frac{k_{j+1\mathrm{z}}}{k_{j+1}} - \frac{k_{\bar{j}+1\mathrm{z}}}{k_{\bar{j}+1}}\right)
\tag{5.15}
$$

and

$$
D_j^2(\boldsymbol{k}_{\mathrm{t}}) = \begin{cases} \eta_3 k_3 k_{2\mathrm{z}} + \eta_2 k_2 k_{3\mathrm{z}}, & j = 1 \\ \eta_3 k_2 k_{3\mathrm{z}} + \eta_2 k_3 k_{2\mathrm{z}}, & j = 2 \end{cases} = \eta_2 k_2 k_3 \left(\frac{\eta_3}{\eta_2}\frac{k_{j+1\mathrm{z}}}{k_{j+1}} + \frac{k_{\bar{j}+1\mathrm{z}}}{k_{\bar{j}+1}}\right)
\tag{5.16}
$$

The Fresnel reflection and transmission coefficients for the surface $z = z_2$ (reflection from the left side of S_2 and transmission from left to right) are

$$\begin{cases} R_j^2(\boldsymbol{k}_\mathrm{t}) = \dfrac{N_j^2(\boldsymbol{k}_\mathrm{t})}{D_j^2(\boldsymbol{k}_\mathrm{t})}\mathrm{e}^{2\mathrm{i}k_{2_z}z_2} \\[2ex] T_j^2(\boldsymbol{k}_\mathrm{t}) = 2\eta_3 k_2 k_3 \dfrac{k_{j+1_z}}{D_j^2(\boldsymbol{k}_\mathrm{t})k_{j+1}}\dfrac{k_{j+1}k_{2_z}}{k_2 k_{j+1_z}}\mathrm{e}^{\mathrm{i}k_{2_z}z_2}\mathrm{e}^{-\mathrm{i}k_{3_z}z_2} \qquad \boldsymbol{k}_\mathrm{t} \in \mathbb{R}^2, \ j = 1,2 \quad (5.17) \\[2ex] \qquad\ = \dfrac{2\eta_3 k_3 k_{2_z}}{D_j^2(\boldsymbol{k}_\mathrm{t})}\mathrm{e}^{\mathrm{i}k_{2_z}z_2}\mathrm{e}^{-\mathrm{i}k_{3_z}z_2} \end{cases}$$

respectively[1], where the exponential factors are due to phase corrections, since the surface S_2 is not located at $z = 0$. The reflection coefficient relation in (5.17) is used in (5.14)

$$\alpha_j^-(\boldsymbol{k}_\mathrm{t}) = R_j^2(\boldsymbol{k}_\mathrm{t})\left(F_j^+(\boldsymbol{k}_\mathrm{t}) + \alpha_j^+(\boldsymbol{k}_\mathrm{t})\right), \quad \boldsymbol{k}_\mathrm{t} \in \mathbb{R}^2, \ j = 1,2$$

which used in (5.13) yields

$$\begin{aligned} T_j^1(\boldsymbol{k}_\mathrm{t})a_j(\boldsymbol{k}_\mathrm{t}) = &\left(1 - \mathcal{R}_j^1(\boldsymbol{k}_\mathrm{t})R_j^2(\boldsymbol{k}_\mathrm{t})\right)\alpha_j^+(\boldsymbol{k}_\mathrm{t}) \\ &- \mathcal{R}_j^1(\boldsymbol{k}_\mathrm{t})\left(F_j^-(\boldsymbol{k}_\mathrm{t}) + R_j^2(\boldsymbol{k}_\mathrm{t})F_j^+(\boldsymbol{k}_\mathrm{t})\right), \\ &\hspace{6cm} \boldsymbol{k}_\mathrm{t} \in \mathbb{R}^2, \ j = 1,2 \end{aligned}$$

Solve for the unknown $\alpha_j^+(\boldsymbol{k}_\mathrm{t})$ and $\alpha_j^-(\boldsymbol{k}_\mathrm{t})$.

$$\alpha_j^+(\boldsymbol{k}_\mathrm{t}) = \frac{T_j^1(\boldsymbol{k}_\mathrm{t})a_j(\boldsymbol{k}_\mathrm{t})}{1 - \mathcal{R}_j^1(\boldsymbol{k}_\mathrm{t})R_j^2(\boldsymbol{k}_\mathrm{t})} + \mathcal{R}_j^1(\boldsymbol{k}_\mathrm{t})\frac{F_j^-(\boldsymbol{k}_\mathrm{t}) + R_j^2(\boldsymbol{k}_\mathrm{t})F_j^+(\boldsymbol{k}_\mathrm{t})}{1 - \mathcal{R}_j^1(\boldsymbol{k}_\mathrm{t})R_j^2(\boldsymbol{k}_\mathrm{t})}, \quad \boldsymbol{k}_\mathrm{t} \in \mathbb{R}^2, \ j = 1,2 \tag{5.18}$$

and

$$\begin{aligned} \alpha_j^-(\boldsymbol{k}_\mathrm{t}) = &\frac{R_j^2(\boldsymbol{k}_\mathrm{t})T_j^1(\boldsymbol{k}_\mathrm{t})a_j(\boldsymbol{k}_\mathrm{t})}{1 - \mathcal{R}_j^1(\boldsymbol{k}_\mathrm{t})R_j^2(\boldsymbol{k}_\mathrm{t})} + R_j^2(\boldsymbol{k}_\mathrm{t})\mathcal{R}_j^1(\boldsymbol{k}_\mathrm{t})\frac{F_j^-(\boldsymbol{k}_\mathrm{t}) + R_j^2(\boldsymbol{k}_\mathrm{t})F_j^+(\boldsymbol{k}_\mathrm{t})}{1 - \mathcal{R}_j^1(\boldsymbol{k}_\mathrm{t})R_j^2(\boldsymbol{k}_\mathrm{t})} \\ &+ R_j^2(\boldsymbol{k}_\mathrm{t})F_j^+(\boldsymbol{k}_\mathrm{t}) = \frac{R_j^2(\boldsymbol{k}_\mathrm{t})T_j^1(\boldsymbol{k}_\mathrm{t})a_j(\boldsymbol{k}_\mathrm{t})}{1 - \mathcal{R}_j^1(\boldsymbol{k}_\mathrm{t})R_j^2(\boldsymbol{k}_\mathrm{t})} \\ &+ R_j^2(\boldsymbol{k}_\mathrm{t})\frac{\mathcal{R}_j^1(\boldsymbol{k}_\mathrm{t})F_j^-(\boldsymbol{k}_\mathrm{t}) + F_j^+(\boldsymbol{k}_\mathrm{t})}{1 - \mathcal{R}_j^1(\boldsymbol{k}_\mathrm{t})R_j^2(\boldsymbol{k}_\mathrm{t})}, \quad \boldsymbol{k}_\mathrm{t} \in \mathbb{R}^2, \ j = 1,2 \end{aligned} \tag{5.19}$$

The coefficients $\alpha_j^\pm(\boldsymbol{k}_\mathrm{t})$ are now expressed in the reflection and transmission properties of the surfaces S_1 and S_2, the given coefficient $a_j(\boldsymbol{k}_\mathrm{t})$, and the factors $F_j^\pm(\boldsymbol{k}_\mathrm{t})$. The later quantity contains the unknown coefficients f_n^p, which contain all interaction contributions from the N finite scatterers. The elimination of these coefficients is made in the next section.

---

[1]Do not misinterpret the super index as the square of the reflection or transmission coefficient. It denotes the surface number — in this case S_2.

5.3   Matrix equation

The elimination of the coefficients f_n^p is done by solving a matrix equation. This matrix equation is developed in this section.

We multiply (4.14) with $T_{nn'}^p$ and sum over the free index (notice change in index p and q in the translation matrix and the use of $\mathcal{P}^{\text{t}}(k\boldsymbol{d}) = \mathcal{P}(-k\boldsymbol{d})$). The use of (4.12) leads to the result ($p = 1, 2, \ldots, N$)

$$
f_n^p = \sum_{n'} T_{nn'}^p \Bigg\{ \sum_{\substack{q=1 \\ q \neq p}}^{N} \sum_{n''} \mathcal{P}_{n'n''}(k_2(\boldsymbol{r}_q - \boldsymbol{r}_p)) f_{n''}^q
$$
$$
+ \sum_{j=1,2} \iint_{\mathbb{R}^2} \left\{ B_{n'j}^{+}{}^{\dagger}(\boldsymbol{k}_{\text{t}}) \mathrm{e}^{\mathrm{i}\boldsymbol{k}_2^{+}\cdot\boldsymbol{r}_p} \alpha_j^{+}(\boldsymbol{k}_{\text{t}}) + B_{n'j}^{-}{}^{\dagger}(\boldsymbol{k}_{\text{t}}) \mathrm{e}^{\mathrm{i}\boldsymbol{k}_2^{-}\cdot\boldsymbol{r}_p} \alpha_j^{-}(\boldsymbol{k}_{\text{t}}) \right\} \, \mathrm{d}k_{\text{x}} \, \mathrm{d}k_{\text{y}} \Bigg\}
$$

Insert the expression of $\alpha_j^{+}(\boldsymbol{k}_{\text{t}})$ and $\alpha_j^{-}(\boldsymbol{k}_{\text{t}})$ given in (5.18) and (5.19) and use (5.3). The result has the form

$$
f_n^p - \sum_{n'n''} \sum_{q=1}^{N} T_{nn''}^p A_{n''n'}^{pq} f_{n'}^q = d_n^p, \quad p = 1, 2, \ldots, N \tag{5.20}
$$

where

$$
A_{n''n'}^{pq} = \mathcal{P}_{n''n'}(k_2(\boldsymbol{r}_q - \boldsymbol{r}_p))(1 - \delta_{pq}) + \sum_{j=1,2} \iint_{\mathbb{R}^2} \frac{2 \, \mathrm{d}k_{\text{x}} \, \mathrm{d}k_{\text{y}}}{k_2 k_{2\text{z}}}
$$
$$
\times \Bigg\{ B_{n''j}^{+}{}^{\dagger}(\boldsymbol{k}_{\text{t}}) \mathrm{e}^{\mathrm{i}\boldsymbol{k}_2^{+}\cdot\boldsymbol{r}_p} \mathcal{R}_j^1(\boldsymbol{k}_{\text{t}}) \frac{B_{n'j}^{-}(\boldsymbol{k}_{\text{t}}) \mathrm{e}^{-\mathrm{i}\boldsymbol{k}_2^{-}\cdot\boldsymbol{r}_q} + R_j^2(\boldsymbol{k}_{\text{t}}) B_{n'j}^{+}(\boldsymbol{k}_{\text{t}}) \mathrm{e}^{-\mathrm{i}\boldsymbol{k}_2^{+}\cdot\boldsymbol{r}_q}}{1 - \mathcal{R}_j^1(\boldsymbol{k}_{\text{t}}) R_j^2(\boldsymbol{k}_{\text{t}})}
$$
$$
+ B_{n''j}^{-}{}^{\dagger}(\boldsymbol{k}_{\text{t}}) \mathrm{e}^{\mathrm{i}\boldsymbol{k}_2^{-}\cdot\boldsymbol{r}_p} R_j^2(\boldsymbol{k}_{\text{t}}) \frac{B_{n'j}^{+}(\boldsymbol{k}_{\text{t}}) \mathrm{e}^{-\mathrm{i}\boldsymbol{k}_2^{+}\cdot\boldsymbol{r}_q} + \mathcal{R}_j^1(\boldsymbol{k}_{\text{t}}) B_{n'j}^{-}(\boldsymbol{k}_{\text{t}}) \mathrm{e}^{-\mathrm{i}\boldsymbol{k}_2^{-}\cdot\boldsymbol{r}_q}}{1 - \mathcal{R}_j^1(\boldsymbol{k}_{\text{t}}) R_j^2(\boldsymbol{k}_{\text{t}})} \Bigg\}
$$

which contains only known geometrical material properties for a given scattering problem, and

$$
d_n^p = \sum_{n'} T_{nn'}^p \sum_{j=1,2} \iint_{\mathbb{R}^2} \Bigg\{ \frac{B_{n'j}^{+}{}^{\dagger}(\boldsymbol{k}_{\text{t}}) \mathrm{e}^{\mathrm{i}\boldsymbol{k}_2^{+}\cdot\boldsymbol{r}_p}}{1 - \mathcal{R}_j^1(\boldsymbol{k}_{\text{t}}) R_j^2(\boldsymbol{k}_{\text{t}})}
$$
$$
+ \frac{R_j^2(\boldsymbol{k}_{\text{t}}) B_{n'j}^{-}{}^{\dagger}(\boldsymbol{k}_{\text{t}}) \mathrm{e}^{\mathrm{i}\boldsymbol{k}_2^{-}\cdot\boldsymbol{r}_p}}{1 - \mathcal{R}_j^1(\boldsymbol{k}_{\text{t}}) R_j^2(\boldsymbol{k}_{\text{t}})} \Bigg\} T_j^1(\boldsymbol{k}_{\text{t}}) a_j(\boldsymbol{k}_{\text{t}}) \, \mathrm{d}k_{\text{x}} \, \mathrm{d}k_{\text{y}}
$$

We are now in a position to summarize the solution procedure of the deterministic problem presented in this paper. The complete solution of the problem, for a given incident field, *i.e.*, given $a_j(\boldsymbol{k}_{\text{t}})$, and consequently known d_n^p, and a scattering

configuration, is found by solving (5.20) for f_n^p. Then, (5.3) is used to get $F_j^\pm(\boldsymbol{k}_\mathrm{t})$ and (5.18) and (5.19) to get $\alpha_j^\pm(\boldsymbol{k}_\mathrm{t})$. The surface fields on S_1 and S_2 are now known.

The coefficients for the expansions of the reflected and transmitted fields, $r_j(\boldsymbol{k}_\mathrm{t})$ and $t_j(\boldsymbol{k}_\mathrm{t})$ are given by (4.4) and (4.18), respectively. The reflected and transmitted fields are then determined by (4.3) and (4.17), respectively. The details of this analysis are given in the next section.

6   The transmitted and reflected fields

We are now in a position of calculating the transmitted and reflected fields from the entire scattering configuration.

6.1   The transmitted field

The transmitted field is, see (4.17)

$$\boldsymbol{E}_\mathrm{t}(\boldsymbol{r}) = \sum_{j=1,2} \iint_{\mathbb{R}^2} t_j(\boldsymbol{k}_\mathrm{t}) \boldsymbol{\varphi}_j^+(\boldsymbol{k}_\mathrm{t}; k_3, \boldsymbol{r})\, \mathrm{d}k_\mathrm{x}\, \mathrm{d}k_\mathrm{y}, \quad z > z_2$$

where the transmission coefficients, with the use of the boundary conditions, are given by (using (4.18), the boundary conditions, (5.5), and (5.7))

$$
\begin{aligned}
t_j(\boldsymbol{k}_\mathrm{t}) &= \frac{k_3 \mathrm{e}^{-\mathrm{i}k_{3\mathrm{z}}z_2} \mathrm{e}^{\mathrm{i}k_{2\mathrm{z}}z_2}}{2k_{3\mathrm{z}}} \left(\frac{\eta_3}{\eta_2} \frac{k_{j+1\mathrm{z}}}{k_{j+1}} + \frac{k_{\bar{j}+1\mathrm{z}}}{k_{\bar{j}+1}} \right) \left(F_j^+(\boldsymbol{k}_\mathrm{t}) + \alpha_j^+(\boldsymbol{k}_\mathrm{t}) \right) \\
&\quad + \frac{k_3 \mathrm{e}^{-\mathrm{i}k_{3\mathrm{z}}z_2} \mathrm{e}^{-\mathrm{i}k_{2\mathrm{z}}z_2}}{2k_{3\mathrm{z}}} (-1)^j \left(\frac{\eta_3}{\eta_2} \frac{k_{j+1\mathrm{z}}}{k_{j+1}} - \frac{k_{\bar{j}+1\mathrm{z}}}{k_{\bar{j}+1}} \right) \alpha_j^-(\boldsymbol{k}_\mathrm{t}) \\
&= \frac{\mathrm{e}^{-\mathrm{i}k_{3\mathrm{z}}z_2} \mathrm{e}^{\mathrm{i}k_{2\mathrm{z}}z_2}}{2k_2 \eta_2 k_{3\mathrm{z}}} D_j^2(\boldsymbol{k}_\mathrm{t}) \left(F_j^+(\boldsymbol{k}_\mathrm{t}) + \alpha_j^+(\boldsymbol{k}_\mathrm{t}) \right) \\
&\quad - \frac{\mathrm{e}^{-\mathrm{i}k_{3\mathrm{z}}z_2} \mathrm{e}^{-\mathrm{i}k_{2\mathrm{z}}z_2}}{2k_2 \eta_2 k_{3\mathrm{z}}} N_j^2(\boldsymbol{k}_\mathrm{t}) \alpha_j^-(\boldsymbol{k}_\mathrm{t}), \quad \boldsymbol{k}_\mathrm{t} \in \mathbb{R}^2,\ j = 1, 2
\end{aligned}
$$

where we used the orthogonality relation (C.5) and the expressions for the numerator and denominator of the reflection coefficient of S_2, see (5.15) and (5.16). Insert (5.18) and (5.19), and we get

$$
\begin{aligned}
t_j(\boldsymbol{k}_\mathrm{t}) &= \frac{\mathrm{e}^{-\mathrm{i}k_{3\mathrm{z}}z_2} \mathrm{e}^{\mathrm{i}k_{2\mathrm{z}}z_2}}{2k_2 \eta_2 k_{3\mathrm{z}}} D_j^2(\boldsymbol{k}_\mathrm{t}) \Bigg(F_j^+(\boldsymbol{k}_\mathrm{t}) + \frac{T_j^1(\boldsymbol{k}_\mathrm{t}) a_j(\boldsymbol{k}_\mathrm{t})}{1 - \mathcal{R}_j^1(\boldsymbol{k}_\mathrm{t}) R_j^2(\boldsymbol{k}_\mathrm{t})} \\
&\quad + \mathcal{R}_j^1(\boldsymbol{k}_\mathrm{t}) \frac{F_j^-(\boldsymbol{k}_\mathrm{t}) + R_j^2(\boldsymbol{k}_\mathrm{t}) F_j^+(\boldsymbol{k}_\mathrm{t})}{1 - \mathcal{R}_j^1(\boldsymbol{k}_\mathrm{t}) R_j^2(\boldsymbol{k}_\mathrm{t})} \Bigg) - \frac{\mathrm{e}^{-\mathrm{i}k_{3\mathrm{z}}z_2} \mathrm{e}^{-\mathrm{i}k_{2\mathrm{z}}z_2}}{2k_2 \eta_2 k_{3\mathrm{z}}} N_j^2(\boldsymbol{k}_\mathrm{t}) \Bigg(\frac{R_j^2(\boldsymbol{k}_\mathrm{t}) T_j^1(\boldsymbol{k}_\mathrm{t}) a_j(\boldsymbol{k}_\mathrm{t})}{1 - \mathcal{R}_j^1(\boldsymbol{k}_\mathrm{t}) R_j^2(\boldsymbol{k}_\mathrm{t})} \\
&\quad + R_j^2(\boldsymbol{k}_\mathrm{t}) \frac{\mathcal{R}_j^1(\boldsymbol{k}_\mathrm{t}) F_j^-(\boldsymbol{k}_\mathrm{t}) + F_j^+(\boldsymbol{k}_\mathrm{t})}{1 - \mathcal{R}_j^1(\boldsymbol{k}_\mathrm{t}) R_j^2(\boldsymbol{k}_\mathrm{t})} \Bigg), \quad \boldsymbol{k}_\mathrm{t} \in \mathbb{R}^2,\ j = 1, 2
\end{aligned}
$$

Simplify, and we get

$$
t_j(\boldsymbol{k}_\mathrm{t}) = \frac{\mathrm{e}^{-\mathrm{i}k_{3\mathrm{z}}z_2}\mathrm{e}^{\mathrm{i}k_{2\mathrm{z}}z_2}}{2k_2\eta_2 k_{3\mathrm{z}}}D_j^2(\boldsymbol{k}_\mathrm{t})\frac{\mathcal{R}_j^1(\boldsymbol{k}_\mathrm{t})F_j^-(\boldsymbol{k}_\mathrm{t}) + F_j^+(\boldsymbol{k}_\mathrm{t})}{1 - \mathcal{R}_j^1(\boldsymbol{k}_\mathrm{t})R_j^2(\boldsymbol{k}_\mathrm{t})}
$$

$$
- \frac{\mathrm{e}^{-\mathrm{i}k_{3\mathrm{z}}z_2}\mathrm{e}^{-\mathrm{i}k_{2\mathrm{z}}z_2}}{2k_2\eta_2 k_{3\mathrm{z}}}N_j^2(\boldsymbol{k}_\mathrm{t})R_j^2(\boldsymbol{k}_\mathrm{t})\frac{\mathcal{R}_j^1(\boldsymbol{k}_\mathrm{t})F_j^-(\boldsymbol{k}_\mathrm{t}) + F_j^+(\boldsymbol{k}_\mathrm{t})}{1 - \mathcal{R}_j^1(\boldsymbol{k}_\mathrm{t})R_j^2(\boldsymbol{k}_\mathrm{t})}
$$

$$
+ \mathrm{e}^{-\mathrm{i}k_{3\mathrm{z}}z_2}\frac{D_j^2(\boldsymbol{k}_\mathrm{t})\mathrm{e}^{\mathrm{i}k_{2\mathrm{z}}z_2} - N_j^2(\boldsymbol{k}_\mathrm{t})\mathrm{e}^{-\mathrm{i}k_{2\mathrm{z}}z_2}R_j^2(\boldsymbol{k}_\mathrm{t})}{1 - \mathcal{R}_j^1(\boldsymbol{k}_\mathrm{t})R_j^2(\boldsymbol{k}_\mathrm{t})}\frac{T_j^1(\boldsymbol{k}_\mathrm{t})a_j(\boldsymbol{k}_\mathrm{t})}{2k_2\eta_2 k_{3\mathrm{z}}}, \quad \boldsymbol{k}_\mathrm{t}\in\mathbb{R}^2,\ j=1,2
$$

Since, see (5.15), (5.16), and (5.17)

$$
D_j^2(\boldsymbol{k}_\mathrm{t})\mathrm{e}^{\mathrm{i}k_{2\mathrm{z}}z_2} - N_j^2(\boldsymbol{k}_\mathrm{t})\mathrm{e}^{-\mathrm{i}k_{2\mathrm{z}}z_2}R_j^2(\boldsymbol{k}_\mathrm{t}) = \frac{4\eta_2\eta_3 k_{2\mathrm{z}}k_{3\mathrm{z}}k_2 k_3}{D_j^2(\boldsymbol{k}_\mathrm{t})}\mathrm{e}^{\mathrm{i}k_{2\mathrm{z}}z_2} = 2k_2\eta_2 k_{3\mathrm{z}}T_j^2(\boldsymbol{k}_\mathrm{t})\mathrm{e}^{\mathrm{i}k_{3\mathrm{z}}z_2}
$$

we can simplify further

$$
t_j(\boldsymbol{k}_\mathrm{t}) = T_j^2(\boldsymbol{k}_\mathrm{t})\frac{\mathcal{R}_j^1(\boldsymbol{k}_\mathrm{t})F_j^-(\boldsymbol{k}_\mathrm{t}) + F_j^+(\boldsymbol{k}_\mathrm{t})}{1 - \mathcal{R}_j^1(\boldsymbol{k}_\mathrm{t})R_j^2(\boldsymbol{k}_\mathrm{t})}
$$

$$
+ \frac{T_j^1(\boldsymbol{k}_\mathrm{t})T_j^2(\boldsymbol{k}_\mathrm{t})}{1 - \mathcal{R}_j^1(\boldsymbol{k}_\mathrm{t})R_j^2(\boldsymbol{k}_\mathrm{t})}a_j(\boldsymbol{k}_\mathrm{t}), \quad \boldsymbol{k}_\mathrm{t}\in\mathbb{R}^2,\ j=1,2
$$

It is convenient to introduce the total transmission coefficient of the slab, which in our notation reads [25, Sec. 10.6.1.1]

$$
T_j(\boldsymbol{k}_\mathrm{t}) = \frac{T_j^1(\boldsymbol{k}_\mathrm{t})T_j^2(\boldsymbol{k}_\mathrm{t})}{1 - \mathcal{R}_j^1(\boldsymbol{k}_\mathrm{t})R_j^2(\boldsymbol{k}_\mathrm{t})} \tag{6.1}
$$

The final expression of the amplitude of the transmitted field is

$$
t_j(\boldsymbol{k}_\mathrm{t}) = T_j^2(\boldsymbol{k}_\mathrm{t})\frac{\mathcal{R}_j^1(\boldsymbol{k}_\mathrm{t})F_j^-(\boldsymbol{k}_\mathrm{t}) + F_j^+(\boldsymbol{k}_\mathrm{t})}{1 - \mathcal{R}_j^1(\boldsymbol{k}_\mathrm{t})R_j^2(\boldsymbol{k}_\mathrm{t})} + T_j(\boldsymbol{k}_\mathrm{t})a_j(\boldsymbol{k}_\mathrm{t}), \quad \boldsymbol{k}_\mathrm{t}\in\mathbb{R}^2,\ j=1,2
$$

$$
\tag{6.2}
$$

The amplitude of the transmitted field, $t_j(\boldsymbol{k}_\mathrm{t})$, consists of two terms — the last term $T_j(\boldsymbol{k}_\mathrm{t})a_j(\boldsymbol{k}_\mathrm{t})$ is the direct transmitted contribution of the slab itself, and the first term is the additional contribution to the transmitted field from the scatterers inside the slab.

6.2   The reflected field

Similarly, the reflected field is, see (4.3)

$$
\boldsymbol{E}_\mathrm{r}(\boldsymbol{r}) = \sum_{j=1,2}\iint\limits_{\mathbb{R}^2} r_j(\boldsymbol{k}_\mathrm{t})\boldsymbol{\varphi}_j^-(\boldsymbol{k}_\mathrm{t}; k_1, \boldsymbol{r})\,\mathrm{d}k_\mathrm{x}\,\mathrm{d}k_\mathrm{y}, \quad z < z_1
$$

where the reflection coefficients are given by (4.4)

$$r_j(\boldsymbol{k}_t) = \frac{2\mathrm{i}k_1}{k_{1z}}\frac{\eta_1}{\eta_2} \iint\limits_{S_1} \boldsymbol{\varphi}_j^{+\dagger}(\boldsymbol{k}_t; k_1, \boldsymbol{r}') \cdot (\hat{\boldsymbol{\nu}} \times \mathrm{i}\eta_0\eta_2\boldsymbol{H}(\boldsymbol{r}'))_- \; \mathrm{d}S'$$

$$+ \frac{2\mathrm{i}k_1}{k_{1z}} \iint\limits_{S_1} \boldsymbol{\varphi}_j^{+\dagger}(\boldsymbol{k}_t; k_1, \boldsymbol{r}') \cdot (\hat{\boldsymbol{\nu}} \times \boldsymbol{E}(\boldsymbol{r}'))_- \; \mathrm{d}S', \quad \boldsymbol{k}_t \in \mathbb{R}^2, \; j = 1, 2$$

were we used the boundary conditions, $\hat{\boldsymbol{\nu}} \times \boldsymbol{E}|_- = \hat{\boldsymbol{\nu}} \times \boldsymbol{E}|_+$ and $\hat{\boldsymbol{\nu}} \times \boldsymbol{H}|_- = \hat{\boldsymbol{\nu}} \times \boldsymbol{H}|_+$ on S_1. The surface expansions (5.4) and (5.6) and the use of the orthogonality in (C.2) imply

$$r_j(\boldsymbol{k}_t) = \frac{k_1\mathrm{e}^{\mathrm{i}k_{1z}z_1}}{2k_{1z}}\frac{\eta_1}{\eta_2}\frac{k_{\bar{j}z}}{k_{\bar{j}}} \left((-1)^j \alpha_j^+(\boldsymbol{k}_t)\mathrm{e}^{\mathrm{i}k_{2z}z_1} + \left(F_j^-(\boldsymbol{k}_t) + \alpha_j^-(\boldsymbol{k}_t)\right)\mathrm{e}^{-\mathrm{i}k_{2z}z_1} \right)$$

$$+ \frac{k_1\mathrm{e}^{\mathrm{i}k_{1z}z_1}}{2k_{1z}}\frac{k_{jz}}{k_j} \left((-1)^{\bar{j}} \alpha_j^+(\boldsymbol{k}_t)\mathrm{e}^{\mathrm{i}k_{2z}z_1} + \left(F_j^-(\boldsymbol{k}_t) + \alpha_j^-(\boldsymbol{k}_t)\right)\mathrm{e}^{-\mathrm{i}k_{2z}z_1} \right)$$

$$= \frac{k_1\mathrm{e}^{\mathrm{i}k_{1z}z_1}\mathrm{e}^{\mathrm{i}k_{2z}z_1}}{2k_{1z}}(-1)^j \left(\frac{\eta_1}{\eta_2}\frac{k_{\bar{j}z}}{k_{\bar{j}}} - \frac{k_{jz}}{k_j} \right)\alpha_j^+(\boldsymbol{k}_t)$$

$$+ \frac{k_1\mathrm{e}^{\mathrm{i}k_{1z}z_1}\mathrm{e}^{-\mathrm{i}k_{2z}z_1}}{2k_{1z}} \left(\frac{\eta_1}{\eta_2}\frac{k_{\bar{j}z}}{k_{\bar{j}}} + \frac{k_{jz}}{k_j} \right)\left(F_j^-(\boldsymbol{k}_t) + \alpha_j^-(\boldsymbol{k}_t)\right),$$

$$\boldsymbol{k}_t \in \mathbb{R}^2, \; j = 1, 2$$

The numerator and denominator of the reflection coefficient on S_1, (5.9) and (5.10), simplify this expression further. We get

$$r_j(\boldsymbol{k}_t) = \frac{\mathrm{e}^{\mathrm{i}k_{1z}z_1}\mathrm{e}^{\mathrm{i}k_{2z}z_1}}{2\eta_2k_2k_{1z}}N_j^1(\boldsymbol{k}_t)\alpha_j^+(\boldsymbol{k}_t)$$

$$+ \frac{\mathrm{e}^{\mathrm{i}k_{1z}z_1}\mathrm{e}^{-\mathrm{i}k_{2z}z_1}}{2\eta_2k_2k_{1z}}D_j^1(\boldsymbol{k}_t)\left(F_j^-(\boldsymbol{k}_t) + \alpha_j^-(\boldsymbol{k}_t)\right), \quad \boldsymbol{k}_t \in \mathbb{R}^2, \; j = 1, 2$$

Insert (5.18) and (5.19), and we get

$$r_j(\boldsymbol{k}_t)$$

$$= \frac{\mathrm{e}^{\mathrm{i}k_{1z}z_1}\mathrm{e}^{\mathrm{i}k_{2z}z_1}}{2\eta_2k_2k_{1z}}N_j^1(\boldsymbol{k}_t)\left\{ \frac{T_j^1(\boldsymbol{k}_t)a_j(\boldsymbol{k}_t)}{1 - \mathcal{R}_j^1(\boldsymbol{k}_t)R_j^2(\boldsymbol{k}_t)} + \mathcal{R}_j^1(\boldsymbol{k}_t)\frac{F_j^-(\boldsymbol{k}_t) + R_j^2(\boldsymbol{k}_t)F_j^+(\boldsymbol{k}_t)}{1 - \mathcal{R}_j^1(\boldsymbol{k}_t)R_j^2(\boldsymbol{k}_t)} \right\}$$

$$+ \frac{\mathrm{e}^{\mathrm{i}k_{1z}z_1}\mathrm{e}^{-\mathrm{i}k_{2z}z_1}}{2\eta_2k_2k_{1z}}D_j^1(\boldsymbol{k}_t)\left\{ \frac{R_j^2(\boldsymbol{k}_t)T_j^1(\boldsymbol{k}_t)a_j(\boldsymbol{k}_t)}{1 - \mathcal{R}_j^1(\boldsymbol{k}_t)R_j^2(\boldsymbol{k}_t)} + \frac{F_j^-(\boldsymbol{k}_t) + R_j^2(\boldsymbol{k}_t)F_j^+(\boldsymbol{k}_t)}{1 - \mathcal{R}_j^1(\boldsymbol{k}_t)R_j^2(\boldsymbol{k}_t)} \right\},$$

$$\boldsymbol{k}_t \in \mathbb{R}^2, \; j = 1, 2$$

We simplify this expression with the use of (5.11)

$$
r_j(\boldsymbol{k}_{\mathrm{t}}) = -\frac{\mathrm{e}^{-\mathrm{i}k_{1\mathrm{z}}z_1}\mathrm{e}^{-\mathrm{i}k_{2\mathrm{z}}z_1}}{2\eta_2 k_2 k_{1\mathrm{z}}} N_j^1(\boldsymbol{k}_{\mathrm{t}})R_j^1(\boldsymbol{k}_{\mathrm{t}})\frac{F_j^-(\boldsymbol{k}_{\mathrm{t}}) + R_j^2(\boldsymbol{k}_{\mathrm{t}})F_j^+(\boldsymbol{k}_{\mathrm{t}})}{1 - \mathcal{R}_j^1(\boldsymbol{k}_{\mathrm{t}})R_j^2(\boldsymbol{k}_{\mathrm{t}})}
$$

$$
+ \frac{\mathrm{e}^{\mathrm{i}k_{1\mathrm{z}}z_1}\mathrm{e}^{-\mathrm{i}k_{2\mathrm{z}}z_1}}{2\eta_2 k_2 k_{1\mathrm{z}}} D_j^1(\boldsymbol{k}_{\mathrm{t}})\frac{F_j^-(\boldsymbol{k}_{\mathrm{t}}) + R_j^2(\boldsymbol{k}_{\mathrm{t}})F_j^+(\boldsymbol{k}_{\mathrm{t}})}{1 - \mathcal{R}_j^1(\boldsymbol{k}_{\mathrm{t}})R_j^2(\boldsymbol{k}_{\mathrm{t}})} + \frac{R_j^1(\boldsymbol{k}_{\mathrm{t}}) + R_j^2(\boldsymbol{k}_{\mathrm{t}})\mathrm{e}^{2\mathrm{i}(k_{1\mathrm{z}}-k_{2\mathrm{z}})z_1}}{1 - \mathcal{R}_j^1(\boldsymbol{k}_{\mathrm{t}})R_j^2(\boldsymbol{k}_{\mathrm{t}})} a_j(\boldsymbol{k}_{\mathrm{t}})
$$

$$
= \mathcal{T}_j^1(\boldsymbol{k}_{\mathrm{t}})\frac{F_j^-(\boldsymbol{k}_{\mathrm{t}}) + R_j^2(\boldsymbol{k}_{\mathrm{t}})F_j^+(\boldsymbol{k}_{\mathrm{t}})}{1 - \mathcal{R}_j^1(\boldsymbol{k}_{\mathrm{t}})R_j^2(\boldsymbol{k}_{\mathrm{t}})} + \frac{R_j^1(\boldsymbol{k}_{\mathrm{t}}) + R_j^2(\boldsymbol{k}_{\mathrm{t}})\mathrm{e}^{2\mathrm{i}(k_{1\mathrm{z}}-k_{2\mathrm{z}})z_1}}{1 - \mathcal{R}_j^1(\boldsymbol{k}_{\mathrm{t}})R_j^2(\boldsymbol{k}_{\mathrm{t}})} a_j(\boldsymbol{k}_{\mathrm{t}}),
$$

$$
\boldsymbol{k}_{\mathrm{t}} \in \mathbb{R}^2, \ j = 1,2
$$

since, see (5.15), (5.16), (5.11) and (5.12)

$$
D_j^1(\boldsymbol{k}_{\mathrm{t}})\mathrm{e}^{\mathrm{i}k_{1\mathrm{z}}z_1} - N_j^1(\boldsymbol{k}_{\mathrm{t}})\mathrm{e}^{-\mathrm{i}k_{1\mathrm{z}}z_1}R_j^1(\boldsymbol{k}_{\mathrm{t}}) = \frac{4\eta_1\eta_2 k_{1\mathrm{z}}k_{2\mathrm{z}}k_1 k_2}{D_j^1(\boldsymbol{k}_{\mathrm{t}})}\mathrm{e}^{\mathrm{i}k_{1\mathrm{z}}z_1} = 2k_2\eta_2 k_{1\mathrm{z}}\mathcal{T}_j^1(\boldsymbol{k}_{\mathrm{t}})\mathrm{e}^{\mathrm{i}k_{2\mathrm{z}}z_1}
$$

It is convenient to introduce the total reflection coefficient of the slab, which in our notation reads [25, Sec. 10.6.1.1]

$$
R_j(\boldsymbol{k}_{\mathrm{t}}) = \frac{R_j^1(\boldsymbol{k}_{\mathrm{t}}) + R_j^2(\boldsymbol{k}_{\mathrm{t}})\mathrm{e}^{2\mathrm{i}(k_{1\mathrm{z}}-k_{2\mathrm{z}})z_1}}{1 - \mathcal{R}_j^1(\boldsymbol{k}_{\mathrm{t}})R_j^2(\boldsymbol{k}_{\mathrm{t}})}
$$

$$
= \frac{R_j^1(\boldsymbol{k}_{\mathrm{t}}) + R_j^2(\boldsymbol{k}_{\mathrm{t}})\left(T_j^1(\boldsymbol{k}_{\mathrm{t}})\mathcal{T}_j^1(\boldsymbol{k}_{\mathrm{t}}) - R_j^1(\boldsymbol{k}_{\mathrm{t}})\mathcal{R}_j^1(\boldsymbol{k}_{\mathrm{t}})\right)}{1 - \mathcal{R}_j^1(\boldsymbol{k}_{\mathrm{t}})R_j^2(\boldsymbol{k}_{\mathrm{t}})}
$$

$$
= R_j^1(\boldsymbol{k}_{\mathrm{t}}) + T_j^1(\boldsymbol{k}_{\mathrm{t}})\frac{R_j^2(\boldsymbol{k}_{\mathrm{t}})}{1 - \mathcal{R}_j^1(\boldsymbol{k}_{\mathrm{t}})R_j^2(\boldsymbol{k}_{\mathrm{t}})}\mathcal{T}_j^1(\boldsymbol{k}_{\mathrm{t}})
$$

where we also used the identity

$$
\mathrm{e}^{2\mathrm{i}(k_{1\mathrm{z}}-k_{2\mathrm{z}})z_1} = T_j^1(\boldsymbol{k}_{\mathrm{t}})\mathcal{T}_j^1(\boldsymbol{k}_{\mathrm{t}}) - R_j^1(\boldsymbol{k}_{\mathrm{t}})\mathcal{R}_j^1(\boldsymbol{k}_{\mathrm{t}})
$$

The final expression of the amplitude of the reflected field then becomes

$$
\boxed{r_j(\boldsymbol{k}_{\mathrm{t}}) = \mathcal{T}_j^1(\boldsymbol{k}_{\mathrm{t}})\frac{F_j^-(\boldsymbol{k}_{\mathrm{t}}) + R_j^2(\boldsymbol{k}_{\mathrm{t}})F_j^+(\boldsymbol{k}_{\mathrm{t}})}{1 - \mathcal{R}_j^1(\boldsymbol{k}_{\mathrm{t}})R_j^2(\boldsymbol{k}_{\mathrm{t}})} + R_j(\boldsymbol{k}_{\mathrm{t}})a_j(\boldsymbol{k}_{\mathrm{t}}), \quad \boldsymbol{k}_{\mathrm{t}} \in \mathbb{R}^2, \ j = 1,2}
$$

$$
(6.3)
$$

The amplitude of the reflected field, $r_j(\boldsymbol{k}_{\mathrm{t}})$, consists of two terms — the last term $R_j(\boldsymbol{k}_{\mathrm{t}})a_j(\boldsymbol{k}_{\mathrm{t}})$ is the direct reflected contribution of the slab itself, and the first term is the additional contribution to the reflected field from the scatterers inside the slab.

7 Statistical problem — ensemble average

The solution of the set of equations in (5.20) for the unknowns, f_n^p, is an unsurmountable task, if the number of scatterers is large. Fortunately, there are statistical

methods that apply in this case, especially if the location and state (material properties, size, shape, and orientation *etc.*) of the scatterers are randomly distributed. Moreover, with a large number of scatterers, we rarely have complete information about the position and the state of each scatterer, and we are often not interested in the physical quantities of a particular configuration, but ensemble averages suffice. In particular, the average of the electric field is an appropriate quantity in several radio and radar applications, but it is of limited value as an optical observable. The presentation in this section follows to some extent the one presented in [23, 31, 52, 60, 61], but deviates in the method of solving the problem.

A statistical evaluation of the relevant physical quantities involves ensemble averages, which we denote by the symbol $\langle \cdot \rangle$. The relation between the ensemble average and the time average and use of the ergodic hypothesis are found in the comprehensive review article [36] and in the excellent textbook [35].

The scatterer locations $\boldsymbol{r}_p$, $p = 1, 2, \ldots, N$, are now random variables. Moreover, the properties of each scatterer (geometry and material) are also random variables, that we collect in a state variable ξ_p, $p = 1, 2, \ldots, N$. The common N-particle probability density function (PDF) is denoted $P(\boldsymbol{r}_1, \ldots, \boldsymbol{r}_N; \xi_1, \ldots, \xi_N)$. More details on this PDF are collected in Appendix E.

The explicit assumptions made about the scatterers in this section are:

1. the number of scatterers N is large, so that statistical methods are appropriate to apply

2. the N scatterers are characterized by a common probability density function

3. the scatterers are indistinguishable insofar as the numbering of the scatterers is arbitrary

4. the state variables of the scatterers, ξ_p, are independent between different scatterers and of the position variables, $\boldsymbol{r}_p$, $p = 1, 2, \ldots, N$

5. no minimum circumscribed spheres of the individual scatterers intersect

The position variables cannot be statistically independent variables for scatterers of finite size, due to the assumption of non-intersecting minimum circumscribed spheres. The assumption of independence in Item 4 makes the averaging of scatterer position separate from the averaging over their states in the transition matrix entries.

The random variables $\boldsymbol{r}_p$ and ξ_p are now dummy variables in the integration over all possible positions and states. As a consequence, the index p is eventually dropped in the analysis below.

7.1 Transmitted and reflected fields

The ensemble average and the use of the conditional probability density function, see Appendix E, imply the following expressions of the reflected and transmitted

24

fields from (4.17) and (4.3)

$$\langle \boldsymbol{E}_{\mathrm{t}}(\boldsymbol{r}) \rangle = \sum_{j=1,2} \iint_{\mathbb{R}^2} \langle t_j(\boldsymbol{k}_{\mathrm{t}}) \rangle \, \boldsymbol{\varphi}_j^+(\boldsymbol{k}_{\mathrm{t}}; k_3, \boldsymbol{r}) \, \mathrm{d}k_{\mathrm{x}} \, \mathrm{d}k_{\mathrm{y}}, \quad z > z_2 \qquad (7.1)$$

and

$$\langle \boldsymbol{E}_{\mathrm{r}}(\boldsymbol{r}) \rangle = \sum_{j=1,2} \iint_{\mathbb{R}^2} \langle r_j(\boldsymbol{k}_{\mathrm{t}}) \rangle \, \boldsymbol{\varphi}_j^-(\boldsymbol{k}_{\mathrm{t}}; k_1, \boldsymbol{r}) \, \mathrm{d}k_{\mathrm{x}} \, \mathrm{d}k_{\mathrm{y}}, \quad z < z_1 \qquad (7.2)$$

These fields are the average or coherent contribution of the electric field outside the slab, and the computation of these fields are the main purpose of this paper.

To evaluate the averaged transmitted and reflected fields, we need to obtain $\langle t_j(\boldsymbol{k}_{\mathrm{t}}) \rangle$ and $\langle r_j(\boldsymbol{k}_{\mathrm{t}}) \rangle$, which both contain the factors $\langle F_j^\pm(\boldsymbol{k}_{\mathrm{t}}) \rangle$, see (6.2) and (6.3). All other quantities in $\langle t_j(\boldsymbol{k}_{\mathrm{t}}) \rangle$ and $\langle r_j(\boldsymbol{k}_{\mathrm{t}}) \rangle$ are deterministic. We have

$$\langle t_j(\boldsymbol{k}_{\mathrm{t}}) \rangle = T_j^2(\boldsymbol{k}_{\mathrm{t}}) \frac{\mathcal{R}_j^1(\boldsymbol{k}_{\mathrm{t}}) \langle F_j^-(\boldsymbol{k}_{\mathrm{t}}) \rangle + \langle F_j^+(\boldsymbol{k}_{\mathrm{t}}) \rangle}{1 - \mathcal{R}_j^1(\boldsymbol{k}_{\mathrm{t}}) R_j^2(\boldsymbol{k}_{\mathrm{t}})}$$
$$+ T_j(\boldsymbol{k}_{\mathrm{t}}) a_j(\boldsymbol{k}_{\mathrm{t}}), \quad \boldsymbol{k}_{\mathrm{t}} \in \mathbb{R}^2, \ j = 1, 2 \quad (7.3)$$

and

$$\langle r_j(\boldsymbol{k}_{\mathrm{t}}) \rangle = \mathcal{T}_j^1(\boldsymbol{k}_{\mathrm{t}}) \frac{\langle F_j^-(\boldsymbol{k}_{\mathrm{t}}) \rangle + R_j^2(\boldsymbol{k}_{\mathrm{t}}) \langle F_j^+(\boldsymbol{k}_{\mathrm{t}}) \rangle}{1 - \mathcal{R}_j^1(\boldsymbol{k}_{\mathrm{t}}) R_j^2(\boldsymbol{k}_{\mathrm{t}})}$$
$$+ R_j(\boldsymbol{k}_{\mathrm{t}}) a_j(\boldsymbol{k}_{\mathrm{t}}), \quad \boldsymbol{k}_{\mathrm{t}} \in \mathbb{R}^2, \ j = 1, 2 \quad (7.4)$$

The factors $\langle F_j^\pm(\boldsymbol{k}_{\mathrm{t}}) \rangle$ are evaluated in the section below.

7.2   Coefficient average

The average of the functions $F_j^\pm(\boldsymbol{k}_t)$ in (5.3) has to be computed. The definition of the conditional probability density function implies, see Appendix E

$$
\left\langle F_j^\pm(\boldsymbol{k}_t)\right\rangle = \frac{2}{k_2 k_{2z}} \sum_n \sum_{p=1}^N B_{nj}^\pm(\boldsymbol{k}_t) \left\langle f_n^p \mathrm{e}^{-\mathrm{i}\boldsymbol{k}_2^\pm \cdot \boldsymbol{r}_p}\right\rangle
$$

$$
= \frac{2}{k_2 k_{2z}} \sum_n \sum_{p=1}^N B_{nj}^\pm(\boldsymbol{k}_t) \iiint_{V_s^N} P(\boldsymbol{r}_1,\dots,\boldsymbol{r}_N) f_n^p(\boldsymbol{r}_1,\dots,\boldsymbol{r}_N) \mathrm{e}^{-\mathrm{i}\boldsymbol{k}_2^\pm \cdot \boldsymbol{r}_p} \prod_{p=1}^N \mathrm{d}v_p
$$

$$
= \frac{2}{k_2 k_{2z}} \sum_n \sum_{p=1}^N B_{nj}^\pm(\boldsymbol{k}_t)
$$

$$
\times \iiint_{V_s^N} P(\boldsymbol{r}_p) P(\boldsymbol{r}_1,\dots,\boldsymbol{r}_{p-1},\boldsymbol{r}_{p+1},\dots\boldsymbol{r}_N|\boldsymbol{r}_p) f_n^p(\boldsymbol{r}_1,\dots,\boldsymbol{r}_N) \mathrm{e}^{-\mathrm{i}\boldsymbol{k}_2^\pm \cdot \boldsymbol{r}_p} \prod_{p=1}^N \mathrm{d}v_p
$$

$$
= \frac{2}{k_2 k_{2z}} \sum_n \sum_{p=1}^N B_{nj}^\pm(\boldsymbol{k}_t) \iiint_{V_s} P(\boldsymbol{r}_p) \left\langle f_n^p\right\rangle(\boldsymbol{r}_p) \mathrm{e}^{-\mathrm{i}\boldsymbol{k}_2^\pm \cdot \boldsymbol{r}_p} \mathrm{d}v_p
$$

$$
= \frac{2N}{k_2 k_{2z}} \sum_n B_{nj}^\pm(\boldsymbol{k}_t) \iiint_{V_s} P(\boldsymbol{r}) \left\langle f_n\right\rangle(\boldsymbol{r}) \mathrm{e}^{-\mathrm{i}\boldsymbol{k}_2^\pm \cdot \boldsymbol{r}} \mathrm{d}v \quad (7.5)
$$

since the variable $\boldsymbol{r}_p$ now is a dummy variable and all integrals in the middle expression are identical. We can also skip the superscript p on f_n. The volume V_s is the volume of possible locations of the local origins $\boldsymbol{r}_p$, $p = 1, 2, \dots, N$. If the number of scatterers $N \to \infty$ and the scatterers are randomly filled in the entire slab (this requires that an appropriate limit procedure is employed), the volume V_s is $\{\boldsymbol{r} : z_1 + a \leq z \leq z_2 - a\}$, where $a = \max_p A_p$. This limit process implies that $NP(\boldsymbol{r}) \to n_0$ as $N \to \infty$, where n_0 is the number density of the scatterers (number of scatterers per unit volume). The geometry of a typical geometry is depicted in Figure 2.[2]

To obtain $\left\langle f_n\right\rangle(\boldsymbol{r})$, we need to take the conditional average of the set of matrix equations in (5.20). Using the conditional probability density function, we obtain

$$
\left\langle f_n^p\right\rangle(\boldsymbol{r}_p; \xi_p) - \sum_{n'n''} \sum_{q=1}^N \iiint_{V_s} P(\boldsymbol{r}_q|\boldsymbol{r}_p) \left\langle T_{nn''}^p A_{n''n'}^{pq} f_{n'}^q\right\rangle(\boldsymbol{r}_p, \boldsymbol{r}_q; \xi_p) \mathrm{d}v_q = \left\langle d_n^p\right\rangle(\boldsymbol{r}_p; \xi_p),
$$

$$
p = 1, 2, \dots, N \quad (7.6)
$$

---

[2]The notation of the slab geometry in this paper differs slightly from the notation employed in Part II [13].
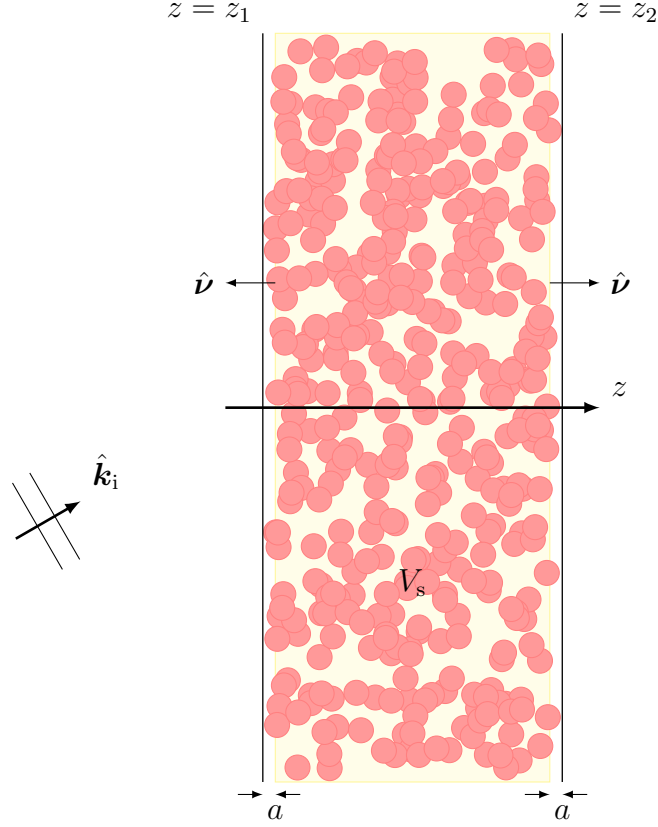
Figure 2: The geometry of the scattering region with randomly located scatterers. In three dimensions the spheres do not intersect. However in this two-dimensional graph some of the projections of the spheres overlap. The yellow region denotes the region V_s, which is the domain of possible locations of local origins, *i.e.*, the interval $[z_1 + a, z_2 - a]$.

where

$$\sum_{n''} \langle T^p_{nn''} A^{pq}_{n''n'} f^q_{n'} \rangle (\boldsymbol{r}_p, \boldsymbol{r}_q; \xi_p)$$

$$= \sum_{n''} T^p_{nn''}(\xi_p) \mathcal{P}_{n''n'}(k_2(\boldsymbol{r}_q - \boldsymbol{r}_p)) \langle f^q_{n'} \rangle (\boldsymbol{r}_p, \boldsymbol{r}_q; \xi_p)(1 - \delta_{pq})$$

$$+ \sum_{n''} T^p_{nn''}(\xi_p) \sum_{j=1,2} \iint_{\mathbb{R}^2} \frac{2}{k_2 k_{2_\mathrm{z}}}$$

$$\times \left\{ B^{+}_{n''j}{}^\dagger(\boldsymbol{k}_\mathrm{t}) \mathrm{e}^{\mathrm{i}\boldsymbol{k}_2^+ \cdot \boldsymbol{r}_p} \mathcal{R}^1_j(\boldsymbol{k}_\mathrm{t}) \frac{B^-_{n'j}(\boldsymbol{k}_\mathrm{t}) \mathrm{e}^{-\mathrm{i}\boldsymbol{k}_2^- \cdot \boldsymbol{r}_q} + R^2_j(\boldsymbol{k}_\mathrm{t}) B^+_{n'j}(\boldsymbol{k}_\mathrm{t}) \mathrm{e}^{-\mathrm{i}\boldsymbol{k}_2^+ \cdot \boldsymbol{r}_q}}{1 - \mathcal{R}^1_j(\boldsymbol{k}_\mathrm{t}) R^2_j(\boldsymbol{k}_\mathrm{t})} \right.$$

$$\left. + B^{-}_{n''j}{}^\dagger(\boldsymbol{k}_\mathrm{t}) \mathrm{e}^{\mathrm{i}\boldsymbol{k}_2^- \cdot \boldsymbol{r}_p} R^2_j(\boldsymbol{k}_\mathrm{t}) \frac{B^+_{n'j}(\boldsymbol{k}_\mathrm{t}) \mathrm{e}^{-\mathrm{i}\boldsymbol{k}_2^+ \cdot \boldsymbol{r}_q} + \mathcal{R}^1_j(\boldsymbol{k}_\mathrm{t}) B^-_{n'j}(\boldsymbol{k}_\mathrm{t}) \mathrm{e}^{-\mathrm{i}\boldsymbol{k}_2^- \cdot \boldsymbol{r}_q}}{1 - \mathcal{R}^1_j(\boldsymbol{k}_\mathrm{t}) R^2_j(\boldsymbol{k}_\mathrm{t})} \right\}$$

$$\times \, \mathrm{d}k_\mathrm{x} \, \mathrm{d}k_\mathrm{y} \, \langle f^q_{n'} \rangle (\boldsymbol{r}_p, \boldsymbol{r}_q; \xi_p)$$

and

$$\langle d_n^p \rangle (\boldsymbol{r}_p; \xi_p) = \sum_{n'} T_{nn'}^p(\xi_p) \sum_{j=1,2} \iint_{\mathbb{R}^2} \left\{ \frac{B_{n'j}^{+\,\dagger}(\boldsymbol{k}_{\mathrm{t}}) \mathrm{e}^{\mathrm{i}\boldsymbol{k}_2^+ \cdot \boldsymbol{r}_p}}{1 - \mathcal{R}_j^1(\boldsymbol{k}_{\mathrm{t}}) R_j^2(\boldsymbol{k}_{\mathrm{t}})} \right.$$

$$\left. + \frac{R_j^2(\boldsymbol{k}_{\mathrm{t}}) B_{n'j}^{-\,\dagger}(\boldsymbol{k}_{\mathrm{t}}) \mathrm{e}^{\mathrm{i}\boldsymbol{k}_2^- \cdot \boldsymbol{r}_p}}{1 - \mathcal{R}_j^1(\boldsymbol{k}_{\mathrm{t}}) R_j^2(\boldsymbol{k}_{\mathrm{t}})} \right\} T_j^1(\boldsymbol{k}_{\mathrm{t}}) a_j(\boldsymbol{k}_{\mathrm{t}}) \, \mathrm{d}k_{\mathrm{x}} \, \mathrm{d}k_{\mathrm{y}}$$

where, as above, $\boldsymbol{k}_2^\pm = \boldsymbol{k}_{\mathrm{t}} \pm k_{2\mathrm{z}}\hat{\boldsymbol{z}}$ and $k_{2\mathrm{z}} = (k_2^2 - k_{\mathrm{t}}^2)^{1/2}$.

7.2.1 Quasi Crystalline Approximations

In practice, higher order density functions are harder to obtain. To break the hierarchy in (7.6) Lax [29] introduced the Quasi Crystalline Approximation (QCA), which states that the conditional average with two positions held fixed, $\langle f_{n'}^q \rangle (\boldsymbol{r}_p, \boldsymbol{r}_q; \xi_p)$, is replaced with the conditional average with one position held fixed, $\langle f_{n'}^q \rangle (\boldsymbol{r}_q; \xi_p)$, i.e.,

$$\langle f_{n'}^q \rangle (\boldsymbol{r}_p, \boldsymbol{r}_q; \xi_p) \approx \langle f_{n'}^q \rangle (\boldsymbol{r}_q; \xi_p)$$

This approximation has been successfully applied in a range of concentrations from tenuous to dense media, and from the low-frequency to intermediate frequency range [66].

The Quasi Crystalline Approximation in (7.6) leads to a set of integral equations in the unknowns, $\langle f_n \rangle (\boldsymbol{r}'; \xi)$, viz., (the indices p and q are now superfluous and $\boldsymbol{r}_p$, $\boldsymbol{r}_q$, and ξ_p are dummy variables)

$$\langle f_n \rangle (\boldsymbol{r}; \xi) - k_2^3 \sum_{n'} \iiint_{V_{\mathrm{s}}} \mathcal{K}_{nn'}(\boldsymbol{r}, \boldsymbol{r}'; \xi) \langle f_{n'} \rangle (\boldsymbol{r}'; \xi) \, \mathrm{d}v' = \langle d_n \rangle (\boldsymbol{r}; \xi), \quad \boldsymbol{r} \in V_{\mathrm{s}} \quad (7.7)$$

where

$$\mathcal{K}_{nn'}(\boldsymbol{r}, \boldsymbol{r}'; \xi) = \frac{N-1}{k_2^3} P(\boldsymbol{r}'|\boldsymbol{r}) \sum_{n''} T_{nn''}(\xi) \mathcal{P}_{n''n'}(k_2(\boldsymbol{r}' - \boldsymbol{r}))$$

$$+ \frac{N}{k_2^3} P(\boldsymbol{r}'|\boldsymbol{r}) \sum_{n''} T_{nn''}(\xi) \sum_{j=1,2} \iint_{\mathbb{R}^2} \frac{2}{k_2 k_{2\mathrm{z}}}$$

$$\left\{ B_{n''j}^{+\,\dagger}(\boldsymbol{k}_{\mathrm{t}}) \mathrm{e}^{\mathrm{i}\boldsymbol{k}_2^+ \cdot \boldsymbol{r}} \mathcal{R}_j^1(\boldsymbol{k}_{\mathrm{t}}) \frac{B_{n'j}^-(\boldsymbol{k}_{\mathrm{t}}) \mathrm{e}^{-\mathrm{i}\boldsymbol{k}_2^- \cdot \boldsymbol{r}'} + R_j^2(\boldsymbol{k}_{\mathrm{t}}) B_{n'j}^+(\boldsymbol{k}_{\mathrm{t}}) \mathrm{e}^{-\mathrm{i}\boldsymbol{k}_2^+ \cdot \boldsymbol{r}'}}{1 - \mathcal{R}_j^1(\boldsymbol{k}_{\mathrm{t}}) R_j^2(\boldsymbol{k}_{\mathrm{t}})} \right.$$

$$\left. + B_{n''j}^{-\,\dagger}(\boldsymbol{k}_{\mathrm{t}}) \mathrm{e}^{\mathrm{i}\boldsymbol{k}_2^- \cdot \boldsymbol{r}} R_j^2(\boldsymbol{k}_{\mathrm{t}}) \frac{B_{n'j}^+(\boldsymbol{k}_{\mathrm{t}}) \mathrm{e}^{-\mathrm{i}\boldsymbol{k}_2^+ \cdot \boldsymbol{r}'} + \mathcal{R}_j^1(\boldsymbol{k}_{\mathrm{t}}) B_{n'j}^-(\boldsymbol{k}_{\mathrm{t}}) \mathrm{e}^{-\mathrm{i}\boldsymbol{k}_2^- \cdot \boldsymbol{r}'}}{1 - \mathcal{R}_j^1(\boldsymbol{k}_{\mathrm{t}}) R_j^2(\boldsymbol{k}_{\mathrm{t}})} \right\} \, \mathrm{d}k_{\mathrm{x}} \, \mathrm{d}k_{\mathrm{y}}$$

and

$$\langle d_n \rangle (\boldsymbol{r}; \xi) = \sum_{n'} T_{nn'}(\xi) \sum_{j=1,2} \iint_{\mathbb{R}^2} \left\{ \frac{{B_{n'j}^+}^\dagger(\boldsymbol{k}_\mathrm{t}) \mathrm{e}^{\mathrm{i}\boldsymbol{k}_2^+ \cdot \boldsymbol{r}}}{1 - \mathcal{R}_j^1(\boldsymbol{k}_\mathrm{t}) R_j^2(\boldsymbol{k}_\mathrm{t})} \right.$$

$$\left. + \frac{R_j^2(\boldsymbol{k}_\mathrm{t}) {B_{n'j}^-}^\dagger(\boldsymbol{k}_\mathrm{t}) \mathrm{e}^{\mathrm{i}\boldsymbol{k}_2^- \cdot \boldsymbol{r}}}{1 - \mathcal{R}_j^1(\boldsymbol{k}_\mathrm{t}) R_j^2(\boldsymbol{k}_\mathrm{t})} \right\} T_j^1(\boldsymbol{k}_\mathrm{t}) a_j(\boldsymbol{k}_\mathrm{t}) \, \mathrm{d}k_\mathrm{x} \, \mathrm{d}k_\mathrm{y}$$

Equation (7.7) is a system of integral equations for the unknown $\langle f_n \rangle (\boldsymbol{r}; \xi)$, which can be simplified under the assumption made in this paper. The state variable ξ acts as a parameter in this system of integral equations. To average over this state variable, we have to solve the system of integral equations for each value of the state variable ξ and then take the ensemble average of the state variable.

7.2.2 Plane wave incidence and uniform distribution of scatterers

In this paper, we apply the result to a plane wave incidence, *i.e.*,

$$\boldsymbol{E}_\mathrm{i}(\boldsymbol{r}) = \boldsymbol{E}_0 \mathrm{e}^{\mathrm{i}k_1 \hat{\boldsymbol{k}}_\mathrm{i} \cdot \boldsymbol{r}}$$

where the complex-valued vector $\boldsymbol{E}_0$ satisfies $\boldsymbol{E}_0 \cdot \hat{\boldsymbol{k}}_\mathrm{i} = 0$ and the real-valued incident direction $\hat{\boldsymbol{k}}_\mathrm{i}$ satisfies $\hat{\boldsymbol{k}}_\mathrm{i} \cdot \hat{\boldsymbol{z}} > 0$. The explicit form of the expansion function $a_j(\boldsymbol{k}_\mathrm{t})$ for a plane wave incident field is

$$a_j(\boldsymbol{k}_\mathrm{t}) = \delta(\boldsymbol{k}_\mathrm{t} - \boldsymbol{k}_\mathrm{it}) A_j \tag{7.8}$$

The factor A_j is a short-hand notation for

$$A_j = 4\pi \boldsymbol{E}_0 \cdot \left\{ \begin{array}{ll} -\dfrac{\hat{\boldsymbol{z}} \times \boldsymbol{k}_\mathrm{it}}{\mathrm{i}k_\mathrm{it}}, & j = 1 \\[2ex] \dfrac{\hat{\boldsymbol{z}} k_\mathrm{it}^2 - \boldsymbol{k}_\mathrm{it} k_{1\mathrm{iz}}}{k_1 k_\mathrm{it}}, & j = 2 \end{array} \right\}$$

where $\boldsymbol{k}_\mathrm{it} = k_1 (\hat{\boldsymbol{x}}\hat{\boldsymbol{x}} + \hat{\boldsymbol{y}}\hat{\boldsymbol{y}}) \cdot \hat{\boldsymbol{k}}_\mathrm{i} = k_1 \mathbf{I}_2 \cdot \hat{\boldsymbol{k}}_\mathrm{i}$, $k_{1\mathrm{iz}} = \left(k_1^2 - k_\mathrm{it}^2\right)^{1/2}$ and $k_\mathrm{it} = |\boldsymbol{k}_\mathrm{it}|$. The delta function implies that the $\boldsymbol{k}_\mathrm{t} = \boldsymbol{k}_\mathrm{it}$ everywhere. This is usually called Snell's law. To derive the factor A_j we have used the dyadic identity

$$\mathbf{I}_3 - \hat{\boldsymbol{k}}\hat{\boldsymbol{k}} = \frac{\hat{\boldsymbol{z}} \times \boldsymbol{k}_\mathrm{t}}{k_\mathrm{t}} \frac{\hat{\boldsymbol{z}} \times \boldsymbol{k}_\mathrm{t}}{k_\mathrm{t}} + \frac{(\boldsymbol{k}_\mathrm{t} + k_\mathrm{z}\hat{\boldsymbol{z}}) \times (\hat{\boldsymbol{z}} \times \boldsymbol{k}_\mathrm{t})}{k_1 k_\mathrm{t}} \frac{(\boldsymbol{k}_\mathrm{t} + k_\mathrm{z}\hat{\boldsymbol{z}}) \times (\hat{\boldsymbol{z}} \times \boldsymbol{k}_\mathrm{t})}{k_1 k_\mathrm{t}}$$

For a plane wave incidence, the excitation term simplifies

$$\langle d_n \rangle (\boldsymbol{r}; \xi) = d_n(z; \xi) \mathrm{e}^{\mathrm{i}\boldsymbol{k}_\mathrm{it} \cdot \boldsymbol{r}_\mathrm{c}} = \mathrm{e}^{\mathrm{i}\boldsymbol{k}_\mathrm{it} \cdot \boldsymbol{r}_\mathrm{c}} \sum_{n'} T_{nn'}(\xi) \sum_{j=1,2} T_j^1(\boldsymbol{k}_\mathrm{it}) A_j$$

$$\times \frac{{B_{n'j}^+}^\dagger(\boldsymbol{k}_\mathrm{it}) \mathrm{e}^{\mathrm{i}k_{2\mathrm{iz}}z} + R_j^2(\boldsymbol{k}_\mathrm{it}) {B_{n'j}^-}^\dagger(\boldsymbol{k}_\mathrm{it}) \mathrm{e}^{-\mathrm{i}k_{2\mathrm{iz}}z}}{1 - \mathcal{R}_j^1(\boldsymbol{k}_\mathrm{it}) R_j^2(\boldsymbol{k}_\mathrm{it})} \tag{7.9}$$

where $\boldsymbol{r}_\mathrm{c} = x\hat{\boldsymbol{x}} + y\hat{\boldsymbol{y}}$ and $k_{2\mathrm{iz}} = (k_2^2 - |\boldsymbol{k}_{\mathrm{it}}|^2)^{1/2}$.

If the scatterers are randomly distributed within the volume between the planes, the solution of the problem shows lateral invariance, which implies that the coefficients must have the form $\langle f_n \rangle (\boldsymbol{r}) = f_n(z)\mathrm{e}^{\mathrm{i}\boldsymbol{k}_{\mathrm{it}}\cdot\boldsymbol{r}_\mathrm{c}}$, where $f_n(z)$ only depends on the depth z of the slab.[3] The integral equation (7.7) then has the form (for simplicity, we suppress the state variable ξ which acts as a parameter)

$$f_n(z) - k_2 \sum_{n'} \int_{z_1+a}^{z_2-a} K_{nn'}(z, z') f_n(z')\,\mathrm{d}z' = d_n(z), \quad z \in [z_1 + a, z_2 - a]$$

(7.10)

where $a = \max_p A_p$, and where

$$K_{nn'}(z, z') = k_2^2 \iint_{\mathbb{R}^2} \mathcal{K}_{nn'}(\boldsymbol{r}, \boldsymbol{r}')\mathrm{e}^{\mathrm{i}\boldsymbol{k}_{\mathrm{it}}\cdot(\boldsymbol{r}_\mathrm{c}{}'-\boldsymbol{r}_\mathrm{c})}\,\mathrm{d}x'\,\mathrm{d}y'$$

Note that, due to invariance under translation in the lateral variables, this expression of the kernel does not depend on $\boldsymbol{r}_\mathrm{c}$, see the explicit expression below. The explicit expression of $K_{nn'}(z, z')$ is ($N \to \infty$ is assumed)

$$\begin{aligned}
K_{nn'}(z, z') = \frac{n_0}{k_2} \sum_{n''} T_{nn''} &\iint_{\mathbb{R}^2} \left\{ \mathrm{e}^{\mathrm{i}\boldsymbol{k}_{\mathrm{it}}\cdot\boldsymbol{r}_\mathrm{c}{}'} \mathcal{P}_{n''n'}(k_2(\boldsymbol{r}_\mathrm{c}{}' + \hat{\boldsymbol{z}}(z' - z))) \right. \\
&+ \sum_{j=1,2} \iint_{\mathbb{R}^2} \frac{2}{k_2 k_{2\mathrm{z}}} \mathrm{e}^{\mathrm{i}(\boldsymbol{k}_{\mathrm{it}} - \boldsymbol{k}_\mathrm{t})\cdot\boldsymbol{r}_\mathrm{c}{}'} \\
&\times \left\{ {B_{n''j}^{+}}^{\dagger}(\boldsymbol{k}_\mathrm{t}) \mathcal{R}_j^1(\boldsymbol{k}_\mathrm{t})\mathrm{e}^{\mathrm{i}k_{2\mathrm{z}}z} \frac{B_{n'j}^{-}(\boldsymbol{k}_\mathrm{t})\mathrm{e}^{\mathrm{i}k_{2\mathrm{z}}z'} + R_j^2(\boldsymbol{k}_\mathrm{t})B_{n'j}^{+}(\boldsymbol{k}_\mathrm{t})\mathrm{e}^{-\mathrm{i}k_{2\mathrm{z}}z'}}{1 - \mathcal{R}_j^1(\boldsymbol{k}_\mathrm{t})R_j^2(\boldsymbol{k}_\mathrm{t})} \right. \\
&+ {B_{n''j}^{-}}^{\dagger}(\boldsymbol{k}_\mathrm{t}) R_j^2(\boldsymbol{k}_\mathrm{t})\mathrm{e}^{-\mathrm{i}k_{2\mathrm{z}}z} \\
&\left. \times \frac{B_{n'j}^{+}(\boldsymbol{k}_\mathrm{t})\mathrm{e}^{-\mathrm{i}k_{2\mathrm{z}}z'} + \mathcal{R}_j^1(\boldsymbol{k}_\mathrm{t})B_{n'j}^{-}(\boldsymbol{k}_\mathrm{t})\mathrm{e}^{\mathrm{i}k_{2\mathrm{z}}z'}}{1 - \mathcal{R}_j^1(\boldsymbol{k}_\mathrm{t})R_j^2(\boldsymbol{k}_\mathrm{t})} \right\} \mathrm{d}k_\mathrm{x}\,\mathrm{d}k_\mathrm{y} \left.\vphantom{\iint}\right\} \\
&\times g(|\boldsymbol{r}_\mathrm{c}{}' + \hat{\boldsymbol{z}}(z' - z)|)\,\mathrm{d}x'\,\mathrm{d}y'
\end{aligned}$$

where we expressed the conditional probability density $P(\boldsymbol{r}'|\boldsymbol{r})$ in terms of the pair distribution function $g(\boldsymbol{r}, \boldsymbol{r}')$, i.e., $(N-1)P(\boldsymbol{r}'|\boldsymbol{r}) = n_0 g(\boldsymbol{r}, \boldsymbol{r}')$, see (E.3). Moreover, for symmetric scatterers, the pair distribution function depends only on the distance between two scatterers $|\boldsymbol{r} - \boldsymbol{r}'|$, i.e., $g(\boldsymbol{r}, \boldsymbol{r}') = g(|\boldsymbol{r} - \boldsymbol{r}|)$, and the spatial integral is invariant w.r.t. lateral translations. The assumption $N \to \infty$ simplifies the factor $N/(N-1) \to 1$ that occurs in the second term.

---

[3]We require the integrand to vanish in an appropriate way as the lateral variables, x and y, approach infinity. One way to accomplish this is to assume an infinitely small positive imaginary part of the wave number k.

At this point, it is convenient to simplify the notation by introducing the following dimension-less quantities:

$$C_{nn'}(\boldsymbol{k}_{\mathrm{t}}; z) = k_2^2 \iint\limits_{\mathbb{R}^2} g(|\boldsymbol{r}_{\mathrm{c}} - \hat{\boldsymbol{z}} z|) \mathcal{P}_{nn'}(k_2(\boldsymbol{r}_{\mathrm{c}} - \hat{\boldsymbol{z}} z)) \mathrm{e}^{\mathrm{i}\boldsymbol{k}_{\mathrm{t}} \cdot \boldsymbol{r}_{\mathrm{c}}} \, \mathrm{d}x \, \mathrm{d}y, \quad |z| \le z_2 - z_1 - 2a$$

(7.11)

and the lateral Fourier transform of the pair correlation function

$$G(\boldsymbol{k}_{\mathrm{t}}; z) = k_2^2 \iint\limits_{\mathbb{R}^2} g(|\boldsymbol{r}_{\mathrm{c}} - \hat{\boldsymbol{z}} z|) \mathrm{e}^{-\mathrm{i}\boldsymbol{k}_{\mathrm{t}} \cdot \boldsymbol{r}_{\mathrm{c}}} \, \mathrm{d}x \, \mathrm{d}y, \quad |z| \le z_2 - z_1 - 2a \qquad (7.12)$$

The simplest model for the pair correlation function $g(r)$ is the hole correction function, *i.e.*, $g(r) = \mathrm{H}(r - 2a)$, where $\mathrm{H}(x)$ denotes the Heaviside function. The function $C_{nn'}(\boldsymbol{0}; z)$ in (7.11) is investigated in Ref. 23.

$$C_{nn'}(\boldsymbol{0}; z) = \sum_{\lambda = |l - l'| + |\tau - \tau'|}^{l + l'} I_\lambda(-z) \mathcal{A}_{nn'\lambda} \qquad (7.13)$$

where $\mathcal{A}_{nn'\lambda}$ is the azimuthal average of the translation matrix $\mathcal{P}_{nn'}(k\boldsymbol{r})$, which are explicitly evaluated in Appendix B.1, and where the important integral $I_\lambda(z)$ is [24]

$$I_l(z) = k_2^2 \int_{d(z)}^\infty g(|\boldsymbol{r}_{\mathrm{c}} + z\hat{\boldsymbol{z}}|) h_l^{(1)}(k_2 \sqrt{r_{\mathrm{c}}^2 + z^2}) P_l(z / \sqrt{r_{\mathrm{c}}^2 + z^2}) r_{\mathrm{c}} \, \mathrm{d}r_{\mathrm{c}}, \quad z \in \mathbb{R}$$

where

$$d(z) = \begin{cases} \sqrt{4a^2 - z^2}, & -2a \le z \le 2a \\ 0, & |z| > 2a \end{cases}$$

Some effective iteration schemes to compute the integrals $I_\lambda(z)$ are presented in [24].

The lateral Fourier transform of the pair correlation function, see (7.12), or the hole correction becomes

$$G(\boldsymbol{k}_{\mathrm{t}}; z) = k_2^2 \iint\limits_{\mathbb{R}^2} \mathrm{H}(|\boldsymbol{r}_{\mathrm{c}} - \hat{\boldsymbol{z}} z| - 2a) \mathrm{e}^{-\mathrm{i}\boldsymbol{k}_{\mathrm{t}} \cdot \boldsymbol{r}_{\mathrm{c}}} \, \mathrm{d}x \, \mathrm{d}y$$

$$= 4\pi^2 k_2^2 \delta(\boldsymbol{k}_{\mathrm{t}}) - k_2^2 \int_0^{2\pi} \int_0^{d(z)} \mathrm{e}^{-\mathrm{i}\boldsymbol{k}_{\mathrm{t}} \cdot \boldsymbol{r}_{\mathrm{c}}} r_{\mathrm{c}} \, \mathrm{d}r_{\mathrm{c}} \, \mathrm{d}\phi$$

$$= 4\pi^2 k_2^2 \delta(\boldsymbol{k}_{\mathrm{t}}) - 2\pi k_2^2 \int_0^{d(z)} J_0(k_{\mathrm{t}} r_{\mathrm{c}}) r_{\mathrm{c}} \, \mathrm{d}r_{\mathrm{c}}$$

$$= 4\pi^2 k_2^2 \delta(\boldsymbol{k}_{\mathrm{t}}) - 2\pi (k_2 d(z))^2 \frac{J_1(k_{\mathrm{t}} d(z))}{k_{\mathrm{t}} d(z)}, \quad |z| \le z_2 - z_1 - 2a$$

where

$$d(z) = \begin{cases} \sqrt{4a^2 - z^2}, & -2a \le z \le 2a \\ 0, & |z| > 2a \end{cases}$$

In this new notation, the kernel $K_{nn'}(z, z')$ reads

$$
K_{nn'}(z, z') = \frac{n_0}{k_2^3} \sum_{n''} T_{nn''} \Bigg\{ C_{n''n'}(\boldsymbol{k}_{\mathrm{it}}; z - z') + \sum_{j=1,2} \iint_{\mathbb{R}^2} \frac{2G(\boldsymbol{k}_{\mathrm{t}} - \boldsymbol{k}_{\mathrm{it}}; z - z')}{k_2 k_{2\mathrm{z}}}
$$
$$
\times \Bigg\{ B_{n''j}^{+\,\dagger}(\boldsymbol{k}_{\mathrm{t}}) \mathcal{R}_j^1(\boldsymbol{k}_{\mathrm{t}}) \mathrm{e}^{\mathrm{i}k_{2\mathrm{z}}z} \frac{B_{n'j}^-(\boldsymbol{k}_{\mathrm{t}})\mathrm{e}^{\mathrm{i}k_{2\mathrm{z}}z'} + R_j^2(\boldsymbol{k}_{\mathrm{t}})B_{n'j}^+(\boldsymbol{k}_{\mathrm{t}})\mathrm{e}^{-\mathrm{i}k_{2\mathrm{z}}z'}}{1 - \mathcal{R}_j^1(\boldsymbol{k}_{\mathrm{t}})R_j^2(\boldsymbol{k}_{\mathrm{t}})}
$$
$$
+ B_{n''j}^{-\,\dagger}(\boldsymbol{k}_{\mathrm{t}})R_j^2(\boldsymbol{k}_{\mathrm{t}})\mathrm{e}^{-\mathrm{i}k_{2\mathrm{z}}z} \frac{B_{n'j}^+(\boldsymbol{k}_{\mathrm{t}})\mathrm{e}^{-\mathrm{i}k_{2\mathrm{z}}z'} + \mathcal{R}_j^1(\boldsymbol{k}_{\mathrm{t}})B_{n'j}^-(\boldsymbol{k}_{\mathrm{t}})\mathrm{e}^{\mathrm{i}k_{2\mathrm{z}}z'}}{1 - \mathcal{R}_j^1(\boldsymbol{k}_{\mathrm{t}})R_j^2(\boldsymbol{k}_{\mathrm{t}})} \Bigg\} \, \mathrm{d}k_{\mathrm{x}} \, \mathrm{d}k_{\mathrm{y}} \Bigg\} \quad (7.14)
$$

The plane wave incidence also simplifies the evaluation of $\langle F_j^\pm(\boldsymbol{k}_{\mathrm{t}}) \rangle$ in (7.5).

$$
\langle F_j^\pm(\boldsymbol{k}_{\mathrm{t}}) \rangle = \frac{2n_0}{k_2 k_{2\mathrm{z}}} \sum_n B_{nj}^\pm(\boldsymbol{k}_{\mathrm{t}}) \iiint_{V_{\mathrm{s}}} f_n(z)\mathrm{e}^{\mathrm{i}\boldsymbol{k}_{\mathrm{it}}\cdot\boldsymbol{r}_{\mathrm{c}} - \mathrm{i}\boldsymbol{k}_2^\pm\cdot\boldsymbol{r}} \, \mathrm{d}\upsilon
$$
$$
= \frac{8\pi^2 n_0 \delta(\boldsymbol{k}_{\mathrm{t}} - \boldsymbol{k}_{\mathrm{it}})}{k_2 k_{2\mathrm{iz}}} \sum_n B_{nj}^\pm(\boldsymbol{k}_{\mathrm{it}}) \int_{z_1+a}^{z_2-a} f_n(z)\mathrm{e}^{\mp\mathrm{i}k_{2\mathrm{iz}}z} \, \mathrm{d}z
$$
$$
= \frac{8\pi^2 n_0 \delta(\boldsymbol{k}_{\mathrm{t}} - \boldsymbol{k}_{\mathrm{it}})}{k_2 k_{2\mathrm{iz}}} C_j^\pm(\boldsymbol{k}_{\mathrm{it}})
$$

where

$$
C_j^\pm(\boldsymbol{k}_{\mathrm{it}}) = \sum_n B_{nj}^\pm(\boldsymbol{k}_{\mathrm{it}}) \int_{z_1+a}^{z_2-a} f_n(z)\mathrm{e}^{\mp\mathrm{i}k_{2\mathrm{iz}}z} \, \mathrm{d}z
$$

From (7.3) and (7.4), we obtain

$$
\langle t_j(\boldsymbol{k}_{\mathrm{t}}) \rangle = T_j^2(\boldsymbol{k}_{\mathrm{it}}) \frac{8\pi^2 n_0 \delta(\boldsymbol{k}_{\mathrm{t}} - \boldsymbol{k}_{\mathrm{it}})}{k_2 k_{2\mathrm{iz}}} \frac{\mathcal{R}_j^1(\boldsymbol{k}_{\mathrm{it}})C_j^-(\boldsymbol{k}_{\mathrm{it}}) + C_j^+(\boldsymbol{k}_{\mathrm{it}})}{1 - \mathcal{R}_j^1(\boldsymbol{k}_{\mathrm{it}})R_j^2(\boldsymbol{k}_{\mathrm{it}})}
$$
$$
+ T_j(\boldsymbol{k}_{\mathrm{it}})A_j\delta(\boldsymbol{k}_{\mathrm{t}} - \boldsymbol{k}_{\mathrm{it}}), \quad \boldsymbol{k}_{\mathrm{t}} \in \mathbb{R}^2, \ j = 1, 2
$$

and

$$
\langle r_j(\boldsymbol{k}_{\mathrm{t}}) \rangle = \mathcal{T}_j^1(\boldsymbol{k}_{\mathrm{it}}) \frac{8\pi^2 n_0 \delta(\boldsymbol{k}_{\mathrm{t}} - \boldsymbol{k}_{\mathrm{it}})}{k_2 k_{2\mathrm{iz}}} \frac{C_j^-(\boldsymbol{k}_{\mathrm{it}}) + R_j^2(\boldsymbol{k}_{\mathrm{it}})C_j^+(\boldsymbol{k}_{\mathrm{it}})}{1 - \mathcal{R}_j^1(\boldsymbol{k}_{\mathrm{it}})R_j^2(\boldsymbol{k}_{\mathrm{it}})}
$$
$$
+ R_j(\boldsymbol{k}_{\mathrm{it}})A_j\delta(\boldsymbol{k}_{\mathrm{t}} - \boldsymbol{k}_{\mathrm{it}}), \quad \boldsymbol{k}_{\mathrm{t}} \in \mathbb{R}^2, \ j = 1, 2
$$

and the transmitted and the reflected fields in (7.1) and (7.2) are

$$
\langle \boldsymbol{E}_{\mathrm{t}}(\boldsymbol{r}) \rangle = \frac{8\pi^2 n_0}{k_2 k_{2\mathrm{iz}}} \sum_{j=1,2} T_j^2(\boldsymbol{k}_{\mathrm{it}}) \frac{\mathcal{R}_j^1(\boldsymbol{k}_{\mathrm{it}})C_j^-(\boldsymbol{k}_{\mathrm{it}}) + C_j^+(\boldsymbol{k}_{\mathrm{it}})}{1 - \mathcal{R}_j^1(\boldsymbol{k}_{\mathrm{it}})R_j^2(\boldsymbol{k}_{\mathrm{it}})} \boldsymbol{\varphi}_j^+(\boldsymbol{k}_{\mathrm{it}}; k_3, \boldsymbol{r})
$$
$$
+ \sum_{j=1,2} T_j(\boldsymbol{k}_{\mathrm{it}})A_j\boldsymbol{\varphi}_j^+(\boldsymbol{k}_{\mathrm{it}}; k_3, \boldsymbol{r}), \quad z > z_2
$$

$$(7.15)$$

and

$$\langle \boldsymbol{E}_{\mathrm{r}}(\boldsymbol{r}) \rangle = \frac{8\pi^2 n_0}{k_2 k_{2\mathrm{iz}}} \sum_{j=1,2} \mathcal{T}_j^1(\boldsymbol{k}_{\mathrm{it}}) \frac{C_j^-(\boldsymbol{k}_{\mathrm{it}}) + R_j^2(\boldsymbol{k}_{\mathrm{it}}) C_j^+(\boldsymbol{k}_{\mathrm{it}})}{1 - \mathcal{R}_j^1(\boldsymbol{k}_{\mathrm{it}}) R_j^2(\boldsymbol{k}_{\mathrm{it}})} \boldsymbol{\varphi}_j^-(\boldsymbol{k}_{\mathrm{it}}; k_1, \boldsymbol{r})$$
$$+ \sum_{j=1,2} R_j(\boldsymbol{k}_{\mathrm{it}}) A_j \boldsymbol{\varphi}_j^-(\boldsymbol{k}_{\mathrm{it}}; k_1, \boldsymbol{r}), \quad z < z_1 \tag{7.16}$$

Both expressions of the transmitted and reflected fields contain one deterministic contribution of the slab itself without scatterers, and one stochastic contribution from the scatterers and their interactions with the slab boundaries and all other scatterers. The latter effects are contained in $C_j^{\pm}(\boldsymbol{k}_{\mathrm{it}})$.

8 Special cases

There are a few special cases of the general result in Section 7 that are worth special investigations. We identify three special cases: 1) the scatterers lie below a homogeneous half space with sources in the other half space, *i.e.*, the material parameters are $\epsilon_2 = \epsilon_3$ and $\mu_2 = \mu_3$, 2) the scatterers lie above a homogeneous half space and in the same half space as the sources, *i.e.*, the material parameters are $\epsilon_2 = \epsilon_1$ and $\mu_2 = \mu_1$, 3) the surface S_2 is a perfectly electric conducting (PEC) surface. Moreover, the absence of a slab background, *i.e.*, the background is homogeneous, $\epsilon_1 = \epsilon_2 = \epsilon_3$ and $\mu_1 = \mu_2 = \mu_3$, recovers the result in [23]. In the subsections below, we exploit these we special cases one by one.

8.1 Scatterers in a half space I

In this section, we show the result for the special case when the material parameters $\epsilon_2 = \epsilon_3$ and $\mu_2 = \mu_3$. This correspond to a geometry when the scatterers are located in a homogeneous half space with sources in the other half space. This special case correspond to letting $R_j^2(\boldsymbol{k}_{\mathrm{it}}) = 0$ and $T_j^2(\boldsymbol{k}_{\mathrm{it}}) = 1$.

From (7.15) and (7.16), we get the transmitted and the reflected fields for this special case. To the right of all scatterers, $z > z_2$, we have

$$\langle \boldsymbol{E}_{\mathrm{t}}(\boldsymbol{r}) \rangle = \sum_{j=1,2} \left\{ \frac{8\pi^2 n_0}{k_2 k_{2\mathrm{iz}}} \left(\mathcal{R}_j^1(\boldsymbol{k}_{\mathrm{it}}) C_j^-(\boldsymbol{k}_{\mathrm{it}}) + C_j^+(\boldsymbol{k}_{\mathrm{it}}) \right) + T_j^1(\boldsymbol{k}_{\mathrm{it}}) A_j \right\} \boldsymbol{\varphi}_j^+(\boldsymbol{k}_{\mathrm{it}}; k_2, \boldsymbol{r})$$

and

$$\langle \boldsymbol{E}_{\mathrm{r}}(\boldsymbol{r}) \rangle = \sum_{j=1,2} \left\{ \frac{8\pi^2 n_0}{k_2 k_{2\mathrm{iz}}} \mathcal{T}_j^1(\boldsymbol{k}_{\mathrm{it}}) C_j^-(\boldsymbol{k}_{\mathrm{it}}) + R_j^1(\boldsymbol{k}_{\mathrm{it}}) A_j \right\} \boldsymbol{\varphi}_j^-(\boldsymbol{k}_{\mathrm{it}}; k_1, \boldsymbol{r}), \quad z < z_1$$

The kernel in the system of integral equations in (7.7) simplifies to

$$\mathcal{K}_{nn'}(\boldsymbol{r}, \boldsymbol{r}'; \xi) = \frac{N-1}{k_2^3} P(\boldsymbol{r}'|\boldsymbol{r}) \sum_{n''} T_{nn''}(\xi) \mathcal{P}_{n''n'}(k_2(\boldsymbol{r}' - \boldsymbol{r}))$$

$$+ \frac{N}{k_2^3} P(\boldsymbol{r}'|\boldsymbol{r}) \sum_{n''} T_{nn''}(\xi) \sum_{j=1,2} \iint_{\mathbb{R}^2} \frac{2{B_{n''j}^+}^\dagger(\boldsymbol{k}_\text{t}) \mathrm{e}^{\mathrm{i}\boldsymbol{k}_2^+ \cdot \boldsymbol{r}}}{k_2 k_{2\text{z}}} \mathcal{R}_j^1(\boldsymbol{k}_\text{t}) B_{n'j}^-(\boldsymbol{k}_\text{t}) \mathrm{e}^{-\mathrm{i}\boldsymbol{k}_2^- \cdot \boldsymbol{r}'} \, \mathrm{d}k_\text{x} \, \mathrm{d}k_\text{y}$$

and the right-hand side simplifies to

$$\langle d_n \rangle (\boldsymbol{r}; \xi) = \sum_{n'} T_{nn'}(\xi) \sum_{j=1,2} \iint_{\mathbb{R}^2} {B_{n'j}^+}^\dagger(\boldsymbol{k}_\text{t}) \mathrm{e}^{\mathrm{i}\boldsymbol{k}_2^+ \cdot \boldsymbol{r}} T_j^1(\boldsymbol{k}_\text{t}) a_j(\boldsymbol{k}_\text{t}) \, \mathrm{d}k_\text{x} \, \mathrm{d}k_\text{y}$$

8.2   Scatterers in a half space II

If the scatterers lie in the same half space as the sources, we let the material parameters $\epsilon_2 = \epsilon_1$ and $\mu_2 = \mu_1$. This special case correspond to letting $R_j^1(\boldsymbol{k}_\text{it}) = 0$, $T_j^1(\boldsymbol{k}_\text{it}) = 1$, $\mathcal{R}_j^1(\boldsymbol{k}_\text{it}) = 0$, and $\mathcal{T}_j^1(\boldsymbol{k}_\text{it}) = 1$. From (7.15) and (7.16), we get the transmitted and the reflected fields.

$$\langle \boldsymbol{E}_\text{t}(\boldsymbol{r}) \rangle = \sum_{j=1,2} T_j^2(\boldsymbol{k}_\text{it}) \left\{ \frac{8\pi^2 n_0}{k_2 k_{2\text{iz}}} C_j^+(\boldsymbol{k}_\text{it}) + A_j \right\} \boldsymbol{\varphi}_j^+(\boldsymbol{k}_\text{it}; k_3, \boldsymbol{r}), \quad z > z_2$$

and in the left half space to the left of all scatterers, $z < z_1$

$$\langle \boldsymbol{E}_\text{r}(\boldsymbol{r}) \rangle = \sum_{j=1,2} \left\{ \frac{8\pi^2 n_0}{k_2 k_{2\text{iz}}} \left(C_j^-(\boldsymbol{k}_\text{it}) + R_j^2(\boldsymbol{k}_\text{it}) C_j^+(\boldsymbol{k}_\text{it}) \right) + R_j^2(\boldsymbol{k}_\text{it}) A_j \right\} \boldsymbol{\varphi}_j^-(\boldsymbol{k}_\text{it}; k_1, \boldsymbol{r})$$

The kernel in the system of integral equations in (7.7) simplifies to

$$\mathcal{K}_{nn'}(\boldsymbol{r}, \boldsymbol{r}'; \xi) = \frac{N-1}{k_2^3} P(\boldsymbol{r}'|\boldsymbol{r}) \sum_{n''} T_{nn''}(\xi) \mathcal{P}_{n''n'}(k_2(\boldsymbol{r}' - \boldsymbol{r}))$$

$$+ \frac{N}{k_2^3} P(\boldsymbol{r}'|\boldsymbol{r}) \sum_{n''} T_{nn''}(\xi) \sum_{j=1,2} \iint_{\mathbb{R}^2} \frac{2{B_{n''j}^-}^\dagger(\boldsymbol{k}_\text{t}) \mathrm{e}^{\mathrm{i}\boldsymbol{k}_2^- \cdot \boldsymbol{r}}}{k_2 k_{2\text{z}}} R_j^2(\boldsymbol{k}_\text{t}) B_{n'j}^+(\boldsymbol{k}_\text{t}) \mathrm{e}^{-\mathrm{i}\boldsymbol{k}_2^+ \cdot \boldsymbol{r}'} \, \mathrm{d}k_\text{x} \, \mathrm{d}k_\text{y}$$

and the right-hand side simplifies to

$$\langle d_n \rangle (\boldsymbol{r}; \xi) = \sum_{n'} T_{nn'}(\xi) \sum_{j=1,2} \iint_{\mathbb{R}^2} \left\{ {B_{n'j}^+}^\dagger(\boldsymbol{k}_\text{t}) \mathrm{e}^{\mathrm{i}\boldsymbol{k}_2^+ \cdot \boldsymbol{r}} \right.$$

$$\left. + R_j^2(\boldsymbol{k}_\text{t}) {B_{n'j}^-}^\dagger(\boldsymbol{k}_\text{t}) \mathrm{e}^{\mathrm{i}\boldsymbol{k}_2^- \cdot \boldsymbol{r}} \right\} a_j(\boldsymbol{k}_\text{t}) \, \mathrm{d}k_\text{x} \, \mathrm{d}k_\text{y}$$

8.3 Perfectly conducting surface

From an application point of view, the special case of a perfectly electric conductive surface S_2 is of interest. This special case corresponds to letting the reflection coefficient $R_j^2(\boldsymbol{k}_{\text{it}}) = (-1)^j e^{2ik_{2\text{iz}}z_2}$ and the transmission coefficient $T_j^2(\boldsymbol{k}_{\text{it}}) = 0$. The reflected field is relevant in this special case, while the transmitted field is inaccessible. From (7.16), we get

$$\langle \boldsymbol{E}_{\text{r}}(\boldsymbol{r})\rangle = \sum_{j=1,2}\left\{\frac{8\pi^2 n_0}{k_2 k_{2\text{iz}}}\mathcal{T}_j^1(\boldsymbol{k}_{\text{it}})\frac{C_j^-(\boldsymbol{k}_{\text{it}}) + (-1)^j e^{2ik_{2\text{iz}}z_2}C_j^+(\boldsymbol{k}_{\text{it}})}{1-(-1)^j e^{2ik_{2\text{iz}}z_2}\mathcal{R}_j^1(\boldsymbol{k}_{\text{it}})}\right.$$
$$\left. + R_j(\boldsymbol{k}_{\text{it}})A_j\right\}\boldsymbol{\varphi}_j^-(\boldsymbol{k}_{\text{it}};k_1,\boldsymbol{r}), \quad z < z_1$$

8.4 Homogeneous background

With a homogeneous background, i.e., $\epsilon_1 = \epsilon_2 = \epsilon_3$ and $\mu_1 = \mu_2 = \mu_3$, which imply $R_j^{1,2}(\boldsymbol{k}_{\text{t}}) = 0$ and $T_j^{1,2}(\boldsymbol{k}_{\text{t}}) = 1$ and $k_1 = k_2 = k_3$. The transmitted and the reflected fields are, see (7.15) and (7.16)

$$\langle \boldsymbol{E}_{\text{t}}(\boldsymbol{r})\rangle = \sum_{j=1,2}\left\{\frac{8\pi^2 n_0}{k_1 k_{1\text{iz}}}C_j^+(\boldsymbol{k}_{\text{it}}) + A_j\right\}\boldsymbol{\varphi}_j^+(\boldsymbol{k}_{\text{it}};k_1,\boldsymbol{r}), \quad z > z_2$$

and

$$\langle \boldsymbol{E}_{\text{r}}(\boldsymbol{r})\rangle = \sum_{j=1,2}\frac{8\pi^2 n_0}{k_1 k_{1\text{iz}}}C_j^-(\boldsymbol{k}_{\text{it}})\boldsymbol{\varphi}_j^-(\boldsymbol{k}_{\text{it}};k_1,\boldsymbol{r}), \quad z < z_1$$

and where

$$C_j^{\pm}(\boldsymbol{k}_{\text{it}}) = \sum_n B_{nj}^{\pm}(\boldsymbol{k}_{\text{it}})\int_{z_1+a}^{z_2-a} f_n(z)e^{\mp ik_{1\text{iz}}z}\,\mathrm{d}z$$

The kernel in the system of integral equations in (7.7) simplifies to

$$\mathcal{K}_{nn'}(\boldsymbol{r},\boldsymbol{r}';\xi) = \frac{N-1}{k_1^3}P(\boldsymbol{r}'|\boldsymbol{r})\sum_{n''}T_{nn''}(\xi)\mathcal{P}_{n''n'}(k_2(\boldsymbol{r}'-\boldsymbol{r}))$$
$$= \frac{g(\boldsymbol{r},\boldsymbol{r}')n_0}{k_1^3}\sum_{n''}T_{nn''}(\xi)\mathcal{P}_{n''n'}(k_2(\boldsymbol{r}'-\boldsymbol{r}))$$

where we used the pair correlation function in (E.3), and the right-hand side simplifies to

$$\langle d_n\rangle(\boldsymbol{r};\xi) = \sum_{n'}T_{nn'}(\xi)\sum_{j=1,2}\iint_{\mathbb{R}^2}B_{n'j}^{+\dagger}(\boldsymbol{k}_{\text{t}})e^{i\boldsymbol{k}_1^+\cdot\boldsymbol{r}}a_j(\boldsymbol{k}_{\text{t}})\,\mathrm{d}k_{\text{x}}\,\mathrm{d}k_{\text{y}}$$

which for a plane wave becomes, see above (7.8)

$$\langle d_n\rangle(\boldsymbol{r};\xi) = \sum_{n'}T_{nn'}(\xi)e^{ik_1\hat{\boldsymbol{k}}_{\text{i}}\cdot\boldsymbol{r}_p}\sum_{j=1,2}B_{nj}^+(\boldsymbol{k}_{\text{it}})(-1)^{l+\tau+j+1}A_j$$
$$= \sum_{n'}T_{nn'}(\xi)e^{ik_1\hat{\boldsymbol{k}}_{\text{i}}\cdot\boldsymbol{r}_p}4\pi i^{l-\tau+1}\boldsymbol{A}_{\tau n}(\hat{\boldsymbol{k}}_{\text{i}})\cdot\boldsymbol{E}_0$$

since

$$\sum_{j=1,2} (-1)^j B_{nj}^+(\boldsymbol{k}_{\mathrm{it}}) A_j = 4\pi \mathrm{i}^{-l+\tau-1} \boldsymbol{A}_{\tau n}(\hat{\boldsymbol{k}}_{\mathrm{i}}) \cdot \boldsymbol{E}_0$$

The expansions coefficients of the incident plane wave in regular spherical vector waves are [25]

$$\boldsymbol{E}_{\mathrm{i}}(\boldsymbol{r}) = \boldsymbol{E}_0 \mathrm{e}^{\mathrm{i}k_1 \hat{\boldsymbol{k}}_{\mathrm{i}} \cdot \boldsymbol{r}}$$

where [25]

$$a_{\tau n} = 4\pi \mathrm{i}^{l-\tau+1} \boldsymbol{A}_{\tau n}(\hat{\boldsymbol{k}}_{\mathrm{i}}) \cdot \boldsymbol{E}_0$$

which implies

$$\langle d_n \rangle (\boldsymbol{r}; \xi) = \mathrm{e}^{\mathrm{i}k_1 \hat{\boldsymbol{k}}_{\mathrm{i}} \cdot \boldsymbol{r}_p} \sum_{n'} T_{nn'}(\xi) a_n$$

This special case is in agreement with the results in [23].

9 Approximations

Two different approximations of the final expression of the transmission and reflection coefficients are of interest — tenuous (sparse) media and the low frequency approximation.

9.1 Tenuous media

If the number density of the scatterers is small, we can approximate the solution to the system of integral equations in (7.10) by the first iteration (first order in the number density n_0)

$$f_n(z) \approx d_n(z), \quad z \in [z_1 + a, z_2 - a]$$

which implies from (7.9)

$$k_2 \int_{z_1+a}^{z_2-a} f_n(z) \mathrm{e}^{\pm \mathrm{i}k_{2\mathrm{iz}}z}\ \mathrm{d}z = \sum_{n'} \langle T_{nn'} \rangle \sum_{j=1,2} T_j^1(\boldsymbol{k}_{\mathrm{it}}) A_j$$

$$\times \frac{B_{n'j}^{+\dagger}(\boldsymbol{k}_{\mathrm{it}}) \begin{pmatrix} I_+ \\ D \end{pmatrix} + R_j^2(\boldsymbol{k}_{\mathrm{it}}) B_{n'j}^{-\dagger}(\boldsymbol{k}_{\mathrm{it}}) \begin{pmatrix} D \\ I_- \end{pmatrix}}{1 - \mathcal{R}_j^1(\boldsymbol{k}_{\mathrm{it}}) R_j^2(\boldsymbol{k}_{\mathrm{it}})}$$

where

$$I_\pm = k_2 \int_{z_1+a}^{z_2-a} \mathrm{e}^{\pm 2\mathrm{i}k_{2\mathrm{iz}}z}\ \mathrm{d}z = \pm \frac{k_2}{2\mathrm{i}k_{2\mathrm{iz}}} \left(\mathrm{e}^{\pm 2\mathrm{i}k_{2\mathrm{iz}}(z_2-a)} - \mathrm{e}^{\pm 2\mathrm{i}k_{2\mathrm{iz}}(z_1+a)} \right)$$

$$= \pm \frac{k_2 \mathrm{e}^{\pm \mathrm{i}k_{2\mathrm{iz}}(z_2+z_1)}}{2\mathrm{i}k_{2\mathrm{iz}}} \left(\mathrm{e}^{\pm \mathrm{i}k_{2\mathrm{iz}}D} - \mathrm{e}^{\mp \mathrm{i}k_{2\mathrm{iz}}D} \right) = \frac{k_2 \mathrm{e}^{\pm \mathrm{i}k_{2\mathrm{iz}}(z_2+z_1)}}{k_{2\mathrm{iz}}} \sin k_{2\mathrm{iz}}D \quad (9.1)$$

and $D = z_2 - z_1 - 2a$. From (7.15) and (7.16) we obtain an explicit expression of the coherent (averaged) transmitted and reflected fields $\langle \boldsymbol{E}_\mathrm{t}(\boldsymbol{r}) \rangle$ and $\langle \boldsymbol{E}_\mathrm{r}(\boldsymbol{r}) \rangle$, respectively.

$$\langle \boldsymbol{E}_\mathrm{t}(\boldsymbol{r}) \rangle = \frac{8\pi^2 n_0}{k_2 k_{2\mathrm{iz}}} \sum_{j=1,2} T_j^2(\boldsymbol{k}_\mathrm{it}) \Bigg\{ \frac{\mathcal{R}_j^1(\boldsymbol{k}_\mathrm{it}) \sum_n B_{nj}^-(\boldsymbol{k}_\mathrm{it}) \int_{z_1+a}^{z_2-a} f_n(z') \mathrm{e}^{\mathrm{i}k_{2\mathrm{iz}}z'}\,\mathrm{d}z'}{1 - \mathcal{R}_j^1(\boldsymbol{k}_\mathrm{it}) R_j^2(\boldsymbol{k}_\mathrm{it})}$$

$$+ \frac{\sum_n B_{nj}^+(\boldsymbol{k}_\mathrm{it}) \int_{z_1+a}^{z_2-a} f_n(z') \mathrm{e}^{-\mathrm{i}k_{2\mathrm{iz}}z'}\,\mathrm{d}z'}{1 - \mathcal{R}_j^1(\boldsymbol{k}_\mathrm{it}) R_j^2(\boldsymbol{k}_\mathrm{it})} \Bigg\} \boldsymbol{\varphi}_j^+(\boldsymbol{k}_\mathrm{it}; k_3, \boldsymbol{r})$$

$$+ \sum_{j=1,2} T_j(\boldsymbol{k}_\mathrm{it}) A_j \boldsymbol{\varphi}_j^+(\boldsymbol{k}_\mathrm{it}; k_3, \boldsymbol{r}), \quad z > z_2$$

and

$$\langle \boldsymbol{E}_\mathrm{r}(\boldsymbol{r}) \rangle = \frac{8\pi^2 n_0}{k_2 k_{2\mathrm{iz}}} \sum_{j=1,2} \mathcal{T}_j^1(\boldsymbol{k}_\mathrm{it}) \Bigg\{ \frac{\sum_n B_{nj}^-(\boldsymbol{k}_\mathrm{it}) \int_{z_1+a}^{z_2-a} f_n(z') \mathrm{e}^{\mathrm{i}k_{2\mathrm{iz}}z'}\,\mathrm{d}z'}{1 - \mathcal{R}_j^1(\boldsymbol{k}_\mathrm{it}) R_j^2(\boldsymbol{k}_\mathrm{it})}$$

$$+ \frac{R_j^2(\boldsymbol{k}_\mathrm{it}) \sum_n B_{nj}^+(\boldsymbol{k}_\mathrm{it}) \int_{z_1+a}^{z_2-a} f_n(z') \mathrm{e}^{-\mathrm{i}k_{2\mathrm{iz}}z'}\,\mathrm{d}z'}{1 - \mathcal{R}_j^1(\boldsymbol{k}_\mathrm{it}) R_j^2(\boldsymbol{k}_\mathrm{it})} \Bigg\} \boldsymbol{\varphi}_j^-(\boldsymbol{k}_\mathrm{it}; k_1, \boldsymbol{r})$$

$$+ \sum_{j=1,2} R_j(\boldsymbol{k}_\mathrm{it}) A_j \boldsymbol{\varphi}_j^-(\boldsymbol{k}_\mathrm{it}; k_1, \boldsymbol{r}), \quad z < z_1$$

9.1.1 Normal incidence

A more comprehensive expression of the coherent transmitted and reflected fields is obtained if we specialize to normal incidence, $\boldsymbol{k}_\mathrm{it} = \boldsymbol{0}$. From (5.11), (5.12), (5.17), and (6.1), we obtain ($j = 1, 2$)

$$\begin{cases} R_j^1(\boldsymbol{0}) = -(-1)^j r_{z_1} \mathrm{e}^{2\mathrm{i}k_1 z_1} \\ \mathcal{R}_j^1(\boldsymbol{0}) = (-1)^j r_{z_1} \mathrm{e}^{-2\mathrm{i}k_2 z_1} \\ R_j^2(\boldsymbol{0}) = -(-1)^j r_{z_2} \mathrm{e}^{2\mathrm{i}k_2 z_2} \\ R_j(\boldsymbol{0}) = -(-1)^j \dfrac{r_{z_1} + r_{z_2} \mathrm{e}^{2\mathrm{i}k_2(z_2-z_1)}}{1 + r_{z_1} r_{z_2} \mathrm{e}^{2\mathrm{i}k_2(z_2-z_1)}} \mathrm{e}^{2\mathrm{i}k_1 z_1} \end{cases}$$

and

$$\begin{cases} T_j^1(\boldsymbol{0}) = t_{z_1} \mathrm{e}^{\mathrm{i}k_1 z_1} \mathrm{e}^{-\mathrm{i}k_2 z_1} \\ \mathcal{T}_j^1(\boldsymbol{0}) = \dfrac{\eta_1}{\eta_2} t_{z_1} \mathrm{e}^{\mathrm{i}k_1 z_1} \mathrm{e}^{-\mathrm{i}k_2 z_1} \\ T_j^2(\boldsymbol{0}) = t_{z_2} \mathrm{e}^{\mathrm{i}k_2 z_2} \mathrm{e}^{-\mathrm{i}k_3 z_2} \\ T_j(\boldsymbol{0}) = \dfrac{t_{z_1} t_{z_2} \mathrm{e}^{\mathrm{i}k_2(z_2-z_1)} \mathrm{e}^{\mathrm{i}k_1 z_1} \mathrm{e}^{-\mathrm{i}k_3 z_2}}{1 + r_{z_1} r_{z_2} \mathrm{e}^{2\mathrm{i}k_2(z_2-z_1)}} \end{cases}$$

where

$$\begin{cases} r_{z_1} = \dfrac{\eta_2 - \eta_1}{\eta_2 + \eta_1} \\ r_{z_2} = \dfrac{\eta_3 - \eta_2}{\eta_3 + \eta_2} \end{cases} \qquad \begin{cases} t_{z_1} = \dfrac{2\eta_2}{\eta_2 + \eta_1} = 1 + r_{z_1} \\ t_{z_2} = \dfrac{2\eta_3}{\eta_3 + \eta_2} = 1 + r_{z_2} \end{cases}$$

and from (D.4)

$$B_{nj}^+(\mathbf{0}) = \mathrm{i}^{-l}\delta_{m1}\sqrt{\frac{2l+1}{8\pi}}\left\{-\mathrm{i}\delta_{\tau j}\left\{\begin{matrix}\cos\beta\\\sin\beta\end{matrix}\right\} - \delta_{\tau\bar{j}}\left\{\begin{matrix}-\sin\beta\\\cos\beta\end{matrix}\right\}\right\}$$

The upper (lower) line in this expression in the brace parentheses corresponds to $\sigma = \mathrm{e}$ ($\sigma = \mathrm{o}$), and

$$B_{nj}^-(\mathbf{0}) = (-1)^{l+\tau+j}B_{nj}^+(\mathbf{0})$$

and

$$B_{nj}^{\pm\,\dagger}(\mathbf{0}) = (-1)^{l+\tau+j+1}B_{nj}^\pm(\mathbf{0})$$

The expansion coefficients of the plane wave are

$$A_j = 4\pi\boldsymbol{E}_0\cdot\left(\mathrm{i}\delta_{j1}\hat{\boldsymbol{\beta}} - \delta_{j2}\hat{\boldsymbol{k}}_{\mathrm{t}}\right)$$

The following sums are needed, see also (A.2):

$$\sum_{j=1,2} B_{nj}^{+\,\dagger}(\mathbf{0})A_j = \mathrm{i}^l\delta_{m1}\sqrt{2\pi}\sqrt{2l+1}\boldsymbol{E}_0\cdot\left\{\delta_{\tau 1}\left\{\begin{matrix}-\hat{\boldsymbol{y}}\\\hat{\boldsymbol{x}}\end{matrix}\right\} - \mathrm{i}\delta_{\tau 2}\left\{\begin{matrix}\hat{\boldsymbol{x}}\\\hat{\boldsymbol{y}}\end{matrix}\right\}\right\}$$
$$= 4\pi\mathrm{i}^{l-\tau+1}\boldsymbol{A}_n(\hat{\boldsymbol{z}})\cdot\boldsymbol{E}_0 \quad (9.2)$$

and

$$\sum_{j=1,2} R_j^2(\mathbf{0})B_{nj}^{-\,\dagger}(\mathbf{0})A_j$$
$$= \mathrm{i}^{-l}\delta_{m1}\sqrt{2\pi}\sqrt{2l+1}r_{z_2}\mathrm{e}^{2\mathrm{i}k_2z_2}\boldsymbol{E}_0\cdot\left\{\delta_{\tau 1}\left\{\begin{matrix}-\hat{\boldsymbol{y}}\\\hat{\boldsymbol{x}}\end{matrix}\right\} + \mathrm{i}\delta_{\tau 2}\left\{\begin{matrix}\hat{\boldsymbol{x}}\\\hat{\boldsymbol{y}}\end{matrix}\right\}\right\}$$
$$= 4\pi\mathrm{i}^{-l+\tau-1}r_{z_2}\mathrm{e}^{2\mathrm{i}k_2z_2}\boldsymbol{A}_n(\hat{\boldsymbol{z}})\cdot\boldsymbol{E}_0 \quad (9.3)$$

and for normal incidence, we get

$$k_2\int_{z_1+a}^{z_2-a} f_n(z)\mathrm{e}^{\pm\mathrm{i}k_2z}\,\mathrm{d}z = 4\pi\frac{t_{z_1}\mathrm{e}^{\mathrm{i}k_1z_1}\mathrm{e}^{-\mathrm{i}k_2z_1}}{1 + r_{z_1}r_{z_2}\mathrm{e}^{2\mathrm{i}k_2(z_2-z_1)}}$$
$$\sum_{n'}\mathrm{i}^{l'-\tau'+1}\langle T_{nn'}\rangle\,\boldsymbol{A}_{n'}(\hat{\boldsymbol{z}})\cdot\boldsymbol{E}_0\left(\begin{matrix}I_+ + (-1)^{l'+\tau'+1}k_2Dr_{z_2}\mathrm{e}^{2\mathrm{i}k_2z_2}\\k_2D + (-1)^{l'+\tau'+1}I_-r_{z_2}\mathrm{e}^{2\mathrm{i}k_2z_2}\end{matrix}\right)$$

where, see (9.1)

$$I_\pm = \mathrm{e}^{\pm\mathrm{i}k_2(z_2+z_1)}\sin(k_2D)$$

and $D = z_2 - z_1 - 2a$.

To proceed, we need the sums

$$\sum_{j=1,2}\mathcal{R}_j^1(\mathbf{0})B_{nj}^-(\mathbf{0})\boldsymbol{\varphi}_j^+(\mathbf{0};k_3,\boldsymbol{r})$$
$$= -\frac{\mathrm{i}^l\delta_{m1}}{4\pi}\sqrt{\frac{2l+1}{8\pi}}r_{z_1}\mathrm{e}^{-2\mathrm{i}k_2z_1}\left\{\delta_{\tau 1}\left\{\begin{matrix}-\hat{\boldsymbol{y}}\\\hat{\boldsymbol{x}}\end{matrix}\right\} - \mathrm{i}\delta_{\tau 2}\left\{\begin{matrix}\hat{\boldsymbol{x}}\\\hat{\boldsymbol{y}}\end{matrix}\right\}\right\}\mathrm{e}^{\mathrm{i}k_3z}$$
$$= -\frac{\mathrm{i}^{l-\tau+1}r_{z_1}\mathrm{e}^{-2\mathrm{i}k_2z_1}}{4\pi}\boldsymbol{A}_n(\hat{\boldsymbol{z}})\mathrm{e}^{\mathrm{i}k_3z}$$

38

and

$$\sum_{j=1,2} B_{nj}^+(\mathbf{0})\boldsymbol{\varphi}_j^+(\mathbf{0};k_3,\boldsymbol{r}) = \frac{\mathrm{i}^{-l}\delta_{m1}}{4\pi}\sqrt{\frac{2l+1}{8\pi}}\left\{\delta_{\tau 1}\left\{\begin{matrix}-\hat{\boldsymbol{y}}\\\hat{\boldsymbol{x}}\end{matrix}\right\} + \mathrm{i}\delta_{\tau 2}\left\{\begin{matrix}\hat{\boldsymbol{x}}\\\hat{\boldsymbol{y}}\end{matrix}\right\}\right\}\mathrm{e}^{\mathrm{i}k_3 z}$$

$$= \frac{\mathrm{i}^{-l+\tau-1}}{4\pi}\boldsymbol{A}_n(\hat{\boldsymbol{z}})\mathrm{e}^{\mathrm{i}k_3 z}$$

Similarly, we get

$$\sum_{j=1,2} B_{nj}^-(\mathbf{0})\boldsymbol{\varphi}_j^-(\mathbf{0};k_1,\boldsymbol{r}) = \frac{\mathrm{i}^{l-\tau+1}}{4\pi}\boldsymbol{A}_n(\hat{\boldsymbol{z}})\mathrm{e}^{-\mathrm{i}k_1 z}$$

and

$$\sum_{j=1,2} R_j^2(\mathbf{0})B_{nj}^+(\mathbf{0})\boldsymbol{\varphi}_j^-(\mathbf{0};k_1,\boldsymbol{r}) = \frac{\mathrm{i}^{-l+\tau-1}r_{z2}\mathrm{e}^{2\mathrm{i}k_2 z_2}}{4\pi}\boldsymbol{A}_n(\hat{\boldsymbol{z}})\mathrm{e}^{-\mathrm{i}k_1 z}$$

and

$$\sum_{j=1,2} A_j\boldsymbol{\varphi}_j^+(\mathbf{0};k_3,\boldsymbol{r}) = \boldsymbol{E}_0\mathrm{e}^{\mathrm{i}k_3 z}, \qquad -\sum_{j=1,2}(-1)^j A_j\boldsymbol{\varphi}_j^-(\mathbf{0};k_1,\boldsymbol{r}) = \boldsymbol{E}_0\mathrm{e}^{-\mathrm{i}k_1 z}$$

These results give the final expressions of the coherent (averaged) transmitted and reflected fields, $\langle\boldsymbol{E}_{\mathrm{t}}(\boldsymbol{r})\rangle$ and $\langle\boldsymbol{E}_{\mathrm{r}}(\boldsymbol{r})\rangle$, respectively, with a plane wave impinging normally to the slab, see (7.15) and (7.16). We get

$$\langle\boldsymbol{E}_{\mathrm{t}}(\boldsymbol{r})\rangle = \sum_{j=1,2}\left\{\frac{8\pi^2 n_0}{k_2^2}T_j^2(\mathbf{0})\left\{\frac{\mathcal{R}_j^1(\mathbf{0})\sum_n B_{nj}^-(\mathbf{0})\int_{z_1+a}^{z_2-a}f_n(z')\mathrm{e}^{\mathrm{i}k_2 z'}\,\mathrm{d}z'}{1-\mathcal{R}_j^1(\mathbf{0})R_j^2(\mathbf{0})}\right.\right.$$

$$+ \left.\left.\frac{\sum_n B_{nj}^+(\mathbf{0})\int_{z_1+a}^{z_2-a}f_n(z')\mathrm{e}^{-\mathrm{i}k_2 z'}\,\mathrm{d}z'}{1-\mathcal{R}_j^1(\mathbf{0})R_j^2(\mathbf{0})}\right\} + T_j(\mathbf{0})A_j\right\}\boldsymbol{\varphi}_j^+(\mathbf{0};k_3,\boldsymbol{r})$$

$$= \frac{8\pi^2 n_0}{k_2^3}\frac{t_{z1}t_{z2}\mathrm{e}^{\mathrm{i}k_1 z_1}\mathrm{e}^{\mathrm{i}k_2(z_2-z_1)}\mathrm{e}^{\mathrm{i}k_3(z-z_2)}}{\left(1+r_{z1}r_{z2}\mathrm{e}^{2\mathrm{i}k_2(z_2-z_1)}\right)^2}\sum_{nn'}\boldsymbol{A}_n(\hat{\boldsymbol{z}})\langle T_{nn'}\rangle\boldsymbol{A}_{n'}(\hat{\boldsymbol{z}})\cdot\boldsymbol{E}_0$$

$$\times\left\{\mathrm{i}^{(l+l')-(\tau+\tau')}r_{z1}\mathrm{e}^{-2\mathrm{i}k_2 z_1}I_+ - \mathrm{i}^{(l-l')-(\tau-\tau')}r_{z1}r_{z2}\mathrm{e}^{2\mathrm{i}k_2(z_2-z_1)}k_2 D\right.$$

$$\left.+ \mathrm{i}^{(l'-l)-(\tau'-\tau)}k_2 D - \mathrm{i}^{-(l+l')+(\tau+\tau')}r_{z2}\mathrm{e}^{2\mathrm{i}k_2 z_2}I_-\right\}$$

$$+ t_{\mathrm{slab}}\mathrm{e}^{\mathrm{i}k_1 z_1}\boldsymbol{E}_0\mathrm{e}^{\mathrm{i}k_3(z-z_2)}, \quad z > z_2$$

where the transmission coefficient for the homogeneous slab is

$$t_{\mathrm{slab}} = \frac{t_{z1}t_{z2}\mathrm{e}^{\mathrm{i}k_2(z_2-z_1)}}{1+r_{z1}r_{z2}\mathrm{e}^{2\mathrm{i}k_2(z_2-z_1)}} \tag{9.4}$$

and

$$\langle \boldsymbol{E}_{\mathrm{r}}(\boldsymbol{r})\rangle = \sum_{j=1,2} \left\{ \frac{8\pi^2 n_0}{k_2^2} \mathcal{T}_j^1(\mathbf{0}) \left\{ \frac{\sum_n B_{nj}^-(\mathbf{0}) \int_{z_1+a}^{z_2-a} f_n(z')\mathrm{e}^{\mathrm{i}k_2 z'}\,\mathrm{d}z'}{1 - \mathcal{R}_j^1(\mathbf{0})R_j^2(\mathbf{0})} \right. \right.$$

$$\left. \left. + \frac{R_j^2(\mathbf{0})\sum_n B_{nj}^+(\mathbf{0}) \int_{z_1+a}^{z_2-a} f_n(z')\mathrm{e}^{-\mathrm{i}k_2 z'}\,\mathrm{d}z'}{1 - \mathcal{R}_j^1(\mathbf{0})R_j^2(\mathbf{0})} \right\} + R_j(\mathbf{0})A_j \right\} \boldsymbol{\varphi}_j^-(\mathbf{0};k_1,\boldsymbol{r})$$

$$= \frac{8\pi^2 n_0}{k_2^3}\frac{\eta_1}{\eta_2} \frac{t_{z_1}^2 \mathrm{e}^{\mathrm{i}k_1 z_1} \mathrm{e}^{-2\mathrm{i}k_2 z_1} \mathrm{e}^{-\mathrm{i}k_1(z-z_1)}}{\left(1 + r_{z_1}r_{z_2}\mathrm{e}^{2\mathrm{i}k_2(z_2-z_1)}\right)^2} \sum_{nn'} \boldsymbol{A}_n(\hat{\boldsymbol{z}}) \langle T_{nn'}\rangle \boldsymbol{A}_{n'}(\hat{\boldsymbol{z}}) \cdot \boldsymbol{E}_0$$

$$\times \left\{ -\mathrm{i}^{(l+l')-(\tau+\tau')}I_+ + \mathrm{i}^{(l-l')-(\tau-\tau')}r_{z_2}\mathrm{e}^{2\mathrm{i}k_2 z_2}k_2 D \right.$$

$$\left. + \mathrm{i}^{(l'-l)-(\tau'-\tau)}r_{z_2}\mathrm{e}^{2\mathrm{i}k_2 z_2}k_2 D - \mathrm{i}^{-(l'+l)+(\tau'+\tau)}r_{z_2}^2\mathrm{e}^{4\mathrm{i}k_2 z_2}I_- \right\}$$

$$+ r_{\mathrm{slab}}\mathrm{e}^{\mathrm{i}k_1 z_1}\boldsymbol{E}_0\mathrm{e}^{-\mathrm{i}k_1(z-z_1)}, \quad z < z_1$$

where the reflection coefficient for the homogeneous slab is

$$r_{\mathrm{slab}} = \frac{r_{z_1} + r_{z_2}\mathrm{e}^{2\mathrm{i}k_2(z_2-z_1)}}{1 + r_{z_1}r_{z_2}\mathrm{e}^{2\mathrm{i}k_2(z_2-z_1)}}$$

This is an explicit expressions of the coherent transmitted and reflected fields in the approximation of tenuous scatterers. The last terms in these expressions are the direct transmitted and reflected fields, and they are obvious. The first terms, however, are more complex, and not easy to derive from elementary physical arguments. In these terms, the transition matrix appears to the first power, which indicates that single scattering approximation has been adopted.

We can simplify this expression further by identifying the forward scattering and backscattering dyadics of a single (deterministic) scatterer in the slab background material [25, Ex. 7.1 and 7.2]

$$\mathbf{S}(\hat{\boldsymbol{z}},\hat{\boldsymbol{z}}) = \frac{4\pi}{\mathrm{i}k_2} \sum_{n,n'} \mathrm{i}^{(l'-l)-(\tau'-\tau)}\boldsymbol{A}_n(\hat{\boldsymbol{z}})T_{nn'}\boldsymbol{A}_{n'}(\hat{\boldsymbol{z}})$$

and

$$\mathbf{S}(-\hat{\boldsymbol{z}},\hat{\boldsymbol{z}}) = -\frac{4\pi}{\mathrm{i}k_2} \sum_{n,n'} \mathrm{i}^{(l+l')-(\tau+\tau')}\boldsymbol{A}_n(\hat{\boldsymbol{z}})T_{nn'}\boldsymbol{A}_{n'}(\hat{\boldsymbol{z}})$$

or by the use of the parity of the vector spherical harmonics (A.1)

$$\mathbf{S}(-\hat{\boldsymbol{z}},-\hat{\boldsymbol{z}}) = \frac{4\pi}{\mathrm{i}k_2} \sum_{n,n'} \mathrm{i}^{(l-l')-(\tau-\tau')}\boldsymbol{A}_n(\hat{\boldsymbol{z}})T_{nn'}\boldsymbol{A}_{n'}(\hat{\boldsymbol{z}})$$

and

$$\mathbf{S}(\hat{\boldsymbol{z}},-\hat{\boldsymbol{z}}) = -\frac{4\pi}{\mathrm{i}k_2} \sum_{n,n'} \mathrm{i}^{-(l+l')+(\tau+\tau')}\boldsymbol{A}_n(\hat{\boldsymbol{z}})T_{nn'}\boldsymbol{A}_{n'}(\hat{\boldsymbol{z}})$$

We get

$$
\begin{aligned}
\langle \boldsymbol{E}_{\mathrm{t}}(\boldsymbol{r})\rangle = \frac{2\pi \mathrm{i} n_0}{k_2^2}\frac{t_{\mathrm{slab}}\mathrm{e}^{\mathrm{i}k_1 z_1}\mathrm{e}^{\mathrm{i}k_3(z-z_2)}}{1+r_{z_1}r_{z_2}\mathrm{e}^{2\mathrm{i}k_2(z_2-z_1)}}\Bigg\{ &-r_{z_1}\mathbf{S}(-\hat{\boldsymbol{z}},\hat{\boldsymbol{z}})\mathrm{e}^{-2\mathrm{i}k_2 z_1}I_+ \\
&-r_{z_1}\mathbf{S}(-\hat{\boldsymbol{z}},-\hat{\boldsymbol{z}})r_{z_2}\mathrm{e}^{2\mathrm{i}k_2(z_2-z_1)}k_2 D + \mathbf{S}(\hat{\boldsymbol{z}},\hat{\boldsymbol{z}})k_2 D \\
&+\mathbf{S}(\hat{\boldsymbol{z}},-\hat{\boldsymbol{z}})r_{z_2}\mathrm{e}^{2\mathrm{i}k_2 z_2}I_- \Bigg\}\cdot \boldsymbol{E}_0 + t_{\mathrm{slab}}\mathrm{e}^{\mathrm{i}k_1 z_1}\boldsymbol{E}_0\mathrm{e}^{\mathrm{i}k_3(z-z_2)}, \quad z>z_2
\end{aligned}
$$

and

$$
\begin{aligned}
\langle \boldsymbol{E}_{\mathrm{r}}(\boldsymbol{r})\rangle = \frac{2\pi \mathrm{i} n_0}{k_2^2}\frac{\eta_1}{\eta_2}\frac{t_{z_1}^2\mathrm{e}^{\mathrm{i}k_1 z_1}\mathrm{e}^{-2\mathrm{i}k_2 z_1}\mathrm{e}^{-\mathrm{i}k_1(z-z_1)}}{\left(1+r_{z_1}r_{z_2}\mathrm{e}^{2\mathrm{i}k_2(z_2-z_1)}\right)^2}\Bigg\{ &\mathbf{S}(-\hat{\boldsymbol{z}},\hat{\boldsymbol{z}})I_+ \\
&+\mathbf{S}(-\hat{\boldsymbol{z}},-\hat{\boldsymbol{z}})r_{z_2}\mathrm{e}^{2\mathrm{i}k_2 z_2}k_2 D + \mathbf{S}(\hat{\boldsymbol{z}},\hat{\boldsymbol{z}})r_{z_2}\mathrm{e}^{2\mathrm{i}k_2 z_2}k_2 D \\
&+\mathbf{S}(\hat{\boldsymbol{z}},-\hat{\boldsymbol{z}})r_{z_2}^2\mathrm{e}^{4\mathrm{i}k_2 z_2}I_- \Bigg\}\cdot \boldsymbol{E}_0 + r_{\mathrm{slab}}\mathrm{e}^{\mathrm{i}k_1 z_1}\boldsymbol{E}_0\mathrm{e}^{-\mathrm{i}k_1(z-z_1)}, \quad z<z_1
\end{aligned}
$$

If we restrict to spherical, dielectric obstacles of radius a and material parameters ϵ and μ so that $T_{nn'}$ is diagonal in its indices (we adopt the notion $t_{\tau l}$ for the transition matrix entries [25, Chap. 8]), the expressions simplify [25, Ex. 7.3]. We get

$$
\mathbf{S}(\hat{\boldsymbol{z}},\hat{\boldsymbol{z}}) = \mathbf{S}(-\hat{\boldsymbol{z}},-\hat{\boldsymbol{z}}) = \frac{\mathbf{I}_2}{2\mathrm{i}k_2}\sum_{l=1}^{\infty}(2l+1)\left(t_{1l}+t_{2l}\right)
$$

and

$$
\mathbf{S}(\hat{\boldsymbol{z}},-\hat{\boldsymbol{z}}) = \mathbf{S}(-\hat{\boldsymbol{z}},\hat{\boldsymbol{z}}) = \frac{\mathbf{I}_2}{2\mathrm{i}k_2}\sum_{l=1}^{\infty}(-1)^l(2l+1)\left(t_{1l}-t_{2l}\right)
$$

The transmission coefficient t defined as $\langle \boldsymbol{E}_{\mathrm{t}}(\boldsymbol{r})\rangle = t\boldsymbol{E}_0\mathrm{e}^{\mathrm{i}k_3(z-z_2)}$ then is

$$
\begin{aligned}
t = \frac{3f}{4(k_2 a)^3}\frac{t_{\mathrm{slab}}\mathrm{e}^{\mathrm{i}k_1 z_1}}{1+r_{z_1}r_{z_2}\mathrm{e}^{2\mathrm{i}k_2(z_2-z_1)}}\Bigg\{ &\left(1-r_{z_1}r_{z_2}\mathrm{e}^{2\mathrm{i}k_2(z_2-z_1)}\right)k_2 D\sum_{l=1}^{\infty}(2l+1)\left(t_{1l}+t_{2l}\right) \\
&+\left(r_{z_2}-r_{z_1}\right)\mathrm{e}^{\mathrm{i}k_2(z_2-z_1)}\sin(k_2 D)\sum_{l=1}^{\infty}(-1)^l(2l+1)\left(t_{1l}-t_{2l}\right)\Bigg\} + t_{\mathrm{slab}}\mathrm{e}^{\mathrm{i}k_1 z_1}
\end{aligned}
$$

where we used the dimensionless volume fraction, $f = n_0 4\pi a^3/3$, and where we also used

$$
\begin{aligned}
-r_{z_1}&\mathrm{e}^{-2\mathrm{i}k_2 z_1}I_+ + r_{z_2}\mathrm{e}^{2\mathrm{i}k_2 z_2}I_- \\
&= -r_{z_1}\mathrm{e}^{-2\mathrm{i}k_2 z_1}\mathrm{e}^{\mathrm{i}k_2(z_2+z_1)}\sin(k_2 D) + r_{z_2}\mathrm{e}^{2\mathrm{i}k_2 z_2}\mathrm{e}^{-\mathrm{i}k_2(z_2+z_1)}\sin(k_2 D) \\
&\qquad\qquad\qquad\qquad\qquad\qquad = (-r_{z_1}+r_{z_2})\mathrm{e}^{\mathrm{i}k_2(z_2-z_1)}\sin(k_2 D)
\end{aligned}
$$

where $D = z_2 - z_1 - 2a$.

Similarly, the reflection coefficient r is defined as $\langle \boldsymbol{E}_{\mathrm{r}}(\boldsymbol{r}) \rangle = r \boldsymbol{E}_0 \mathrm{e}^{-\mathrm{i}k_1(z-z_1)}$ where

$$
\begin{aligned}
r = \frac{3f}{4(k_2 a)^3} \frac{\eta_1}{\eta_2} \frac{t_{z_1}^2 \mathrm{e}^{\mathrm{i}k_1 z_1} \mathrm{e}^{-2\mathrm{i}k_2 z_1}}{\left(1 + r_{z_1} r_{z_2} \mathrm{e}^{2\mathrm{i}k_2(z_2-z_1)}\right)^2} &\left\{ 2r_{z_2} \mathrm{e}^{2\mathrm{i}k_2 z_2} k_2 D \sum_{l=1}^{\infty} (2l+1)\left(t_{1l} + t_{2l}\right) \right. \\
&\left. + \left(\mathrm{e}^{2\mathrm{i}k_2 z_1} + r_{z_2}^2 \mathrm{e}^{2\mathrm{i}k_2 z_2}\right) \mathrm{e}^{\mathrm{i}k_2(z_2-z_1)} \sin(k_2 D) \sum_{l=1}^{\infty} (-1)^l (2l+1)\left(t_{1l} - t_{2l}\right) \right\} + r_{\mathrm{slab}} \mathrm{e}^{\mathrm{i}k_1 z_1}
\end{aligned}
$$

where we used

$$
\begin{aligned}
I_+ + r_{z_2}^2 \mathrm{e}^{4\mathrm{i}k_2 z_2} I_- &= \mathrm{e}^{\mathrm{i}k_2(z_2+z_1)} \sin(k_2 D) + r_{z_2}^2 \mathrm{e}^{4\mathrm{i}k_2 z_2} \mathrm{e}^{-\mathrm{i}k_2(z_2+z_1)} \sin(k_2 D) \\
&= \left(\mathrm{e}^{2\mathrm{i}k_2 z_1} + r_{z_2}^2 \mathrm{e}^{2\mathrm{i}k_2 z_2}\right) \mathrm{e}^{\mathrm{i}k_2(z_2-z_1)} \sin(k_2 D)
\end{aligned}
$$

Further simplifications occur if the material on both sides of the slab are identical, i.e., $\epsilon_1 = \epsilon_3$ and $\mu_1 = \mu_3$. Then $r_{z_2} = -r_{z_1}$ and

$$
\begin{aligned}
t = t_{\mathrm{slab}} \mathrm{e}^{\mathrm{i}k_1 z_1} &\left\{ 1 + \frac{3f}{4(k_2 a)^3} \frac{k_2 D \left(1 + r_{z_1}^2 \mathrm{e}^{2\mathrm{i}k_2(z_2-z_1)}\right)}{1 - r_{z_1}^2 \mathrm{e}^{2\mathrm{i}k_2(z_2-z_1)}} \sum_{l=1}^{\infty} (2l+1)\left(t_{1l} + t_{2l}\right) \right. \\
&\left. - \frac{6f}{4(k_2 a)^3} \frac{r_{z_1} \sin(k_2 D) \mathrm{e}^{\mathrm{i}k_2(z_2-z_1)}}{1 - r_{z_1}^2 \mathrm{e}^{2\mathrm{i}k_2(z_2-z_1)}} \sum_{l=1}^{\infty} (-1)^l (2l+1)\left(t_{1l} - t_{2l}\right) \right\} \quad (9.5)
\end{aligned}
$$

where

$$
t_{\mathrm{slab}} = \frac{\left(1 - r_{z_1}^2\right) \mathrm{e}^{\mathrm{i}k_2(z_2-z_1)}}{1 - r_{z_1}^2 \mathrm{e}^{2\mathrm{i}k_2(z_2-z_1)}}
$$

This result shows several similarities with the corresponding result with no slab present [23], and a numerical implementation of the result in this section, simulating air bubbles ($\epsilon = \epsilon_1 = \epsilon_3$ and $\mu = \mu_1 = \mu_3$) in a dielectric slab of resin, is illustrated in Figure 3.

9.2 Low-frequency approximation

The aim of this section is to solve the integral equation (7.10) for low frequencies for spherical particles of radius a, or, more precisely, small $k_2 a$.

9.2.1 Normal incidence

To simplify the analysis, we assume $\epsilon_1 = \epsilon_3$ and $\mu_1 = \mu_2 = \mu_3$ (the same materials on both sides of the slab, and all materials have the same magnetic properties) and we assume the plane wave impinges normally to the slab, i.e., $\boldsymbol{k}_{\mathrm{it}} = \boldsymbol{0}$.

If the spherical particles of radius a are of the same magnetic properties as the slab, $\mu = \mu_2$, and with a permittivity ϵ, then the transition matrix entries of the scatterers to leading order in powers of $k_2 a$ are [25]

$$
t_{21} = T_{2\sigma 11, 2\sigma 11} = \frac{2\mathrm{i}(k_2 a)^3}{3} y, \quad \sigma = \mathrm{e, o} \quad (9.6)
$$
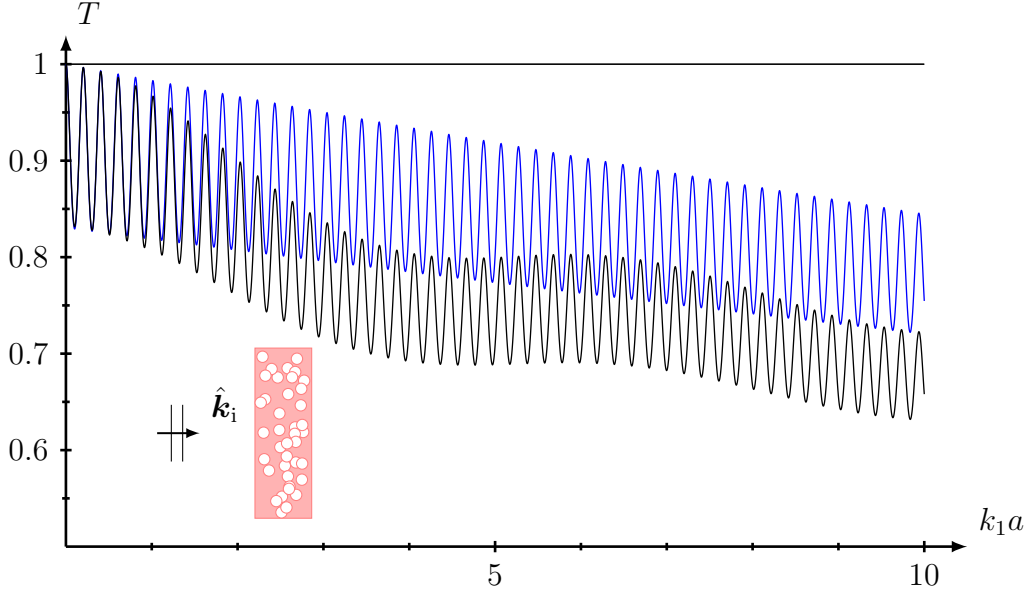
Figure 3: The transmissivity $T = |t|^2$ (t given in (9.5)) as a function of the electrical size k_1a for a slab of thickness $(z_2 - z_1)/a = 10$ and constant volume fraction $f = 0.01$ consisting of spherical voids of radius a (same material as the outside the slab). The materials parameters are identical on both sides of the slab, *i.e.*, $\epsilon_1 = \epsilon_3$ and $\mu_1 = \mu_3$. The material parameters of the slab are $\epsilon_2/\epsilon_1 = 2.4(1 + 0.001i)$ and $\mu_2/\mu_1 = 1$. The tenuous approximation of the transmissivity with a slab background is depicted in black. The blue curve corresponds to the transmissivity without scatterers, and the curve $T = 1$ is also shown.

where

$$y = \frac{\epsilon - \epsilon_2}{\epsilon + 2\epsilon_2}$$

All other entries of the transition matrix contribute with higher order terms in k_2a.

We proceed by identifying the dominant power in k_2a in the kernel $K_{nn'}(z, z'; \xi)$, see (7.14), which originates from $l = 1$. The simplest model for the pair correlation function $g(r)$ is the hole correction function, *i.e.*, $g(r) = \mathrm{H}(r - 2a)$, where $\mathrm{H}(x)$ denotes the Heaviside function. With only $l = 1$ and $m = 1$ contributing, the function $C_{nn'}(\boldsymbol{k}_\mathrm{t}; z)$ in (7.13), to leading order in powers of k_2a, the transition matrix entries are [23, 24]

$$C_{\tau\sigma11,\tau\sigma11}(\boldsymbol{0}; z) = -2\pi \begin{cases} O(1), & |z| \geq 2a \\ \mathrm{i}\dfrac{12 - 3(z/a)^2}{32k_2a} + O(1), & |z| < 2a \end{cases} \quad \tau = 1, 2 \; \sigma = \mathrm{e}, \mathrm{o}$$

The lateral Fourier transform of the pair correlation function, see (7.12), for the hole correction becomes

$$G(\boldsymbol{k}_\mathrm{t}; z) = 4\pi^2 k_2^2 \delta(\boldsymbol{k}_\mathrm{t}) - 2\pi(k_2 d(z))^2 \frac{J_1(k_\mathrm{t} d(z))}{k_\mathrm{t} d(z)} = O(1)$$

These estimates imply that the kernel $K_{nn'}(z, z')$ in (7.14) has the dominant term (only $\tau = 2$ contributes due to the assumption that the scatterers have the same magnetic properties as the surrounding slab)

$$K_{2\sigma 11, 2\sigma 11}(z, z') = -\frac{3ft_{21}}{2(k_2 a)^3} \begin{cases} O(1), & |z - z'| \geq 2a \\ i\dfrac{12 - 3\left(\frac{z-z'}{a}\right)^2}{32 k_2 a} + O(1), & |z - z'| < 2a \end{cases} \quad \sigma = e, o$$

where the dimensionless volume fraction, $f = n_0 4\pi a^3/3$. All other components of the kernel contributes with higher order terms in $k_2 a$. The integral equation (7.10) to leading order in $k_2 a$ is (we suppress the index $\tau = 2$, $m = 1$, and $l = 1$)

$$f_\sigma(z) + \frac{3ifk_2 t_{21}}{64(k_2 a)^4} \int_{z_1+a}^{z_2-a} H(2a - |z - z'|) \left(12 - 3\left(\frac{z-z'}{a}\right)^2\right) f_\sigma(z') \, dz'$$
$$= d_\sigma(z), \quad z \in [z_1, z_2], \ \sigma = e, o$$

where $H(x)$ is the Heaviside function. We notice that the two integral decouple, and it suffices to solve one of them. Under the assumptions made in this section, the right-hand side $d_\sigma(z)$ in (7.9) is

$$d_\sigma(z) = t_{21} \sum_{j=1,2} T_j^1(\mathbf{0}) A_j \frac{B_{2\sigma 11 j}^{+}{}^\dagger(\mathbf{0}) e^{ik_2 z} + R_j^2(\mathbf{0}) B_{2\sigma 11 j}^{-}{}^\dagger(\mathbf{0}) e^{-ik_2 z}}{1 - \mathcal{R}_j^1(\mathbf{0}) R_j^2(\mathbf{0})}$$

$$= 4\pi t_{21} t_{z_1} e^{ik_1 z_1} e^{-ik_2 z_1} \mathbf{A}_{2\sigma 11}(\hat{\mathbf{z}}) \cdot \mathbf{E}_0 \frac{e^{ik_2 z} + r_{z_2} e^{2ik_2 z_2} e^{-ik_2 z}}{1 + r_{z_1} r_{z_2} e^{2ik_2(z_2-z_1)}}$$

$$= \sqrt{6\pi} t_{21} t_{z_1} e^{ik_1 z_1} e^{-ik_2 z_1} \begin{Bmatrix} \hat{\mathbf{x}} \\ \hat{\mathbf{y}} \end{Bmatrix} \cdot \mathbf{E}_0 \frac{e^{ik_2 z} + r_{z_2} e^{2ik_2 z_2} e^{-ik_2 z}}{1 + r_{z_1} r_{z_2} e^{2ik_2(z_2-z_1)}}, \quad \sigma = e, o$$

where we used (9.2) and (9.3).

Our main goal is to evaluate the transmitted and reflected fields, and for this we need to compute the dominant contribution to the integrals $\int_{z_1+a}^{z_2-a} f_\sigma(z) e^{\pm ik_2 z} \, dz$. Therefore, multiply the integral equation with $k_2 e^{\pm ik_2 z}$ and integrate over $z \in [z_1 + a, z_2 - a]$. The result is (the domain of integration is depicted in Figure 4)

$$y_\sigma^{\pm} + \frac{3ifk_2^2 t_{21}}{64(k_2 a)^4} \int_{z_1+a}^{z_2-a} \int_{z_1+a}^{z_2-a} H(2a - |z - z'|) \left(12 - 3\left(\frac{z-z'}{a}\right)^2\right) e^{\pm ik_2(z-z')}$$
$$\times e^{\pm ik_2 z'} f_\sigma(z') \, dz' \, dz = D_\sigma^{\pm}, \quad \sigma = e, o$$

where

$$y_\sigma^{\pm} = k_2 \int_{z_1+a}^{z_2-a} f_\sigma(z) e^{\pm ik_2 z} \, dz$$

and where the right-hand side is

$$D_\sigma^{\pm} = k_2 \int_{z_1+a}^{z_2-a} d_\sigma(z) e^{\pm ik_2 z} \, dz =$$

$$\sqrt{6\pi} t_{21} \frac{t_{z_1} e^{ik_1 z_1} e^{-ik_2 z_1}}{1 + r_{z_1} r_{z_2} e^{2ik_2(z_2-z_1)}} \begin{Bmatrix} \hat{\mathbf{x}} \\ \hat{\mathbf{y}} \end{Bmatrix} \cdot \mathbf{E}_0 \begin{pmatrix} I_+ + k_2 D r_{z_2} e^{2ik_2 z_2} \\ k_2 D + I_- r_{z_2} e^{2ik_2 z_2} \end{pmatrix}$$
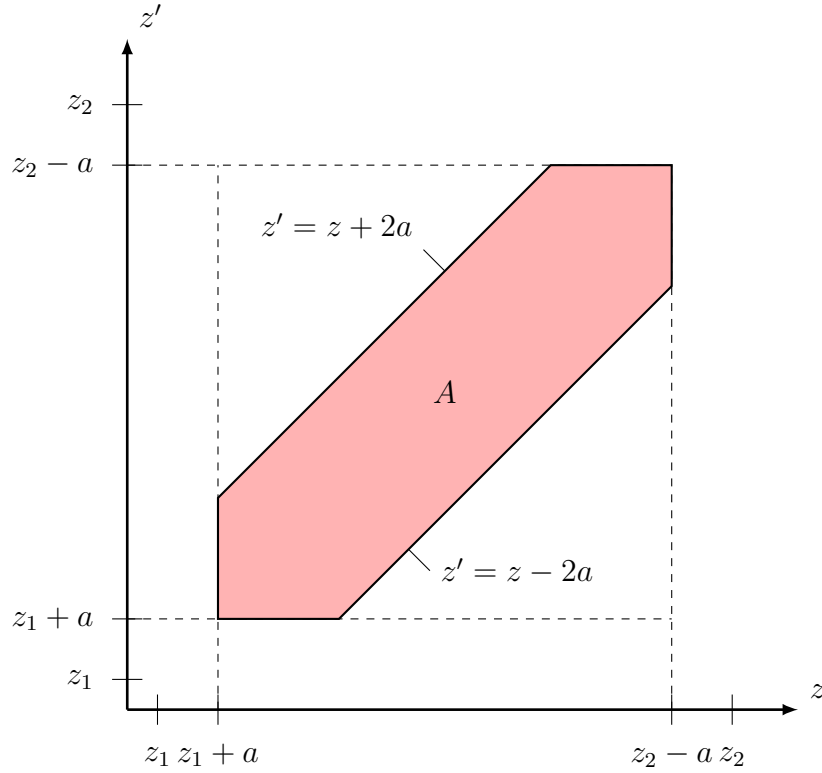
Figure 4: The domain of integration in z and z'. The red area A shows the region where the kernel $K(z - z')$ is non-zero. The domain A is exaggerated.
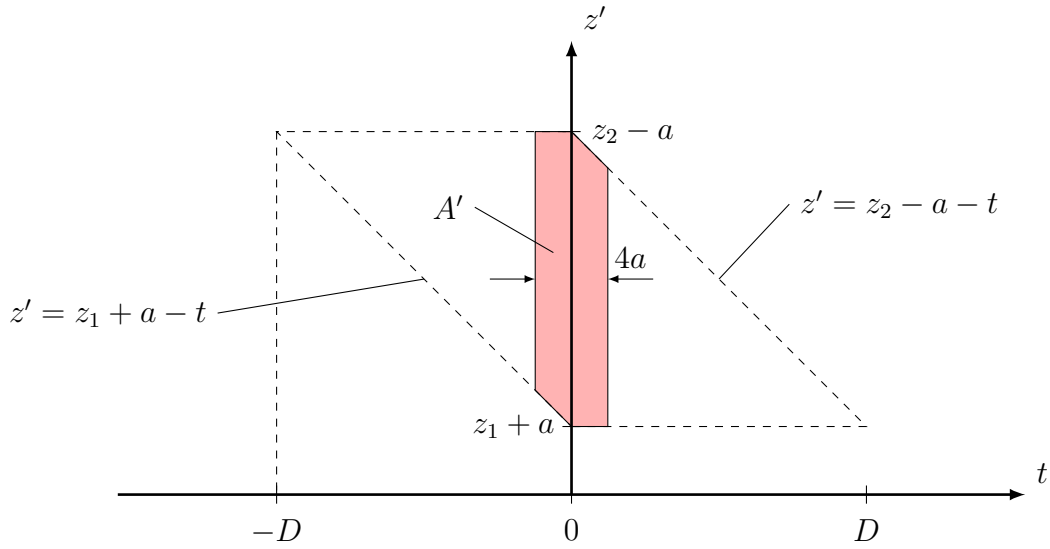
where, see (9.1)

$$I_{\pm} = \mathrm{e}^{\pm \mathrm{i}k_2(z_2+z_1)} \sin(k_2 D)$$

and $D = z_2 - z_1 - 2a$. The upper (lower) line in the parentheses corresponds to the plus (minus) sign in the exponent on the left-hand side. Moreover, the upper (lower) line in the braces corresponds to $\sigma = \mathrm{e}$ ($\sigma = \mathrm{o}$).

Make a change in variables in the integral equation, $z \to t = z - z'$. The new domain of integration is depicted in Figure 5. The integral equation (7.10) becomes to leading order in $k_2 a$

$$y_\sigma^{\pm} + \frac{3\mathrm{i}f k_2^2 t_{21}}{64(k_2 a)^4} \iint\limits_{A'} \left(12 - 3\left(\frac{t}{a}\right)^2\right) \mathrm{e}^{\pm \mathrm{i}k_2 t} \mathrm{e}^{\pm \mathrm{i}k_2 z'} f_\sigma(z')\, \mathrm{d}z'\, \mathrm{d}t = D_\sigma^{\pm}, \quad \sigma = \mathrm{e, o}$$

Figure 5: The domain of integration in t and z'. The red area A' shows the region where the kernel $K(z-z')$ is non-zero, and $D = z_2 - z_1 - 2a$. The domain A' is exaggerated.

To leading order in powers of $k_2 a$, the integral is

$$k_2^2 \iint\limits_{A'} \left(12 - 3\left(\frac{t}{a}\right)^2\right) e^{\pm ik_2 t} e^{\pm ik_2 z'} f_\sigma(z') \, dz' \, dt$$

$$\approx k_2 y_\sigma^\pm \int_{-2a}^{2a} \left(12 - 3\left(\frac{t}{a}\right)^2\right) e^{\pm ik_2 t} \, dt$$

$$= k_2 a y_\sigma^\pm \int_{-2}^{2} \left(12 - 3u^2\right) e^{\pm ik_2 a u} \, du = 32 k_2 a y_\sigma^\pm + O((k_2 a)^2)$$

which implies to leading order in $k_2 a$

$$y_\sigma^\pm = \frac{D_\sigma^\pm}{1 + \frac{3 i f t_{21}}{2(k_2 a)^3}}, \qquad \sigma = \mathrm{e}, \mathrm{o}$$

Finally, we can now form the transmitted field $\langle \boldsymbol{E}_\mathrm{t}(\boldsymbol{r}) \rangle$, see (7.15), by the use of

the sums over j that is found in Section 9.1.1. The result is

$$\langle \boldsymbol{E}_\mathrm{t}(\boldsymbol{r})\rangle = \sum_{j=1,2}\left\{\frac{8\pi^2 n_0}{k_2^2}T_j^2(\boldsymbol{0})\left\{\frac{\mathcal{R}_j^1(\boldsymbol{0})\sum_n B_{nj}^-(\boldsymbol{0})\int_{z_1+a}^{z_2-a}f_n(z')\mathrm{e}^{\mathrm{i}k_2 z'}\,\mathrm{d}z'}{1-\mathcal{R}_j^1(\boldsymbol{0})R_j^2(\boldsymbol{0})}\right.\right.$$

$$+\left.\left.\frac{\sum_n B_{nj}^+(\boldsymbol{0})\int_{z_1+a}^{z_2-a}f_n(z')\mathrm{e}^{-\mathrm{i}k_2 z'}\,\mathrm{d}z'}{1-\mathcal{R}_j^1(\boldsymbol{0})R_j^2(\boldsymbol{0})}\right\}+T_j(\boldsymbol{0})A_j\right\}\boldsymbol{\varphi}_j^+(\boldsymbol{0};k_3,\boldsymbol{r})$$

$$=\frac{9ft_{21}}{4(k_2 a)^3}\frac{t_{z_1}t_{z_2}\mathrm{e}^{\mathrm{i}k_1 z_1}\mathrm{e}^{\mathrm{i}k_2(z_2-z_1)}\mathrm{e}^{\mathrm{i}k_3(z-z_2)}}{\left(1+r_{z_1}r_{z_2}\mathrm{e}^{2\mathrm{i}k_2(z_2-z_1)}\right)^2}\frac{\boldsymbol{E}_0}{1+\frac{3\mathrm{i}ft_{21}}{2(k_2 a)^3}}$$

$$\times\left\{-r_{z_1}\mathrm{e}^{-2\mathrm{i}k_2 z_1}I_+ -r_{z_1}r_{z_2}\mathrm{e}^{2\mathrm{i}k_2(z_2-z_1)}k_2 D+k_2 D+r_{z_2}\mathrm{e}^{2\mathrm{i}k_2 z_2}I_-\right\}$$

$$+t_\mathrm{slab}\mathrm{e}^{\mathrm{i}k_1 z_1}\boldsymbol{E}_0\mathrm{e}^{\mathrm{i}k_3(z-z_2)},\quad z>z_2$$

where the dimensionless volume fraction, $f=n_0 4\pi a^3/3$. The transmission coefficient t defined as $\langle\boldsymbol{E}_\mathrm{t}(\boldsymbol{r})\rangle=t\boldsymbol{E}_0\mathrm{e}^{\mathrm{i}k_3(z-z_2)}$ then is

$$t=\frac{9ft_{21}t_\mathrm{slab}\mathrm{e}^{\mathrm{i}k_1 z_1}}{4(k_2 a)^3+6\mathrm{i}ft_{21}}\left\{\frac{(r_{z_2}-r_{z_1})\,\mathrm{e}^{\mathrm{i}k_2(z_2-z_1)}\sin(k_2 D)}{1+r_{z_1}r_{z_2}\mathrm{e}^{2\mathrm{i}k_2(z_2-z_1)}}+\frac{\left(1-r_{z_1}r_{z_2}\mathrm{e}^{2\mathrm{i}k_2(z_2-z_1)}\right)k_2 D}{1+r_{z_1}r_{z_2}\mathrm{e}^{2\mathrm{i}k_2(z_2-z_1)}}\right\}$$

$$+t_\mathrm{slab}\mathrm{e}^{\mathrm{i}k_1 z_1}\quad(9.7)$$

Similarly, the reflected field is, see (7.16)

$$\langle\boldsymbol{E}_\mathrm{r}(\boldsymbol{r})\rangle=\sum_{j=1,2}\left\{\frac{8\pi^2 n_0}{k_2^2}\mathcal{T}_j^1(\boldsymbol{0})\left\{\frac{\sum_n B_{nj}^-(\boldsymbol{0})\int_{z_1+a}^{z_2-a}f_n(z')\mathrm{e}^{\mathrm{i}k_2 z'}\,\mathrm{d}z'}{1-\mathcal{R}_j^1(\boldsymbol{0})R_j^2(\boldsymbol{0})}\right.\right.$$

$$+\left.\left.\frac{R_j^2(\boldsymbol{0})\sum_n B_{nj}^+(\boldsymbol{0})\int_{z_1+a}^{z_2-a}f_n(z')\mathrm{e}^{-\mathrm{i}k_2 z'}\,\mathrm{d}z'}{1-\mathcal{R}_j^1(\boldsymbol{0})R_j^2(\boldsymbol{0})}\right\}+R_j(\boldsymbol{0})A_j\right\}\boldsymbol{\varphi}_j^-(\boldsymbol{0};k_1,\boldsymbol{r})$$

$$=\frac{9ft_{21}}{4(k_2 a)^3}\frac{\eta_1}{\eta_2}\frac{t_{z_1}^2\mathrm{e}^{\mathrm{i}k_1 z_1}\mathrm{e}^{-2\mathrm{i}k_2 z_1}}{\left(1+r_{z_1}r_{z_2}\mathrm{e}^{2\mathrm{i}k_2(z_2-z_1)}\right)^2}\frac{\boldsymbol{E}_0}{1+\frac{3\mathrm{i}ft_{21}}{2(k_2 a)^3}}$$

$$\left\{I_++r_{z_2}\mathrm{e}^{2\mathrm{i}k_2 z_2}k_2 D+r_{z_2}\mathrm{e}^{2\mathrm{i}k_2 z_2}k_2 D+r_{z_2}^2\mathrm{e}^{4\mathrm{i}k_2 z_2}I_-\right\}\mathrm{e}^{-\mathrm{i}k_1(z-z_1)}$$

$$+r_\mathrm{slab}\mathrm{e}^{\mathrm{i}k_1 z_1}\boldsymbol{E}_0\mathrm{e}^{-\mathrm{i}k_1(z-z_1)},\quad z<z_1$$

The reflection coefficient r defined as $\langle\boldsymbol{E}_\mathrm{r}(\boldsymbol{r})\rangle=r\boldsymbol{E}_0\mathrm{e}^{-\mathrm{i}k_1(z-z_1)}$ then is

$$r=9ft_{21}\frac{\eta_1}{\eta_2}\frac{t_{z_1}^2\mathrm{e}^{\mathrm{i}k_1 z_1}\mathrm{e}^{-2\mathrm{i}k_2 z_1}}{\left(1+r_{z_1}r_{z_2}\mathrm{e}^{2\mathrm{i}k_2(z_2-z_1)}\right)^2}\frac{1}{4(k_2 a)^3+6\mathrm{i}ft_{21}}$$

$$\left\{2r_{z_2}\mathrm{e}^{2\mathrm{i}k_2 z_2}k_2 D+\left(\mathrm{e}^{2\mathrm{i}k_2 z_1}+r_{z_2}^2\mathrm{e}^{2\mathrm{i}k_2 z_2}\right)\mathrm{e}^{\mathrm{i}k_2(z_2-z_1)}\sin(k_2 D)\right\}+r_\mathrm{slab}\mathrm{e}^{\mathrm{i}k_1 z_1}$$

To leading order in the volume fraction f, we get further simplifications of the

transmission and reflection coefficients.

$$t = \frac{9ft_{21}t_{\text{slab}}e^{ik_1z_1}}{4(k_2a)^3}\left\{\frac{(r_{z_2} - r_{z_1})e^{ik_2(z_2-z_1)}\sin(k_2D)}{1 + r_{z_1}r_{z_2}e^{2ik_2(z_2-z_1)}} + \frac{\left(1 - r_{z_1}r_{z_2}e^{2ik_2(z_2-z_1)}\right)k_2D}{1 + r_{z_1}r_{z_2}e^{2ik_2(z_2-z_1)}}\right\}$$
$$+ t_{\text{slab}}e^{ik_1z_1}$$

and

$$r = \frac{9ft_{21}}{4(k_2a)^3}\frac{\eta_1}{\eta_2}\frac{t_{z_1}^2 e^{ik_1z_1}e^{-2ik_2z_1}}{\left(1 + r_{z_1}r_{z_2}e^{2ik_2(z_2-z_1)}\right)^2}$$
$$\left\{2r_{z_2}e^{2ik_2z_2}k_2D + \left(e^{2ik_2z_1} + r_{z_2}^2 e^{2ik_2z_2}\right)e^{ik_2(z_2-z_1)}\sin(k_2D)\right\} + r_{\text{slab}}e^{ik_1z_1}$$

which agree with the results in Section 9.1.1 for a non-magnetic material at low frequencies.

9.2.2 Further simplifications and approximations

Further simplifications occur if the material on both sides of the slab are identical, *i.e.*, $\epsilon_1 = \epsilon_3$ and $\mu_1 = \mu_3$. Then $r_{z_2} = -r_{z_1}$ and (9.4) reads

$$t_{\text{slab}} = \frac{\left(1 - r_{z_1}^2\right)e^{ik_2(z_2-z_1)}}{1 - r_{z_1}^2 e^{2ik_2(z_2-z_1)}}$$

and from (9.7) $(k_2d = k_2(z_2 - z_1))$

$$\frac{te^{-ik_1z_1}}{t_{\text{slab}}} = 1 + \frac{3i}{2}\frac{fy}{1 - fy}\left\{\frac{-2r_{z_1}e^{ik_2d}\sin(k_2d)}{1 - r_{z_1}^2 e^{2ik_2d}} + \frac{\left(1 + r_{z_1}^2 e^{2ik_2d}\right)k_2d}{1 - r_{z_1}^2 e^{2ik_2d}}\right\}$$

where we approximated $D = d$ and introduced the low-frequency expansion of the transition matrix, see (9.6), and $y = (\epsilon - \epsilon_2)/(\epsilon + 2\epsilon_2)$.

The result in this section is illustrated in Figures 6 and 7, simulating air bubbles in a dielectric slab of resin. The low-frequency behaviour shown in Figure 6 shows that all three curves agree in the interval $k_1a \in [0, 0.5]$ — which approximately corresponds to the interval $\text{Re}\,k_2a \in [0, 1.25]$ in the slab parameters.

If also the volume fraction f is low, we have agreement with the corresponding expression in Section 9.1.

The dominant contribution in powers of the electric thickness $k_1d = k_1(z_2 - z_1)$ is also of interest. The transmission coefficient for the homogeneous slab has the following expansion in powers of $k_1d = k_1ad/a$ [25]:

$$t_{\text{slab}}e^{-ik_1d} = \frac{\left(1 - r_{z_1}^2\right)e^{i(k_2-k_1)d}}{1 - r_{z_1}^2 e^{2ik_2d}}$$

$$= \left(1 + i(k_2 - k_1)d + O\left((k_1d)^2\right)\right)\left(1 + 2i\frac{r_{z_1}^2}{1 - r_{z_1}^2}k_2d + O\left((k_1d)^2\right)\right)$$

$$= 1 + i\frac{1 + r_{z_1}^2}{1 - r_{z_1}^2}k_2d - ik_1d + O\left((k_1d)^2\right) = 1 + i\frac{\epsilon_1 + \epsilon_2}{2\sqrt{\epsilon_1\epsilon_2}}k_2d - ik_1d + O\left((k_1d)^2\right)$$

$$= 1 + i\frac{\epsilon_1 + \epsilon_2}{2\epsilon_1}k_1d - ik_1d + O\left((k_1d)^2\right) = 1 + i\frac{\epsilon_2 - \epsilon_1}{2\epsilon_1}k_1d + O\left((k_1d)^2\right)$$
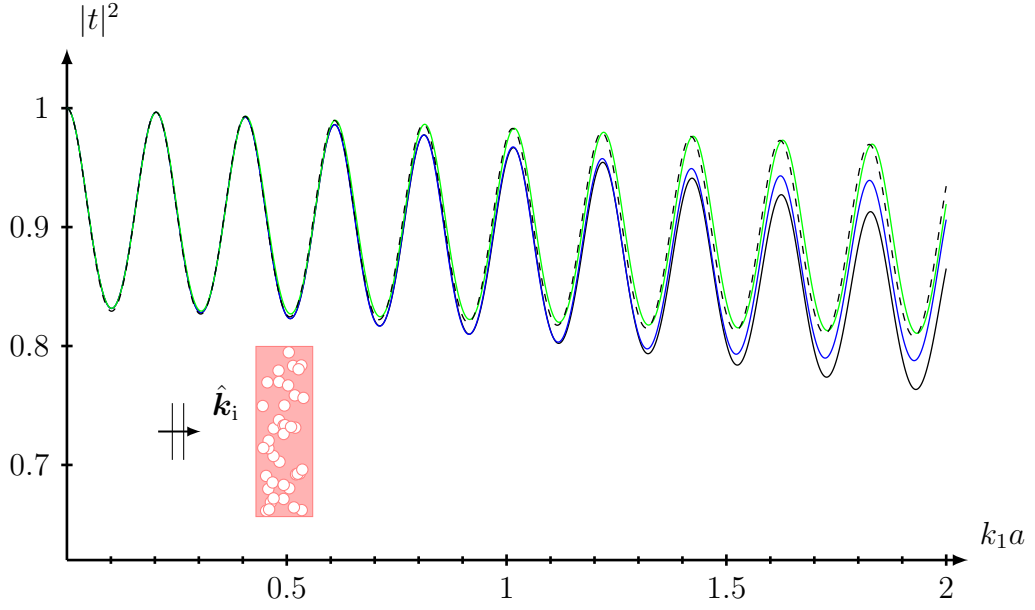
Figure 6: The low-frequency behavior of the transmissivity $T = |t|^2$ (t given in (9.7)) as a function of the electrical size $k_1 a$ for a slab of thickness $(z_2 - z_1)/a = 10$ and constant volume fraction $f = 0.01$ consisting of spherical voids of radius a (same material as the outside the slab). The materials parameters are identical to the ones in Figure 3. The black curve depicts the tenuous media approximation and the blue curve the low-frequency approximation. The green curve gives the transmissivity for a homogeneous slab with the homogenized permittivity in (9.8) and the transmissivity for the slab without any voids is given in dashed curve.

and (to leading order in $k_1 d$)

$$\frac{t\mathrm{e}^{-\mathrm{i}k_1 z_1}}{t_{\mathrm{slab}}} = 1 + \frac{3\mathrm{i}}{2}\frac{fy}{1 - fy}\frac{\left(1 - r_{z_1}\mathrm{e}^{\mathrm{i}k_2 d}\right)^2}{1 - r_{z_1}^2\,\mathrm{e}^{2\mathrm{i}k_2 d}}k_2 d = 1 + \frac{3\mathrm{i}}{2}\frac{fy}{1 - fy}\frac{1 - r_{z_1}\mathrm{e}^{\mathrm{i}k_2 d}}{1 + r_{z_1}\mathrm{e}^{\mathrm{i}k_2 d}}k_2 d$$

$$= 1 + \frac{3\mathrm{i}}{2}\frac{fy}{1 - fy}\frac{1 - r_{z_1}}{1 + r_{z_1}}k_2 d + O\left((k_1 d)^2\right) = 1 + \frac{3\mathrm{i}}{2}\frac{fy}{1 - fy}\sqrt{\frac{\epsilon_2}{\epsilon_1}}k_2 d + O\left((k_1 d)^2\right)$$

These approximations imply (to leading order in $k_1 d$)

$$t\mathrm{e}^{-\mathrm{i}k_1 d} = \left(1 + \mathrm{i}\frac{\epsilon_2 - \epsilon_1}{2\epsilon_1}k_1 d\right)\left(1 + \frac{3\mathrm{i}}{2}\frac{fy}{1 - fy}\frac{\epsilon_2}{\epsilon_1}k_1 d\right)\mathrm{e}^{\mathrm{i}k_1 z_1}$$

$$= \left(1 + \mathrm{i}\frac{\epsilon_2 - \epsilon_1}{2\epsilon_1}k_1 d + \frac{3\mathrm{i}}{2}\frac{fy}{1 - fy}\frac{\epsilon_2}{\epsilon_1}k_1 d\right)\mathrm{e}^{\mathrm{i}k_1 z_1}$$

and the transmitted electric field is

$$\langle \boldsymbol{E}_{\mathrm{t}}(\boldsymbol{r})\rangle = \left(1 + 1 + \mathrm{i}\frac{\epsilon_2 - \epsilon_1}{2\epsilon_1}k_1 d + \frac{3\mathrm{i}}{2}\frac{fy}{1 - fy}\frac{\epsilon_2}{\epsilon_1}k_1 d\right)\boldsymbol{E}_0\mathrm{e}^{\mathrm{i}k_1 z}, \quad z > z_2$$
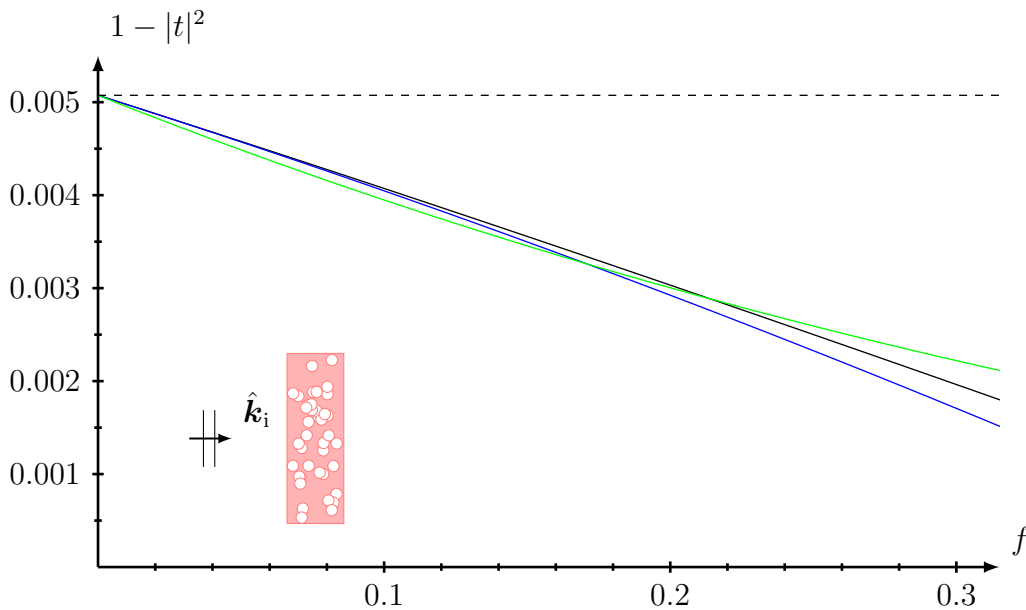
Figure 7: The transmissivity $|t|^2$ as a function of the volume fraction f for a slab of thickness $d/a = 10$ and constant electric size $k_1 a = 0.01$ consisting of spherical voids of radius a (same material as the outside the slab). The materials parameters are identical to the ones in Figure 3. The low-frequency approximation of the transmissivity is displayed in black and the tenuous approximation is given in blue. The dashed line depicts the transmissivity in a slab without scatterers. The green curve gives the transmissivity for a homogeneous slab with the homogenized permittivity in (9.8).

This expression of the transmission coefficient t can be compared with the transmission coefficient of a non-magnetic, dielectric slab of thickness $d = z_2 - z_1$ with permittivity ϵ' in a background material ϵ_1. The thin thickness approximation is

$$\langle \boldsymbol{E}_{\mathrm{t}}(\boldsymbol{r}) \rangle = \left(1 + \mathrm{i}\frac{\epsilon' - \epsilon_1}{2\epsilon_1}k_1 d + O\left((k_1 d)^2\right)\right)\boldsymbol{E}_0 \mathrm{e}^{\mathrm{i}k_1 z}$$

Equating these expressions gives

$$\frac{\epsilon'}{\epsilon_1} = \frac{\epsilon_2}{\epsilon_1} + \frac{3fy}{1 - fy}\frac{\epsilon_2}{\epsilon_1}$$

or

$$\epsilon' = \epsilon_2 + \frac{3fy\epsilon_2}{1 - fy} = \epsilon_2\frac{1 + 2fy}{1 - fy} \tag{9.8}$$

which is the Clausius-Mossotti relation [17].

10   Conclusions

The results presented in this paper generalize the analysis reported in [23], where the background material was identical everywhere. The generalization reported in

50
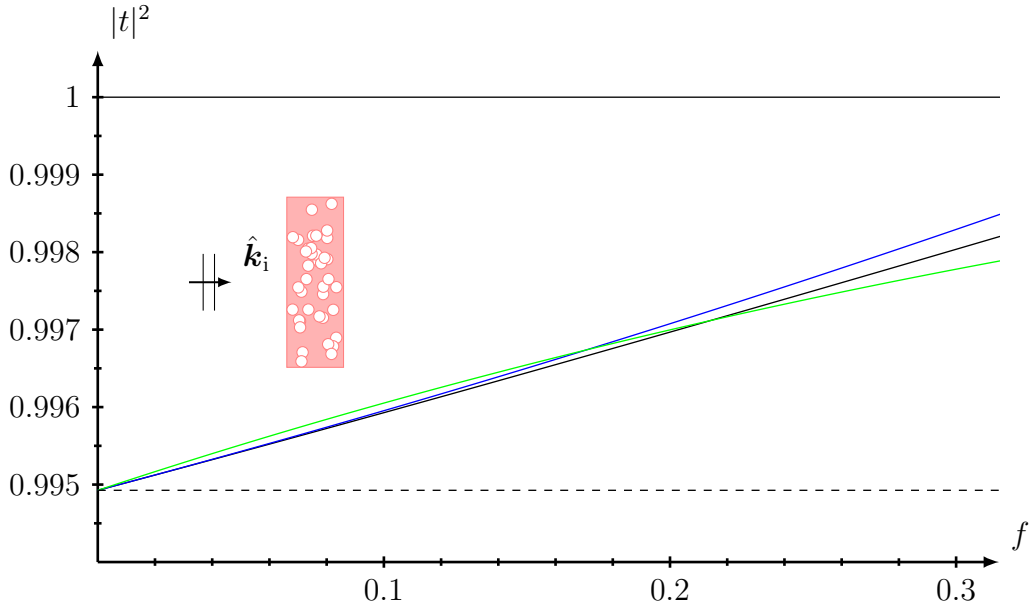
Figure 8: The transmissivity $|t|^2$ as a function of the volume fraction f for a slab of thickness $d/a = 10$ and constant electric size $k_1 a = 0.01$ consisting of spherical voids of radius a (same material as the outside the slab). The materials parameters are identical to the ones in Figure 3. The low-frequency approximation of the transmissivity is displayed in black and the tenuous approximation is given in blue. The dashed line depicts the transmissivity in a slab without scatterers. The green curve gives the transmissivity for a homogeneous slab with the homogenized permittivity in (9.8).

this paper extends the results such that defects in a slab can be handled, *e.g.*, air bubbles. The analysis solves the boundary value with an arbitrary number of general scatterers inside a slab with different material parameters. Moreover, the results explicitly identify the scattering contribution from the particles themselves. In particular, a potentially lossy background material hosting the particles is covered. A lossy background material has been causing controversial arguments over time regarding extinction [2, 32, 33]. The method developed in this paper avoids this controversy.

The complex scattering problem of randomly located obstacles in a slab with different material is solved employing a systematic use of two main tools: 1) the integral representation of the solution of the Maxwell equations, 2) decomposition of the Green dyadic for the electric field in free space in spherical and planar vector waves. In addition, we also employ transformations between planar and spherical vector waves. The statistical treatment is general, but the details is only analyzed in full detail for the uniformly distributed obstacles and for the hole correction. Several generalizations of the results presented in this paper are possible as well as a numerical implementation of the theory. These extensions and numerical implementations are reported elsewhere.

Appendix A Spherical vector waves

The vector spherical harmonics defined on the unit sphere are [4, 25]

$$
\begin{cases}
\boldsymbol{A}_{1n}(\hat{\boldsymbol{r}}) = \dfrac{1}{\sqrt{l(l+1)}} \nabla \times (\boldsymbol{r} Y_n(\hat{\boldsymbol{r}})) = \dfrac{1}{\sqrt{l(l+1)}} \nabla Y_n(\hat{\boldsymbol{r}}) \times \boldsymbol{r} \\[3mm]
\boldsymbol{A}_{2n}(\hat{\boldsymbol{r}}) = \dfrac{1}{\sqrt{l(l+1)}} r \nabla Y_n(\hat{\boldsymbol{r}}) \\[3mm]
\boldsymbol{A}_{3n}(\hat{\boldsymbol{r}}) = \hat{\boldsymbol{r}} Y_n(\hat{\boldsymbol{r}})
\end{cases}
$$

where the (scalar) spherical harmonics are denoted by $Y_n(\hat{\boldsymbol{r}})$ defined as

$$
Y_n(\hat{\boldsymbol{r}}) = Y_n(\theta, \phi) = \sqrt{\frac{\varepsilon_m}{2\pi}} \sqrt{\frac{2l+1}{2} \frac{(l-m)!}{(l+m)!}} P_l^m(\cos\theta) \begin{Bmatrix} \cos m\phi \\ \sin m\phi \end{Bmatrix}
$$

where $P_l^m(x)$ are the associated Legendre functions, and where the Neumann factor is defined as

$$
\varepsilon_m = 2 - \delta_{m0}, \ \ i.e., \ \ \begin{cases} \varepsilon_0 = 1 \\ \varepsilon_m = 2, \quad m > 0 \end{cases}
$$

The index n is a multi-index for the integer indices $l = 1, 2, 3, \ldots$, $m = 0, 1, \ldots, l$, and $\sigma = $ e,o (even and odd in the azimuthal angle).[4] From these definitions we see that the first two vector spherical harmonics, $\boldsymbol{A}_{1n}(\hat{\boldsymbol{r}})$ and $\boldsymbol{A}_{2n}(\hat{\boldsymbol{r}})$, are tangential to the unit sphere Ω in $\mathbb{R}^3$ and they are related as

$$
\begin{cases}
\hat{\boldsymbol{r}} \times \boldsymbol{A}_{1n}(\hat{\boldsymbol{r}}) = \boldsymbol{A}_{2n}(\hat{\boldsymbol{r}}) \\
\hat{\boldsymbol{r}} \times \boldsymbol{A}_{2n}(\hat{\boldsymbol{r}}) = -\boldsymbol{A}_{1n}(\hat{\boldsymbol{r}})
\end{cases}
$$

The vector spherical harmonics form an orthonormal set over the unit sphere Ω in $\mathbb{R}^3$, $i.e.$,

$$
\iint\limits_{\Omega} \boldsymbol{A}_{\tau n}(\hat{\boldsymbol{r}}) \cdot \boldsymbol{A}_{\tau' n'}(\hat{\boldsymbol{r}}) \, \mathrm{d}\Omega = \delta_{nn'} \delta_{\tau\tau'}
$$

where $\mathrm{d}\Omega$ is the surface measure on the unit sphere.

The parity of the vector spherical harmonics is

$$
\boldsymbol{A}_{\tau n}(-\hat{\boldsymbol{r}}) = (-1)^{l+\tau+1} \boldsymbol{A}_{\tau n}(\hat{\boldsymbol{r}}), \quad \tau = 1, 2 \tag{A.1}
$$

The explicit values for $\hat{\boldsymbol{r}} = \hat{\boldsymbol{z}}$ are

$$
\begin{cases}
\boldsymbol{A}_{1\sigma ml}(\hat{\boldsymbol{z}}) = \delta_{m1} \sqrt{\dfrac{2l+1}{8\pi}} \begin{Bmatrix} -\hat{\boldsymbol{y}} \\ \hat{\boldsymbol{x}} \end{Bmatrix} = -\delta_{m1} \sqrt{\dfrac{2l+1}{8\pi}} \hat{\boldsymbol{z}} \times \begin{Bmatrix} \hat{\boldsymbol{x}} \\ \hat{\boldsymbol{y}} \end{Bmatrix} \\[5mm]
\boldsymbol{A}_{2\sigma ml}(\hat{\boldsymbol{z}}) = \delta_{m1} \sqrt{\dfrac{2l+1}{8\pi}} \begin{Bmatrix} \hat{\boldsymbol{x}} \\ \hat{\boldsymbol{y}} \end{Bmatrix}
\end{cases} \tag{A.2}
$$

---

[4]The index set at several places in this paper also denotes a four index set, and includes the τ index. That is, the index n can denote $n = \{\sigma, l, m\}$ or $n = \{\tau, \sigma, l, m\}$.

The radiating solutions to the Maxwell equations in vacuum are defined as (outgoing spherical vector waves)

$$\begin{cases} \boldsymbol{u}_{1n}(k\boldsymbol{r}) = \dfrac{\xi_l(kr)}{kr}\boldsymbol{A}_{1n}(\hat{\boldsymbol{r}}) \\[3mm] \boldsymbol{u}_{2n}(k\boldsymbol{r}) = \dfrac{1}{k}\nabla \times \left(\dfrac{\xi_l(kr)}{kr}\boldsymbol{A}_{1n}(\hat{\boldsymbol{r}}) \right) \end{cases}$$

Here, we use the Riccati-Bessel functions $\xi_l(x) = xh_l^{(1)}(x)$, where $h_l^{(1)}(x)$ is the spherical Hankel function of the first kind [46]. These vector waves satisfy

$$\nabla \times (\nabla \times \boldsymbol{u}_{\tau n}(k\boldsymbol{r})) - k^2\boldsymbol{u}_{\tau n}(k\boldsymbol{r}) = \boldsymbol{0}, \qquad \tau = 1, 2$$

and they also satisfy the Silver-Müller radiation condition [6]. Another representation of the definition of the vector waves is

$$\begin{cases} \boldsymbol{u}_{1n}(k\boldsymbol{r}) = \dfrac{\xi_l(kr)}{kr}\boldsymbol{A}_{1n}(\hat{\boldsymbol{r}}) \\[3mm] \boldsymbol{u}_{2n}(k\boldsymbol{r}) = \dfrac{\xi_l'(kr)}{kr}\boldsymbol{A}_{2n}(\hat{\boldsymbol{r}}) + \sqrt{l(l+1)}\dfrac{\xi_l(kr)}{(kr)^2}\boldsymbol{A}_{3n}(\hat{\boldsymbol{r}}) \end{cases}$$

A simple consequence of these definitions is

$$\begin{cases} \boldsymbol{u}_{1n}(k\boldsymbol{r}) = \dfrac{1}{k}\nabla \times \boldsymbol{u}_{2n}(k\boldsymbol{r}) \\[3mm] \boldsymbol{u}_{2n}(k\boldsymbol{r}) = \dfrac{1}{k}\nabla \times \boldsymbol{u}_{1n}(k\boldsymbol{r}). \end{cases}$$

In a similar way, the regular spherical vector waves $\boldsymbol{v}_{\tau n}(k\boldsymbol{r})$ are defined [4].

$$\begin{cases} \boldsymbol{v}_{1n}(k\boldsymbol{r}) = \dfrac{\psi_l(kr)}{kr}\boldsymbol{A}_{1n}(\hat{\boldsymbol{r}}) \\[3mm] \boldsymbol{v}_{2n}(k\boldsymbol{r}) = \dfrac{\psi_l'(kr)}{kr}\boldsymbol{A}_{2n}(\hat{\boldsymbol{r}}) + \sqrt{l(l+1)}\dfrac{\psi_l(kr)}{(kr)^2}\boldsymbol{A}_{3n}(\hat{\boldsymbol{r}}) \end{cases}$$

where the Riccati-Bessel functions $\psi_l(x) = xj_l(x)$, where $j_l(x)$ is the spherical Bessel function [46].

Appendix B   The translation matrices

The translation properties of the spherical vector waves are instrumental for the formulation and the solution of the scattering problem of many individual scatterers. These translation properties are well know, and we refer to, *e.g.*, [4] for details.

Let $\boldsymbol{r}' = \boldsymbol{r} + \boldsymbol{d}$, see Figure 9. Then

$$\boldsymbol{u}_n(k\boldsymbol{r}') = \sum_{n'} \mathcal{P}_{nn'}(k\boldsymbol{d})\boldsymbol{v}_{n'}(k\boldsymbol{r}), \quad r < d$$
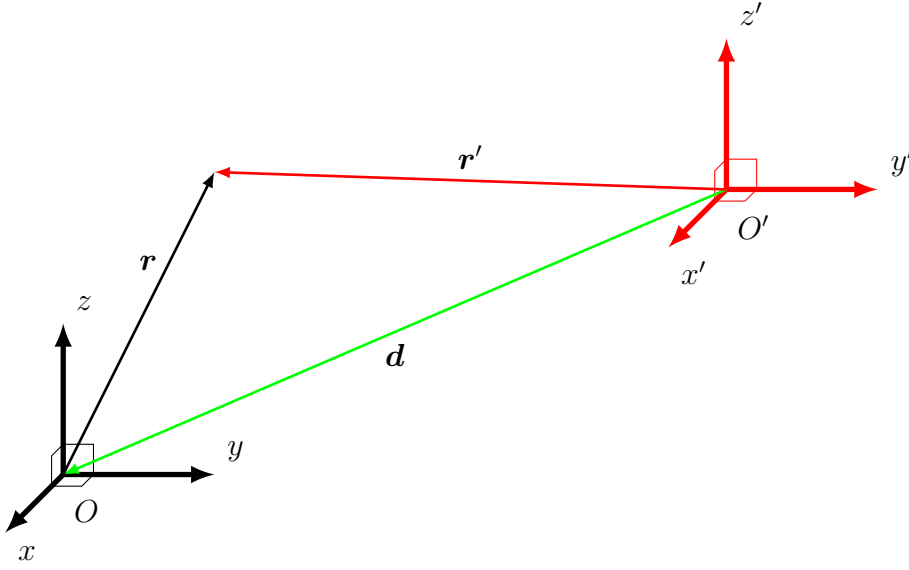
Figure 9: The relation between the translated origins O and O' and the position vectors $\boldsymbol{r}$ and $\boldsymbol{r}'$ at the different origins.

Translation in the opposite direction is identical to the transpose of the translation matrices, *i.e.*,

$$\mathcal{P}^{\mathrm{t}}(k\boldsymbol{d}) = \mathcal{P}(-k\boldsymbol{d})$$

Denote the spherical coordinates of $\boldsymbol{r}$, $\boldsymbol{r}'$, and $\boldsymbol{d}$ by (r, θ, ϕ), (r', θ', ϕ'), and (d, η, ψ), respectively. The translation matrices for a translation $\boldsymbol{d}$ ($d \leq 0$) are [4]

$$\mathcal{P}_{1\sigma ml, 1\sigma m'l'}(k\boldsymbol{d}) = (-1)^{m'} C_{ml,m'l'}(kd, \eta) \cos(m - m')\psi$$
$$+ (-1)^{\sigma} C_{ml,-m'l'}(kd, \eta) \cos(m + m')\psi$$

$$\mathcal{P}_{1\sigma ml, 1\sigma' m'l'}(k\boldsymbol{d}) = (-1)^{m'+\sigma'} C_{ml,m'l'}(kd, \eta) \sin(m - m')\psi$$
$$+ C_{ml,-m'l'}(kd, \eta) \sin(m + m')\psi, \quad \sigma \neq \sigma'$$

$$\mathcal{P}_{1\sigma ml, 2\sigma' m'l'}(k\boldsymbol{d}) = (-1)^{m'+\sigma} D_{ml,m'l'}(kd, \eta) \cos(m - m')\psi$$
$$- D_{ml,-m'l'}(kd, \eta) \cos(m + m')\psi, \quad \sigma \neq \sigma'$$

$$\mathcal{P}_{1\sigma ml, 2\sigma m'l'}(k\boldsymbol{d}) = (-1)^{m'} D_{ml,m'l'}(kd, \eta) \sin(m - m')\psi$$
$$+ (-1)^{\sigma} D_{ml,-m'l'}(kd, \eta) \sin(m + m')\psi$$

$$\mathcal{P}_{2\sigma ml, \tau \sigma' m'l'}(k\boldsymbol{d}) = \mathcal{P}_{1\sigma ml, \bar{\tau}\sigma' m'l'}(k\boldsymbol{d}), \quad \tau = 1, 2$$

where

$$C_{ml,m'l'}(kd,\eta) = \frac{(-1)^{m+m'}}{2}\sqrt{\frac{\varepsilon_m\varepsilon_{m'}}{4}}$$

$$\times \sum_{\lambda=|l-l'|}^{l+l'} i^{l'-l+\lambda}(2\lambda+1)\sqrt{\frac{(2l+1)(2l'+1)(\lambda-(m-m'))!}{l(l+1)l'(l'+1)(\lambda+(m-m'))!}}$$

$$\times \begin{pmatrix} l & l' & \lambda \\ 0 & 0 & 0 \end{pmatrix}\begin{pmatrix} l & l' & \lambda \\ m & -m' & m'-m \end{pmatrix}[l(l+1)+l'(l'+1)-\lambda(\lambda+1)]$$

$$\times h_\lambda^{(1)}(kd)P_\lambda^{m-m'}(\cos\eta)$$

$$D_{ml,m'l'}(kd,\eta) = \frac{(-1)^{m+m'}}{2}\sqrt{\frac{\varepsilon_m\varepsilon_{m'}}{4}}$$

$$\times \sum_{\lambda=|l-l'|+1}^{l+l'} i^{l'-l+\lambda+1}(2\lambda+1)\sqrt{\frac{(2l+1)(2l'+1)(\lambda-(m-m'))!}{l(l+1)l'(l'+1)(\lambda+(m-m'))!}}$$

$$\times \begin{pmatrix} l & l' & \lambda-1 \\ 0 & 0 & 0 \end{pmatrix}\begin{pmatrix} l & l' & \lambda \\ m & -m' & m'-m \end{pmatrix}\sqrt{\lambda^2-(l-l')^2}$$

$$\times \sqrt{(l+l'+1)^2-\lambda^2}h_\lambda^{(1)}(kd)P_\lambda^{m-m'}(\cos\eta)$$

where $\varepsilon_m = 2 - \delta_{m,0}$ is the Neumann factor, and where $\begin{pmatrix} \cdot & \cdot & \cdot \\ \cdot & \cdot & \cdot \end{pmatrix}$ denotes Wigner's 3j symbol [11], and

$$(-1)^\sigma = \begin{cases} 1, & \sigma = \mathrm{e} \\ -1, & \sigma = \mathrm{o} \end{cases}$$

Note that the factors $i^{l'-l+\lambda}$ in $C_{ml,m'l'}(d,\eta)$ and $i^{l'-l+\lambda+1}$ in $D_{ml,m'l'}(d,\eta)$ are always real numbers, due to the conditions on the Wigner's 3j symbol.

We notice that the translation matrices have the form

$$\mathcal{P}_{nn'}(k\boldsymbol{d}) = \sum_{\lambda=|l-l'|+|\tau-\tau'|}^{l+l'} h_\lambda^{(1)}(kd)\left(A_{nn'\lambda}(\psi)P_\lambda^{m-m'}(\cos\eta) + B_{nn'\lambda}(\psi)P_\lambda^{m+m'}(\cos\eta)\right)$$

B.1   Average w.r.t. the azimuthal angle ψ

The integral of the translational matrix w.r.t. the azimuthal variable ψ is relevant, see (7.13). Explicitly, the non-zero contributions for a general $m \geq 0$ are

$$\begin{cases} \displaystyle\int_0^{2\pi} A_{1eml,1em'l'\lambda}(\psi)\,\mathrm{d}\psi = 2\pi(-1)^m\delta_{mm'}C_{mll'\lambda} \\[2mm] \displaystyle\int_0^{2\pi} A_{1eml,2om'l'\lambda}(\psi)\,\mathrm{d}\psi = 2\pi(-1)^m\delta_{mm'}D_{mll'\lambda} \\[2mm] \displaystyle\int_0^{2\pi} A_{2oml,1em'l'\lambda}(\psi)\,\mathrm{d}\psi = \int_0^{2\pi} A_{1oml,2em'l'\lambda}(\psi)\,\mathrm{d}\psi \\[2mm] \displaystyle\int_0^{2\pi} A_{2oml,2om'l'\lambda}(\psi)\,\mathrm{d}\psi = \int_0^{2\pi} A_{1oml,1om'l'\lambda}(\psi)\,\mathrm{d}\psi \end{cases}$$

$$
\begin{cases}
\displaystyle\int_0^{2\pi} A_{1oml,1om'l'\lambda}(\psi)\ \mathrm{d}\psi = 2\pi(-1)^m \delta_{mm'} C_{mll'\lambda} \\[2ex]
\displaystyle\int_0^{2\pi} A_{1oml,2em'l'\lambda}(\psi)\ \mathrm{d}\psi = -2\pi(-1)^m \delta_{mm'} D_{mll'\lambda} \\[2ex]
\displaystyle\int_0^{2\pi} A_{2eml,1om'l'\lambda}(\psi)\ \mathrm{d}\psi = \int_0^{2\pi} A_{1eml,2om'l'\lambda}(\psi)\ \mathrm{d}\psi \\[2ex]
\displaystyle\int_0^{2\pi} A_{2eml,2em'l'\lambda}(\psi)\ \mathrm{d}\psi = \int_0^{2\pi} A_{1eml,1em'l'\lambda}(\psi)\ \mathrm{d}\psi
\end{cases}
$$

and the average over the function B becomes

$$
\begin{cases}
\displaystyle\int_0^{2\pi} B_{1eml,1em'l'\lambda}(\psi)\ \mathrm{d}\psi = 2\pi\delta_{mm'}\delta_{m,0} C_{mll'\lambda} \\[2ex]
\displaystyle\int_0^{2\pi} B_{1eml,2om'l'\lambda}(\psi)\ \mathrm{d}\psi = -2\pi\delta_{mm'}\delta_{m,0} D_{mll'\lambda} \\[2ex]
\displaystyle\int_0^{2\pi} B_{2oml,1em'l'\lambda}(\psi)\ \mathrm{d}\psi = \int_0^{2\pi} B_{1oml,2em'l'\lambda}(\psi)\ \mathrm{d}\psi \\[2ex]
\displaystyle\int_0^{2\pi} B_{2oml,2om'l'\lambda}(\psi)\ \mathrm{d}\psi = \int_0^{2\pi} B_{1oml,1om'l'\lambda}(\psi)\ \mathrm{d}\psi
\end{cases}
$$

$$
\begin{cases}
\displaystyle\int_0^{2\pi} B_{1oml,1om'l'\lambda}(\psi)\ \mathrm{d}\psi = -2\pi\delta_{mm'}\delta_{m,0} C_{mll'\lambda} \\[2ex]
\displaystyle\int_0^{2\pi} B_{1oml,2em'l'\lambda}(\psi)\ \mathrm{d}\psi = -2\pi\delta_{mm'}\delta_{m,0} D_{ml,ml'\lambda} \\[2ex]
\displaystyle\int_0^{2\pi} B_{2eml,1om'l'\lambda}(\psi)\ \mathrm{d}\psi = \int_0^{2\pi} B_{1eml,2om'l'\lambda}(\psi)\ \mathrm{d}\psi \\[2ex]
\displaystyle\int_0^{2\pi} B_{2eml,2em'l'\lambda}(\psi)\ \mathrm{d}\psi = \int_0^{2\pi} B_{1eml,1em'l'\lambda}(\psi)\ \mathrm{d}\psi
\end{cases}
$$

The explicit form of the average is, see (7.13)

$$
\mathcal{A}_{nn'\lambda} = \int_0^{2\pi} A_{nn'\lambda}(\phi)\ \mathrm{d}\phi + \int_0^{2\pi} B_{nn'\lambda}(\phi)\ \mathrm{d}\phi
$$

$$
= 2\pi(-1)^m \delta_{mm'} \;
\begin{array}{c}
\begin{array}{cccc} 1e & 2o & 1o & 2e \end{array} \\
\begin{array}{c} 1e \\ 2o \\ 1o \\ 2e \end{array}
\left(
\begin{array}{cccc}
C & D & 0 & 0 \\
-D & C & 0 & 0 \\
0 & 0 & C & -D \\
0 & 0 & D & C
\end{array}
\right)
\end{array}, \quad m = 1,2,\dots
$$

and

$$\mathcal{A}_{nn'\lambda} = \int_0^{2\pi} A_{nn'\lambda}(\phi)\ \mathrm{d}\phi + \int_0^{2\pi} B_{nn'\lambda}(\phi)\ \mathrm{d}\phi$$

$$= 2\pi\delta_{mm'} \begin{array}{c} \\ \text{1e} \\ \text{2o} \\ \text{1o} \\ \text{2e} \end{array} \begin{pmatrix} \overset{\text{1e}}{C} & \overset{\text{2o}}{0} & \overset{\text{1o}}{0} & \overset{\text{2e}}{0} \\ 0 & 0 & 0 & 0 \\ 0 & 0 & 0 & 0 \\ 0 & 0 & 0 & C \end{pmatrix}, \quad m = 0$$

where

$$C = C_{mll'\lambda} = \frac{\mathrm{i}^{l'-l+\lambda}(2\lambda+1)}{2}\sqrt{\frac{(2l+1)(2l'+1)}{l(l+1)l'(l'+1)}}$$

$$\times \begin{pmatrix} l & l' & \lambda \\ 0 & 0 & 0 \end{pmatrix} \begin{pmatrix} l & l' & \lambda \\ m & -m & 0 \end{pmatrix} [l(l+1) + l'(l'+1) - \lambda(\lambda+1)]$$

$$D = D_{mll'\lambda} = \frac{\mathrm{i}^{l'-l+\lambda+1}(2\lambda+1)}{2}\sqrt{\frac{(2l+1)(2l'+1)}{l(l+1)l'(l'+1)}}$$

$$\times \begin{pmatrix} l & l' & \lambda-1 \\ 0 & 0 & 0 \end{pmatrix} \begin{pmatrix} l & l' & \lambda \\ m & -m & 0 \end{pmatrix} \sqrt{\lambda^2 - (l-l')^2}\sqrt{(l+l'+1)^2 - \lambda^2}$$

Appendix C   Planar vector waves

Planar vector waves are commonly used in this paper. The planar vector waves $\boldsymbol{\varphi}_j^{\pm}(\boldsymbol{k}_{\mathrm{t}}; k, \boldsymbol{r})$, $j = 1, 2$, are defined as [4, 25]

$$\boldsymbol{\varphi}_1^{\pm}(\boldsymbol{k}_{\mathrm{t}}; k, \boldsymbol{r}) = \frac{\hat{\boldsymbol{z}} \times \boldsymbol{k}_{\mathrm{t}}}{4\pi \mathrm{i} k_{\mathrm{t}}} \mathrm{e}^{\mathrm{i}\boldsymbol{k}_{\mathrm{t}}\cdot\boldsymbol{r}_{\mathrm{c}} \pm \mathrm{i} k_{\mathrm{z}} z}, \quad \boldsymbol{\varphi}_2^{\pm}(\boldsymbol{k}_{\mathrm{t}}; k, \boldsymbol{r}) = \frac{\mp \boldsymbol{k}_{\mathrm{t}} k_{\mathrm{z}} + k_{\mathrm{t}}^2 \hat{\boldsymbol{z}}}{4\pi k k_{\mathrm{t}}} \mathrm{e}^{\mathrm{i}\boldsymbol{k}_{\mathrm{t}}\cdot\boldsymbol{r}_{\mathrm{c}} \pm \mathrm{i} k_{\mathrm{z}} z} \quad \text{(C.1)}$$

where the lateral distance $\boldsymbol{r}_{\mathrm{c}} = x\hat{\boldsymbol{x}} + y\hat{\boldsymbol{y}}$, the lateral wave vector $\boldsymbol{k}_{\mathrm{t}} = k_{\mathrm{x}}\hat{\boldsymbol{x}} + k_{\mathrm{y}}\hat{\boldsymbol{y}}$, the lateral wave number, $k_{\mathrm{t}} = |\boldsymbol{k}_{\mathrm{t}}|$, and the longitudinal wave number k_{z} is defined by

$$k_{\mathrm{z}} = \left(k^2 - k_{\mathrm{t}}^2\right)^{1/2} = \begin{cases} \sqrt{k^2 - k_{\mathrm{t}}^2} \text{ for } k_{\mathrm{t}} < k \\ \mathrm{i}\sqrt{k_{\mathrm{t}}^2 - k^2} \text{ for } k_{\mathrm{t}} > k \end{cases}$$

From these definitions, we identify $j = 1$ with a TE mode or $\perp$ electric polarization, and $j = 2$ with a TM or $\parallel$ electric polarization.

The planar vector waves satisfy

$$\nabla \times \boldsymbol{\varphi}_j^{\pm}(\boldsymbol{k}_{\mathrm{t}}; k, \boldsymbol{r}) = k\boldsymbol{\varphi}_{\bar{j}}^{\pm}(\boldsymbol{k}_{\mathrm{t}}; k, \boldsymbol{r}), \quad j = 1, 2$$

where the dual index $\bar{j}$ of j is $\bar{1} = 2$ and $\bar{2} = 1$. Consequently,

$$\nabla \times \left(\nabla \times \boldsymbol{\varphi}_j^{\pm}(\boldsymbol{k}_{\mathrm{t}}; k, \boldsymbol{r})\right) = k^2\boldsymbol{\varphi}_j^{\pm}(\boldsymbol{k}_{\mathrm{t}}; k, \boldsymbol{r}), \quad j = 1, 2$$

The planar vector waves satisfy orthogonality relations. These are collected in Appendix C.1.

C.1 Orthogonality relations for the planar vector waves

In this appendix we collect a series of orthogonality relation of the planar vector waves that is used in the analysis.

On a general plane surface S, which is defined as $z = z_0$, we have

$$
\begin{cases}
\displaystyle \iint\limits_{S} \boldsymbol{\varphi}_j^{\pm\dagger}(\boldsymbol{k}_{\mathrm{t}}; k, \boldsymbol{r}) \cdot \left(\hat{\boldsymbol{z}} \times \boldsymbol{\varphi}_{j'}^{\mp}(\boldsymbol{k}_{\mathrm{t}}'; k, \boldsymbol{r})\right) \, \mathrm{d}x \, \mathrm{d}y = \mp \dfrac{k_{\mathrm{z}}}{4\mathrm{i}k} \delta_{\bar{j}j'} \delta(\boldsymbol{k}_{\mathrm{t}} - \boldsymbol{k}_{\mathrm{t}}') \\[3ex]
\displaystyle \iint\limits_{S} \boldsymbol{\varphi}_j^{\pm\dagger}(\boldsymbol{k}_{\mathrm{t}}; k, \boldsymbol{r}) \cdot \left(\hat{\boldsymbol{z}} \times \boldsymbol{\varphi}_{j'}^{\pm}(\boldsymbol{k}_{\mathrm{t}}'; k, \boldsymbol{r})\right) \, \mathrm{d}x \, \mathrm{d}y = \pm \dfrac{(-1)^{j'} k_{\mathrm{z}}}{4\mathrm{i}k} \mathrm{e}^{\pm 2\mathrm{i}k_{\mathrm{z}}z_0} \delta_{\bar{j}j'} \delta(\boldsymbol{k}_{\mathrm{t}} - \boldsymbol{k}_{\mathrm{t}}')
\end{cases}
$$

where the dagger $\dagger$ denotes a planar vector wave with reversed argument $\boldsymbol{k}_{\mathrm{t}}$, $i.e.$, $\boldsymbol{\varphi}_j^{\pm\dagger}(\boldsymbol{k}_{\mathrm{t}}; k, \boldsymbol{r}) = \boldsymbol{\varphi}_j^{\pm}(-\boldsymbol{k}_{\mathrm{t}}; k, \boldsymbol{r})$.

Explicitly, on the planar surface S_1, we have

$$
\iint\limits_{S_1} \boldsymbol{\varphi}_j^{+\dagger}(\boldsymbol{k}_{\mathrm{t}}; k_1, \boldsymbol{r}) \cdot \left(-\hat{\boldsymbol{z}} \times \boldsymbol{\varphi}_{j'}^{\pm}(\boldsymbol{k}_{\mathrm{t}}'; k_2, \boldsymbol{r})\right) \, \mathrm{d}x \, \mathrm{d}y
$$

$$
= \frac{\delta(\boldsymbol{k}_{\mathrm{t}} - \boldsymbol{k}_{\mathrm{t}}') \delta_{\bar{j}j'} \mathrm{e}^{\mathrm{i}(k_{1\mathrm{z}} \pm k_{2\mathrm{z}})z_1}}{4\mathrm{i}}
\begin{cases}
\mp \dfrac{k_{2\mathrm{z}}}{k_2}, & j = 1 \\[2ex]
\dfrac{k_{1\mathrm{z}}}{k_1}, & j = 2
\end{cases}
$$

$$
= \frac{(\mp 1)^j \delta(\boldsymbol{k}_{\mathrm{t}} - \boldsymbol{k}_{\mathrm{t}}') \delta_{\bar{j}j'} \mathrm{e}^{\mathrm{i}(k_{1\mathrm{z}} \pm k_{2\mathrm{z}})z_1} \frac{k_{\bar{j}\mathrm{z}}}{k_{\bar{j}}}}{4\mathrm{i}} \tag{C.2}
$$

and

$$
\iint\limits_{S_1} \boldsymbol{\varphi}_j^{-\dagger}(\boldsymbol{k}_{\mathrm{t}}; k_1, \boldsymbol{r}) \cdot \left(-\hat{\boldsymbol{z}} \times \boldsymbol{\varphi}_{j'}^{\pm}(\boldsymbol{k}_{\mathrm{t}}'; k_2, \boldsymbol{r})\right) \, \mathrm{d}x \, \mathrm{d}y
$$

$$
= \frac{\delta(\boldsymbol{k}_{\mathrm{t}} - \boldsymbol{k}_{\mathrm{t}}') \delta_{\bar{j}j'} \mathrm{e}^{-\mathrm{i}(k_{1\mathrm{z}} \mp k_{2\mathrm{z}})z_1}}{4\mathrm{i}}
\begin{cases}
\mp \dfrac{k_{2\mathrm{z}}}{k_2}, & j = 1 \\[2ex]
-\dfrac{k_{1\mathrm{z}}}{k_1}, & j = 2
\end{cases}
$$

$$
= -\frac{(\pm 1)^j \delta(\boldsymbol{k}_{\mathrm{t}} - \boldsymbol{k}_{\mathrm{t}}') \delta_{\bar{j}j'} \mathrm{e}^{-\mathrm{i}(k_{1\mathrm{z}} \mp k_{2\mathrm{z}})z_1} \frac{k_{\bar{j}\mathrm{z}}}{k_{\bar{j}}}}{4\mathrm{i}} \tag{C.3}
$$

On the planar surface S_2 we have use for

$$
\iint\limits_{S_2} \boldsymbol{\varphi}_j^{+\dagger}(\boldsymbol{k}_{\mathrm{t}}; k_3, \boldsymbol{r}) \cdot \left(\hat{\boldsymbol{z}} \times \boldsymbol{\varphi}_{j'}^{\pm}(\boldsymbol{k}_{\mathrm{t}}'; k_2, \boldsymbol{r})\right) \, \mathrm{d}x \, \mathrm{d}y
$$

$$
= \frac{\delta(\boldsymbol{k}_{\mathrm{t}} - \boldsymbol{k}_{\mathrm{t}}') \delta_{\bar{j}j'} \mathrm{e}^{\mathrm{i}(k_{3\mathrm{z}} \pm k_{2\mathrm{z}})z_2}}{4\mathrm{i}} \begin{cases} \pm \dfrac{k_{2\mathrm{z}}}{k_2}, & j = 1 \\[2mm] -\dfrac{k_{3\mathrm{z}}}{k_3}, & j = 2 \end{cases}
$$

$$
= -\frac{(\mp 1)^j \delta(\boldsymbol{k}_{\mathrm{t}} - \boldsymbol{k}_{\mathrm{t}}') \delta_{\bar{j}j'} \mathrm{e}^{\mathrm{i}(k_{3\mathrm{z}} \pm k_{2\mathrm{z}})z_2} \frac{k_{j+1\mathrm{z}}}{k_{j+1}}}{4\mathrm{i}} \quad (\text{C.4})
$$

and

$$
\iint\limits_{S_2} \boldsymbol{\varphi}_j^{-\dagger}(\boldsymbol{k}_{\mathrm{t}}; k_3, \boldsymbol{r}) \cdot \left(\hat{\boldsymbol{z}} \times \boldsymbol{\varphi}_{j'}^{\pm}(\boldsymbol{k}_{\mathrm{t}}'; k_2, \boldsymbol{r})\right) \, \mathrm{d}x \, \mathrm{d}y
$$

$$
= \frac{\delta(\boldsymbol{k}_{\mathrm{t}} - \boldsymbol{k}_{\mathrm{t}}') \delta_{\bar{j}j'} \mathrm{e}^{-\mathrm{i}(k_{3\mathrm{z}} \mp k_{2\mathrm{z}})z_2}}{4\mathrm{i}} \begin{cases} \pm \dfrac{k_{2\mathrm{z}}}{k_2}, & j = 1 \\[2mm] \dfrac{k_{3\mathrm{z}}}{k_3}, & j = 2 \end{cases}
$$

$$
= \frac{(\pm 1)^j \delta(\boldsymbol{k}_{\mathrm{t}} - \boldsymbol{k}_{\mathrm{t}}') \delta_{\bar{j}j'} \mathrm{e}^{-\mathrm{i}(k_{3\mathrm{z}} \mp k_{2\mathrm{z}})z_2} \frac{k_{j+1\mathrm{z}}}{k_{j+1}}}{4\mathrm{i}} \quad (\text{C.5})
$$

C.2 Expansion function for a given incident field

There is an alternative representation of the expansion functions $a_j(\boldsymbol{k}_{\mathrm{t}})$ for the incident fields $\boldsymbol{E}_{\mathrm{i}}$ and $\boldsymbol{H}_{\mathrm{i}}$ in (4.2), see [25]

$$
\begin{aligned}
a_j(\boldsymbol{k}_{\mathrm{t}}) = &- \frac{2\mathrm{i}k_1}{k_{1\mathrm{z}}} \iint\limits_{S} \boldsymbol{\varphi}_j^{-\dagger}(\boldsymbol{k}_{\mathrm{t}}; k_1, \boldsymbol{r}) \cdot (\hat{\boldsymbol{\nu}} \times \mathrm{i}\eta_0\eta_1 \boldsymbol{H}_{\mathrm{i}}(\boldsymbol{r})) \, \mathrm{d}S \\
&- \frac{2\mathrm{i}k_1}{k_{1\mathrm{z}}} \iint\limits_{S} \boldsymbol{\varphi}_{\bar{j}}^{-\dagger}(\boldsymbol{k}_{\mathrm{t}}; k_1, \boldsymbol{r}) \cdot (\hat{\boldsymbol{\nu}} \times \boldsymbol{E}_{\mathrm{i}}(\boldsymbol{r})) \, \mathrm{d}S, \quad \boldsymbol{k}_{\mathrm{t}} \in \mathbb{R}^2, \; j = 1, 2
\end{aligned} \quad (\text{C.6})
$$

where the surface S is any plane surface to the left of S_1, but to the right of the volume V_{i}, which contains the sources of the incident field. For a given incident field, this expression gives an explicit formula for the computation of the expansion functions $a_j(\boldsymbol{k}_{\mathrm{t}})$.

Appendix D   The Green dyadic

An important tool is the decomposition of the Green dyadic for the electric field in free space. We decompose the Green dyadic in spherical vector waves, see [4, 25].

$$
\mathbf{G}_{\mathrm{e}}(k, |\boldsymbol{r} - \boldsymbol{r}'|) = \mathrm{i}k \sum_n \boldsymbol{v}_n(k\boldsymbol{r}_<) \boldsymbol{u}_n(k\boldsymbol{r}_>) \quad (\text{D.1})
$$

where the index n is a multi-index,[5] and where $\boldsymbol{r}_<$ $(\boldsymbol{r}_>)$ is the position vector with the smallest (largest) distance to the origin, *i.e.*, if $r < r'$ then $\boldsymbol{r}_< = \boldsymbol{r}$ and $\boldsymbol{r}_> = \boldsymbol{r}'$. This expansion is uniformly convergent in finite domains, provided $r \neq r'$ in the domain [7]. The regular spherical vector waves $\boldsymbol{v}_n(k\boldsymbol{r})$ and the radiating (out-going) spherical vector waves $\boldsymbol{u}_n(k\boldsymbol{r})$ are defined in Appendix A.

The Green dyadic can also be decomposed in planar vector waves [4, 25].

$$\mathbf{G}_{\mathrm{e}}(k, |\boldsymbol{r} - \boldsymbol{r}'|) = 2\mathrm{i}k \sum_{j=1,2} \iint_{\mathbb{R}^2} \boldsymbol{\varphi}_j^{\pm}(\boldsymbol{k}_{\mathrm{t}}; k, \boldsymbol{r}) \boldsymbol{\varphi}_j^{\mp\dagger}(\boldsymbol{k}_{\mathrm{t}}; k, \boldsymbol{r}') \frac{k}{k_{\mathrm{z}}} \frac{\mathrm{d}k_{\mathrm{x}}\,\mathrm{d}k_{\mathrm{y}}}{k^2} \qquad (\mathrm{D.2})$$

where the upper (lower) is used if $z > z'$ $(z < z')$, and where $\boldsymbol{\varphi}_j^{\pm\dagger}(\boldsymbol{k}_{\mathrm{t}}; k, \boldsymbol{r}) = \boldsymbol{\varphi}_j^{\pm}(-\boldsymbol{k}_{\mathrm{t}}; k, \boldsymbol{r})$.

D.1 Transformation spherical and planar vector waves

Of frequent use in this paper is the comparison between the two types of solutions of the Maxwell equations — the spherical vector waves and the planar vector waves.

The outgoing spherical vector waves, $\boldsymbol{u}_n(k\boldsymbol{r})$, can be expressed in the planar vector waves, $\boldsymbol{\varphi}_j^{\pm}(\boldsymbol{k}_{\mathrm{t}}; \boldsymbol{r})$, $j = 1, 2$. This transformation reads, see [4, p. 183]

$$\boldsymbol{u}_n(k\boldsymbol{r}) = 2 \sum_{j=1,2} \iint_{\mathbb{R}^2} B_{nj}^{\pm}(\boldsymbol{k}_{\mathrm{t}}) \boldsymbol{\varphi}_j^{\pm}(\boldsymbol{k}_{\mathrm{t}}; k, \boldsymbol{r}) \frac{k}{k_{\mathrm{z}}} \frac{\mathrm{d}k_{\mathrm{x}}\,\mathrm{d}k_{\mathrm{y}}}{k^2}, \quad z \gtrless 0 \qquad (\mathrm{D.3})$$

where[6]

$$B_{nj}^{+}(\boldsymbol{k}_{\mathrm{t}}) = \mathrm{i}^{-l} C_{lm} \left\{ -\mathrm{i}\delta_{\tau j} \Delta_l^m(k_{\mathrm{z}}/k) \left\{ \begin{matrix} \cos m\beta \\ \sin m\beta \end{matrix} \right\} - \delta_{\tau\bar{j}} \pi_l^m(k_{\mathrm{z}}/k) \left\{ \begin{matrix} -\sin m\beta \\ \cos m\beta \end{matrix} \right\} \right\} \quad (\mathrm{D.4})$$

and

$$B_{nj}^{-}(\boldsymbol{k}_{\mathrm{t}}) = (-1)^{l+m+\tau+j+1} B_{nj}^{+}(\boldsymbol{k}_{\mathrm{t}})$$

where again the index $\bar{j}$ is the dual index of j, defined by $\bar{1} = 2$ and $\bar{2} = 1$, and where $\boldsymbol{k}_{\mathrm{t}} = k_{\mathrm{t}}(\hat{\boldsymbol{x}} \cos \beta + \hat{\boldsymbol{y}} \sin \beta)$, and

$$C_{lm} = \sqrt{\frac{\varepsilon_m}{2\pi}} \sqrt{\frac{2l+1}{2} \frac{(l-m)!}{(l+m)!}}$$

---

[5]Depending on the context, the index n consists of three or four different indices, *i.e.*, $n = \sigma m l$ or $n = \tau \sigma m l$, where $\tau = 1, 2$, $\sigma = \mathrm{e}, \mathrm{o}$, $m = 0, 1, 2, \ldots, l$, and $l = 1, 2, 3, \ldots$. Both conventions are used in this paper. For more details abut this convention, we refer to Ref. 25.

[6]There is an alternative definition of the transformation coefficients $B_{nj}^{+}(\boldsymbol{k}_{\mathrm{t}})$.

$$B_{nj}^{+}(\boldsymbol{k}_{\mathrm{t}}) = \mathrm{i}^{-l} \left\{ -\mathrm{i}\delta_{\tau j} \hat{\boldsymbol{\alpha}} \cdot \boldsymbol{A}_{2n}(\hat{\boldsymbol{k}}) - \delta_{\tau\bar{j}} \hat{\boldsymbol{\beta}} \cdot \boldsymbol{A}_{2n}(\hat{\boldsymbol{k}}) \right\} = \mathrm{i}^{-l} \left\{ \mathrm{i}\delta_{\tau j} \hat{\boldsymbol{\beta}} \cdot \boldsymbol{A}_{1n}(\hat{\boldsymbol{k}}) - \delta_{\tau\bar{j}} \hat{\boldsymbol{\alpha}} \cdot \boldsymbol{A}_{1n}(\hat{\boldsymbol{k}}) \right\}$$

where $\hat{\boldsymbol{k}} = \hat{\boldsymbol{x}} \sin \alpha \cos \beta + \hat{\boldsymbol{y}} \sin \alpha \sin \beta + \hat{\boldsymbol{z}} \cos \alpha = (\boldsymbol{k}_{\mathrm{t}} + \hat{\boldsymbol{z}}k_z)/k$, $\cos \alpha > 0$.

The Neumann factor is defined as $\varepsilon_m = 2 - \delta_{m0}$, and

$$\Delta_l^m(t) = -\frac{(1-t^2)^{1/2}}{\sqrt{l(l+1)}}P_l^{m\prime}(t), \quad \pi_l^m(t) = \frac{m}{\sqrt{l(l+1)}\,(1-t^2)^{1/2}}P_l^m(t)$$

where $P_l^m(t)$ are the associated Legendre functions. Notice that the argument t can take complex values.

Moreover, we make use of [4]

$$\varphi_j^\pm(\boldsymbol{k}_{\mathrm{t}}; k, \boldsymbol{r}) = \sum_n B_{nj}^{\pm\,\dagger}(\boldsymbol{k}_{\mathrm{t}})\boldsymbol{v}_n(k\boldsymbol{r}) \tag{D.5}$$

where $B_{nj}^{\pm\,\dagger}(\boldsymbol{k}_{\mathrm{t}}) = (-1)^{l+\tau+j+1}B_{nj}^\pm(\boldsymbol{k}_{\mathrm{t}})$.

Appendix E Probability density functions

The statistical distribution of the N scatterers, positioned at $\boldsymbol{r}_p$, $p = 1, 2, \ldots, N$, and the state, which is collected in one symbol ξ_p, $p = 1, 2, \ldots, N$, is described by the N-particle probability density function $P(\boldsymbol{r}_1, \ldots, \boldsymbol{r}_N; \xi_1, \ldots, \xi_N)$. This function quantifies the probability of finding the first scatterer in a volume element $\mathrm{d}v_1$ centered at $\boldsymbol{r}_1$ with its state in $\mathrm{d}\xi_1$ centered at ξ_1, the second scatterer in a volume element $\mathrm{d}v_2$ centered at $\boldsymbol{r}_2$ with its state in $\mathrm{d}\xi_2$ centered at ξ_2, and, in general, the pth scatterer within a volume element $\mathrm{d}v_p$ centered at position $\boldsymbol{r}_p$ with its state in $\mathrm{d}\xi_p$ centered at ξ_p as

$$P(\boldsymbol{r}_1, \ldots, \boldsymbol{r}_N; \xi_1, \ldots, \xi_N)\prod_{p=1}^{N}\mathrm{d}v_p\,\mathrm{d}\xi_p$$

The assumption of the independence of the state and position variables implies that the N-particle probability density function takes the form

$$P(\boldsymbol{r}_1, \ldots, \boldsymbol{r}_N; \xi_1, \ldots, \xi_N) = P(\boldsymbol{r}_1, \ldots, \boldsymbol{r}_N)\prod_{p=1}^{N}P_{\mathrm{s}}(\xi_p)$$

where $P(\boldsymbol{r}_1, \ldots, \boldsymbol{r}_N)$ denotes the probability density function depending on the location of the individual scatterer, and $P_{\mathrm{s}}(\xi_p)$ the probability density function depending on the state of the pth scatterer. Conservation of probability implies

$$\int_{V_{\mathrm{s}}^N} P(\boldsymbol{r}_1, \ldots, \boldsymbol{r}_N)\prod_{p=1}^{N}\mathrm{d}v_p = 1$$

and

$$\int_{\Omega_{\mathrm{s}}} P_{\mathrm{s}}(\xi)\,\mathrm{d}\xi = 1$$

where the integration is taken over V_{s}, which is the entire range of the scatterers' positions,[7] and the states is assumed to take values in the abstract space Ω_{s}.

The probability density function $P(\boldsymbol{r}_1, \ldots, \boldsymbol{r}_N)$ is expressed in terms of conditional probability densities according to the definition of conditional probability density functions[8],[9]

$$
\begin{aligned}
P(\boldsymbol{r}_1, \ldots, \boldsymbol{r}_N) &= P(\boldsymbol{r}_1) P(\boldsymbol{r}_2, \ldots, \boldsymbol{r}_N | \boldsymbol{r}_1) \\
&= P(\boldsymbol{r}_1) P(\boldsymbol{r}_2 | \boldsymbol{r}_1) P(\boldsymbol{r}_3, \ldots, \boldsymbol{r}_N | \boldsymbol{r}_1, \boldsymbol{r}_2)
\end{aligned}
$$

where $P(\boldsymbol{r}_1)$ denotes the probability density of finding scatterer 1 in a volume element $\mathrm{d}v_1$ centered at $\boldsymbol{r}_1$, and where the function $P(\boldsymbol{r}_2, \ldots, \boldsymbol{r}_N | \boldsymbol{r}_1)$ is the conditional probability density of finding scatterer 2 in a volume element $\mathrm{d}v_2$ centered at $\boldsymbol{r}_2$ and scatterer 3 in a volume element $\mathrm{d}v_3$ centered at $\boldsymbol{r}_3$ *etc.*, given scatterer 1 in a volume element $\mathrm{d}v_1$ centered at $\boldsymbol{r}_1$. $P(\boldsymbol{r}_2 | \boldsymbol{r}_1)$ denotes the conditional probability density of finding scatterer 2 in a volume element $\mathrm{d}v_2$ centered at $\boldsymbol{r}_2$ provided scatterer 1 is known to be in a volume element $\mathrm{d}v_1$ centered at $\boldsymbol{r}_1$, and the function $P(\boldsymbol{r}_3, \ldots, \boldsymbol{r}_N | \boldsymbol{r}_1, \boldsymbol{r}_2)$ is the conditional probability density of finding scatterer 3 in a volume element $\mathrm{d}v_3$ centered at $\boldsymbol{r}_3$ and scatterer 4 in a volume element $\mathrm{d}v_4$ centered at $\boldsymbol{r}_4$ *etc.*, given scatterer 1 in a volume element $\mathrm{d}v_1$ centered at $\boldsymbol{r}_1$ and scatterer 2 in a volume element $\mathrm{d}v_2$ centered at $\boldsymbol{r}_2$.

The single-scatterer and two-scatterer probability density functions $P(\boldsymbol{r}_p)$ and $P(\boldsymbol{r}_p, \boldsymbol{r}_q)$ are computed as

$$
P(\boldsymbol{r}_p) = \int\limits_{V_{\mathrm{s}}^{N-1}} P(\boldsymbol{r}_1, \boldsymbol{r}_2, \ldots, \boldsymbol{r}_N) \prod_{\substack{r=1 \\ r \neq p}}^{N} \mathrm{d}v_r, \qquad \iiint\limits_{V_{\mathrm{s}}} P(\boldsymbol{r}) \, \mathrm{d}v = 1 \qquad \text{(E.1)}
$$

and

$$
P(\boldsymbol{r}_p, \boldsymbol{r}_q) = \int\limits_{V_{\mathrm{s}}^{N-2}} P(\boldsymbol{r}_1, \boldsymbol{r}_2, \boldsymbol{r}_3, \ldots, \boldsymbol{r}_N) \prod_{\substack{r=1 \\ r \neq p,q}}^{N} \mathrm{d}v_r, \qquad \int\limits_{V_{\mathrm{s}}^2} P(\boldsymbol{r}_1, \boldsymbol{r}_2) \, \mathrm{d}v_1 \, \mathrm{d}v_2 = 1 \quad \text{(E.2)}
$$

respectively. Moreover, we have by definition

$$
\iiint\limits_{V_{\mathrm{s}}} P(\boldsymbol{r}_p, \boldsymbol{r}_q) \, \mathrm{d}v_q = P(\boldsymbol{r}_p)
$$

---

[7]To be exact, the volume that the local origins, $\boldsymbol{r}_p$, can occupy. This volume is not the same as the convex hull of all scatterer.

[8]The conditional probability density function is defined as [47, Sec. 7.2]

$$
P(\boldsymbol{r}_{k+1}, \ldots, \boldsymbol{r}_N | \boldsymbol{r}_1, \ldots, \boldsymbol{r}_k) = \frac{P(\boldsymbol{r}_1, \ldots, \boldsymbol{r}_N)}{P(\boldsymbol{r}_1, \ldots, \boldsymbol{r}_k)}
$$

[9]Since the order of numbering is arbitrary, we specialize to scatterers 1 and 2. Any other combination of scatterers follows with a similar notation.

From these definitions and the definition of the conditional probability density function, we also have

$$P(\boldsymbol{r}_1) \int_{V_{\mathrm{s}}^{N-1}} P(\boldsymbol{r}_2, \ldots, \boldsymbol{r}_N | \boldsymbol{r}_1) \prod_{r=2}^{N} \mathrm{d}v_r = \int_{V_{\mathrm{s}}^{N-1}} P(\boldsymbol{r}_1, \boldsymbol{r}_2, \ldots, \boldsymbol{r}_N) \prod_{r=2}^{N} \mathrm{d}v_r = P(\boldsymbol{r}_1)$$

and therefore

$$\int_{V_{\mathrm{s}}^{N-1}} P(\boldsymbol{r}_2, \ldots, \boldsymbol{r}_N | \boldsymbol{r}_1) \prod_{r=2}^{N} \mathrm{d}v_r = 1$$

The two-scatterer probability density functions $P(\boldsymbol{r}_p, \boldsymbol{r}_q)$ and the conditional probability density function $P(\boldsymbol{r}_q | \boldsymbol{r}_p)$ are related as

$$P(\boldsymbol{r}_p, \boldsymbol{r}_q) = P(\boldsymbol{r}_p) P(\boldsymbol{r}_q | \boldsymbol{r}_p)$$

and

$$\iiint_{V_{\mathrm{s}}} P(\boldsymbol{r}_q | \boldsymbol{r}_p) \, \mathrm{d}v_q = 1$$

The average of a function $f(\boldsymbol{r}_1, \ldots, \boldsymbol{r}_N; \xi_1, \ldots, \xi_N)$ over all position variables is denoted

$$\langle f \rangle = \int_{\Omega_{\mathrm{s}}^{N}} \int_{V_{\mathrm{s}}^{N}} P(\boldsymbol{r}_1, \ldots, \boldsymbol{r}_N) \prod_{p=1}^{N} P_{\mathrm{s}}(\xi_p) f(\boldsymbol{r}_1, \ldots, \boldsymbol{r}_N; \xi_1, \ldots, \xi_N) \prod_{p=1}^{N} \mathrm{d}v_p \, \mathrm{d}\xi_p$$

If the position and state of the first scatterer are held fixed and all other scatterers are averaged over, we use the notion

$$\langle f \rangle (\boldsymbol{r}_1; \xi_1) = \int_{\Omega_{\mathrm{s}}^{N-1}} \int_{V_{\mathrm{s}}^{N-1}} P(\boldsymbol{r}_2, \ldots, \boldsymbol{r}_N | \boldsymbol{r}_1) \prod_{p=2}^{N} P_{\mathrm{s}}(\xi_p)$$

$$\times f(\boldsymbol{r}_1, \ldots, \boldsymbol{r}_N; \xi_1, \ldots, \xi_N) \prod_{p=2}^{N} \mathrm{d}v_p \, \mathrm{d}\xi_p$$

and

$$\langle f \rangle (\boldsymbol{r}_1) = \int_{\Omega_{\mathrm{s}}^{N}} \int_{V_{\mathrm{s}}^{N-1}} P(\boldsymbol{r}_2, \ldots, \boldsymbol{r}_N | \boldsymbol{r}_1) \prod_{p=1}^{N} P_{\mathrm{s}}(\xi_p)$$

$$\times f(\boldsymbol{r}_1, \ldots, \boldsymbol{r}_N; \xi_1, \ldots, \xi_N) \prod_{p=2}^{N} \mathrm{d}v_p \prod_{p=1}^{N} \mathrm{d}\xi_p$$

if we also include the average over the state variable ξ_1.

With scatterer 1 and 2 held fixed, we use the notion

$$\langle f \rangle \, (\boldsymbol{r}_1, \boldsymbol{r}_2; \xi_1, \xi_2) = \int\limits_{\Omega_{\mathrm{s}}^{N-2}} \int\limits_{V_{\mathrm{s}}^{N-2}} P(\boldsymbol{r}_3, \ldots, \boldsymbol{r}_N | \boldsymbol{r}_1, \boldsymbol{r}_2) \prod_{p=3}^{N} P_{\mathrm{s}}(\xi_p)$$

$$\times f(\boldsymbol{r}_1, \ldots, \boldsymbol{r}_N; \xi_1, \ldots, \xi_N) \prod_{p=3}^{N} \mathrm{d}v_p \, \mathrm{d}\xi_p$$

and a similar notation for any other combination of scatterers.

E.1 Number density functions

Of special interest is (single-scatterer) number density function $n_1(\boldsymbol{r})$ defined by

$$n_1(\boldsymbol{r}) = \sum_{p=1}^{N} \delta(\boldsymbol{r} - \boldsymbol{r}_p)$$

This definition implies

$$\iiint\limits_{V_{\mathrm{s}}} n_1(\boldsymbol{r}) \, \mathrm{d}v = N$$

which gives the total number of scatterers in V_{s}. The average number density is (use (E.1))

$$\langle n_1(\boldsymbol{r}) \rangle = \int\limits_{V_{\mathrm{s}}^{N}} P(\boldsymbol{r}_1, \ldots, \boldsymbol{r}_N) n_1(\boldsymbol{r}) \prod_{p=1}^{N} \mathrm{d}v_p = \sum_{p=1}^{N} P(\boldsymbol{r}) = N P(\boldsymbol{r})$$

If the medium is statistically homogeneous, the single-particle probability density function is simple (denote the volume of V_{s} by $|V_{\mathrm{s}}|$)

$$P(\boldsymbol{r}) = \begin{cases} \dfrac{1}{|V_{\mathrm{s}}|} = \dfrac{n_0}{N}, & \boldsymbol{r} \in V_{\mathrm{s}} \\ 0, & \boldsymbol{r} \notin V_{\mathrm{s}} \end{cases}$$

where the number density is[10]

$$n_0 = \langle n_1(\boldsymbol{r}) \rangle = \frac{N}{|V_{\mathrm{s}}|}$$

The two-scatterer number density function $n_2(\boldsymbol{r}, \boldsymbol{r}')$ is defined as

$$n_2(\boldsymbol{r}, \boldsymbol{r}') = \sum_{p=1}^{N} \sum_{\substack{q=1 \\ q \neq p}}^{N} \delta(\boldsymbol{r} - \boldsymbol{r}_p) \delta(\boldsymbol{r}' - \boldsymbol{r}_q)$$

---

[10]More exactly, the density or concentration of local origins.

The definition implies

$$\iiint\limits_{V_s} n_2(\boldsymbol{r}, \boldsymbol{r}') \, \mathrm{d}v' = (N-1)n_1(\boldsymbol{r})$$

The average two-particle number density is (use (E.2))

$$\langle n_2(\boldsymbol{r}, \boldsymbol{r}')\rangle = \int\limits_{V_s^N} P(\boldsymbol{r}_1, \ldots, \boldsymbol{r}_N) n_2(\boldsymbol{r}, \boldsymbol{r}') \prod_{p=1}^{N} \mathrm{d}v_p$$

$$= \sum_{p=1}^{N} \sum_{\substack{q=1 \\ q \neq p}} P(\boldsymbol{r}, \boldsymbol{r}') = N(N-1)P(\boldsymbol{r}, \boldsymbol{r}')$$

The pair distribution function $g(\boldsymbol{r}, \boldsymbol{r}')$ is now defined in terms of the one- and two-scatterer number densities. The definition of the pair distribution function is

$$\langle n_2(\boldsymbol{r}, \boldsymbol{r}')\rangle = \langle n_1(\boldsymbol{r})\rangle \langle n_1(\boldsymbol{r}')\rangle g(\boldsymbol{r}, \boldsymbol{r}')$$

We expect the two-scatterer probability density function $P(\boldsymbol{r}, \boldsymbol{r}') \to P(\boldsymbol{r})P(\boldsymbol{r}')$ (independent random variables) as $|\boldsymbol{r} - \boldsymbol{r}'| \to \infty$, and we therefore predict $g(\boldsymbol{r}, \boldsymbol{r}') \to 1$ in this limit. We can express the two-scatterer probability density function $P(\boldsymbol{r}, \boldsymbol{r}')$ in terms of the pair distribution function as

$$P(\boldsymbol{r}, \boldsymbol{r}') = \frac{\langle n_1(\boldsymbol{r})\rangle \langle n_1(\boldsymbol{r}')\rangle g(\boldsymbol{r}, \boldsymbol{r}')}{N(N-1)} = \frac{NP(\boldsymbol{r})P(\boldsymbol{r}')g(\boldsymbol{r}, \boldsymbol{r}')}{N-1}$$

or in terms of the conditional probability density function $P(\boldsymbol{r}'|\boldsymbol{r})$ as

$$P(\boldsymbol{r}'|\boldsymbol{r}) = \frac{NP(\boldsymbol{r}')g(\boldsymbol{r}, \boldsymbol{r}')}{N-1}$$

For a homogeneous medium, we get

$$\langle n_2(\boldsymbol{r}, \boldsymbol{r}')\rangle = n_0^2 g(\boldsymbol{r}, \boldsymbol{r}')$$

and

$$P(\boldsymbol{r}, \boldsymbol{r}') = \frac{Ng(\boldsymbol{r}, \boldsymbol{r}')}{|V_s|^2(N-1)} = \frac{n_0^2 g(\boldsymbol{r}, \boldsymbol{r}')}{N(N-1)}, \qquad P(\boldsymbol{r}'|\boldsymbol{r}) = \frac{n_0 g(\boldsymbol{r}, \boldsymbol{r}')}{N-1} \tag{E.3}$$

As the number of scatterers becomes large, the two-scatterer probability density function $P(\boldsymbol{r}, \boldsymbol{r}') \to g(\boldsymbol{r}, \boldsymbol{r}')/|V_s|^2$ and the conditional probability density function $P(\boldsymbol{r}'|\boldsymbol{r}) \to g(\boldsymbol{r}, \boldsymbol{r}')/|V_s|$.

Appendix F   Overview of the notation

This paper contains many symbols and variables. In the following table selection of the most important symbol are explained.

Symbol	Explained	Page
$\boldsymbol{E}$	Electric field	3
$\boldsymbol{H}$	Magnetic field	3
$\boldsymbol{E}_\mathrm{i}$	Incident electric field	6
$\boldsymbol{E}_\mathrm{r}$	Reflected electric field	6
$\boldsymbol{E}_\mathrm{t}$	Transmitted electric field	12
$\mathbf{G}_\mathrm{e}$	Green dyadic for the electric field in free space	4
$\boldsymbol{\varphi}_j^\pm$	Planar vector waves	56
$\boldsymbol{u}_n$	Radiating spherical vector waves	52
$\boldsymbol{v}_n$	Regular spherical vector waves	52
$\boldsymbol{A}_n$	Vector spherical harmonics	51
$\mathcal{P}_{nn'}(k\boldsymbol{d})$	Translation matrix of spherical vector waves	52
$B_{nj}^\pm, B_{nj}^{\pm\,\dagger}$	Transformation operators between spherical and planar waves	59
$F_j^\pm(\boldsymbol{k}_\mathrm{t})$	Expansion coefficients	13
$C_j^\pm(\boldsymbol{k}_\mathrm{it})$	Averaged expansion coefficients	31
$T_{nn'}$	Transition matrix for the particles	8
η_0	Wave impedance of vacuum	3
η	Relative wave impedance	3
ϵ	Relative permittivity	3
μ	Relative permeability	3
k	Wave number	3
z_1	Position of the left interface of the slab	3
z_2	Position of the right interface of the slab	3
d	Thickness of the slab, $i.e.$, $d = z_2 - z_1$	
a	Radius of the spherical particles	
D	z interval of possible origins, $i.e.$, $D = z_2 - z_1 - 2a = d - 2a$	
R_j^1	Reflection coefficient from the left side of the left interface	15
T_j^1	Transmission coefficient (left to right) of the left interface	15
$\mathcal{R}_j^1$	Reflection coefficient from the right side of the left interface	16
$\mathcal{T}_j^1$	Transmission coefficient (right to left) of the left interface	16
R_j^2	Reflection coefficient from the left side of the right interface	17
T_j^2	Transmission coefficient (left to right) of the right interface	17
r_{z_1}	Reflection coefficient at normal incidence of the left interface	36
r_{z_2}	Reflection coefficient at normal incidence of the right interface	36
t_{z_1}	Transmission coefficient at normal incidence of the left interface	36
t_{z_2}	Transmission coefficient at normal incidence of the right interface	36
r_slab	Reflection coefficient at normal incidence of the slab	39
t_slab	Transmission coefficient at normal incidence of the slab	38
$t_j(\boldsymbol{k}_\mathrm{t})$	Amplitude of the transmitted field	20
$r_j(\boldsymbol{k}_\mathrm{t})$	Amplitude of the reflected field	22

$\boldsymbol{k}$	Wave vector
$\boldsymbol{k}_{\mathrm{t}}$	Transverse wave vector
k_{z}	z component of the wave vector
α, β	Polar and azimuth angle of the wave vector
f	Volume fraction of particles
n_0	Number density of particles

References

[1] K. Aydin and A. Hizal. On the completeness of the spherical vector wave functions. *J. Math. Anal. Appl.*, **117**(2), 428–440, 1986.

[2] C. F. Bohren and D. P. Gilra. Extinction by a spherical particle in an absorbing medium. *Journal of Colloid and Interface Science*, **72**(2), 215–221, 1979.

[3] F. Borghese, P. Denti, R. Saija, G. Toscano, and O. Sindoni. Multiple electromagnetic scattering from a cluster of spheres. I. Theory. *Aerosol Science and Technology*, **3**(2), 227–235, 1984.

[4] A. Boström, G. Kristensson, and S. Ström. Transformation properties of plane, spherical and cylindrical scalar and vector wave functions. In V. V. Varadan, A. Lakhtakia, and V. K. Varadan, editors, *Field Representations and Introduction to Scattering*, Acoustic, Electromagnetic and Elastic Wave Scattering, chapter 4, pages 165–210. Elsevier Science Publishers, Amsterdam, 1991.

[5] V. Bringi, V. Varadan, and V. Varadan. Coherent wave attenuation by a random distribution of particles. *Radio Science*, **17**(5), 946–952, 1982.

[6] D. Colton and R. Kress. *Integral Equation Methods in Scattering Theory*. John Wiley & Sons, New York, NY, 1983.

[7] D. Colton and R. Kress. *Inverse Acoustic and Electromagnetic Scattering Theory*, volume 93 of *Applied Mathematical Sciences*. Springer-Verlag, Berlin, third edition, 2013.

[8] A. G. Dallas. Basis properties of traces and normal derivatives of spherical-separable solutions of the Helmholtz equation. Technical Report No. 2000-6:1-42, Dept. of Mathematical Sciences, University of Delaware, 2000.

[9] A. G. Dallas. On the convergence and numerical stability of the second Waterman scheme for approximation of the acoustic field scattered by a hard object. Technical Report No. 2000-7:1-35, Dept. of Mathematical Sciences, University of Delaware, 2000.

[10] A. Doicu, Y. Eremin, and T. Wriedt. *Acoustic and Electromagnetic Scattering Analysis Using Discrete Sources*. Academic Press, London, 2000.

[11] A. R. Edmonds. *Angular Momentum in Quantum Mechanics*. Princeton University Press, Princeton, NJ, 3 edition, 1974.

[12] J. Fikioris and P. Waterman. Multiple scattering of waves. III. The electromagnetic case. *J. Quant. Spectrosc. Radiat. Transfer*, **123**, 8–16, 2013.

[13] M. Gustavsson, G. Kristensson, and N. Wellander. Multiple scattering by a collection of randomly located obstacles. Part II: Numerical implementation — coherent fields. Technical Report LUTEDX/(TEAT-7236)/1–15/(2014), Lund University, Department of Electrical and Information Technology, P.O. Box 118, S-221 00 Lund, Sweden, 2014.

[14] M. Gustavsson, G. Kristensson, and N. Wellander. Multiple scattering by a collection of randomly located obstacles — numerical implementation of the coherent fields. *J. Quant. Spectrosc. Radiat. Transfer*, **185**, 95–100, 2016.

[15] A. Ishimaru. *Wave propagation and scattering in random media. Volume 1. Single scattering and transport theory.* Academic Press, New York, NY, 1978.

[16] A. Ishimaru. *Wave propagation and scattering in random media. Volume 2. Multiple scattering, turbulence, rough surfaces, and remote sensing.* Academic Press, New York, NY, 1978.

[17] J. D. Jackson. *Classical Electrodynamics*. John Wiley & Sons, New York, NY, third edition, 1999.

[18] A. Karlsson and G. Kristensson. Electromagnetic scattering from subterranean obstacles in a stratified ground. *Radio Sci.*, **18**(3), 345–356, 1983.

[19] G. Kristensson. Electromagnetic scattering from buried inhomogeneities—a general three-dimensional formalism. *J. Appl. Phys.*, **51**(7), 3486–3500, 1980.

[20] G. Kristensson. The electromagnetic field in a layered earth induced by an arbitrary stationary current distribution. *Radio Sci.*, **18**(3), 357–368, 1983.

[21] G. Kristensson, A. G. Ramm, and S. Ström. Convergence of the T-matrix approach in scattering theory. II. *J. Math. Phys.*, **24**(11), 2619–2631, 1983.

[22] G. Kristensson. Electromagnetic scattering by a bounded obstacle in a parallel plate waveguide. *J. Quant. Spectrosc. Radiat. Transfer*, **123**, 92–102, 2013.

[23] G. Kristensson. Coherent scattering by a collection of randomly located obstacles — an alternative integral equation formulation. *J. Quant. Spectrosc. Radiat. Transfer*, **164**, 97–108, 2015.

[24] G. Kristensson. Evaluation of some integrals relevant to multiple scattering by randomly distributed obstacles. *Journal of Mathematical Analysis and Applications*, **432**(1), 324–337, 2015.

[25] G. Kristensson. *Scattering of Electromagnetic Waves by Obstacles.* Mario Boella Series on Electromagnetism in Information and Communication. SciTech Publishing, Edison, NJ, USA, 2016.

[26] G. Kristensson and S. Ström. Scattering from buried inhomogeneities — a general three-dimensional formalism. *J. Acoust. Soc. Am.*, **64**(3), 917–936, 1978.

[27] G. Kristensson and S. Ström. Electromagnetic scattering from geophysical targets by means of the T matrix approach: A review of some recent results. *Radio Sci.*, **17**(5), 903–912, 1982.

[28] M. Lax. Multiple scattering of waves. *Reviews of Modern Physics*, **23**(4), 287–310, 1951.

[29] M. Lax. Multiple scattering of waves. II. The effective field in dense systems. *Phys. Rev.*, **85**, 621–629, Feb 1952.

[30] P. A. Martin. *Multiple Scattering: Interaction of Time-Harmonic Waves with N Obstacles*, volume 107 of *Encyclopedia of Mathematics and its Applications*. Cambridge University Press, Cambridge, 2006.

[31] N. C. Mathur and K. C. Yeh. Multiple scattering of electromagnetic waves by random scatterers of finite size. *J. Math. Phys.*, **5**, 1619–1628, 1964.

[32] M. I. Mishchenko. Multiple scattering by particles embedded in an absorbing medium. 1. foldy-lax equations, order-of-scattering expansion, and coherent field. *Opt. Express*, **16**(3), 2288–2301, 2008.

[33] M. I. Mishchenko. Multiple scattering by particles embedded in an absorbing medium. 2. radiative transfer equation. *J. Quant. Spectrosc. Radiat. Transfer*, **109**(14), 2386–2390, 2008.

[34] M. I. Mishchenko. Multiple scattering, radiative transfer, and weak localization in discrete random media: unified microphysical approach. *Reviews of Geophysics*, **46**(2), 2008.

[35] M. I. Mishchenko. *Electromagnetic Scattering by Particles and Particle Groups. An Introduction.* Cambridge University Press, New York, NY, 2014.

[36] M. I. Mishchenko, J. M. Dlugach, M. A. Yurkin, L. Bi, B. Cairns, L. Liu, R. L. Panetta, L. D. Travis, P. Yang, and N. T. Zakharova. First-principles modeling of electromagnetic scattering by discrete and discretely heterogeneous random media. *Physics Reports*, **632**, 1–75, 2016.

[37] M. I. Mishchenko, L. D. Travis, and A. A. Lacis. *Multiple scattering of light by particles: radiative transfer and coherent backscattering.* Cambridge University Press, Cambridge, 2006.

[38] M. I. Mishchenko, L. D. Travis, and D. W. Mackowski. T-matrix method and its applications to electromagnetic scattering by particles: A current perspective. *J. Quant. Spectrosc. Radiat. Transfer*, **111**(11), 1700–1703, 2010.

[39] M. I. Mishchenko, G. Videen, V. A. Babenko, N. G. Khlebtsov, and T. Wriedt. T-matrix theory of electromagnetic scattering by particles and its applications: a comprehensive reference database. *J. Quant. Spectrosc. Radiat. Transfer*, **88**(1-3), 357–406, 2004.

[40] M. I. Mishchenko, G. Videen, V. A. Babenko, N. G. Khlebtsov, and T. Wriedt. Comprehensive T-matrix reference database: A 2004–06 update. *J. Quant. Spectrosc. Radiat. Transfer*, **106**(1), 304–324, 2007.

[41] M. I. Mishchenko, G. Videen, N. G. Khlebtsov, and T. Wriedt. Comprehensive T-matrix reference database: A 2012–2013 update. *J. Quant. Spectrosc. Radiat. Transfer*, **123**, 145–152, 2013.

[42] M. I. Mishchenko, G. Videen, N. G. Khlebtsov, T. Wriedt, and N. T. Zakharova. Comprehensive T-matrix reference database: A 2006–07 update. *J. Quant. Spectrosc. Radiat. Transfer*, **109**(8), 1447–1460, 2008.

[43] M. I. Mishchenko, N. T. Zakharova, N. G. Khlebtsov, G. Videen, and T. Wriedt. Comprehensive thematic t-matrix reference database: a 2015–2017 update. *J. Quant. Spectrosc. Radiat. Transfer*, **202**, 240–246, 2017.

[44] M. I. Mishchenko, N. T. Zakharova, N. G. Khlebtsov, T. Wriedt, and G. Videen. Comprehensive thematic T-matrix reference database: A 2013–2014 update. *J. Quant. Spectrosc. Radiat. Transfer*, **146**, 349 – 354, 2014.

[45] M. I. Mishchenko, N. T. Zakharova, G. Videen, N. G. Khlebtsov, and T. Wriedt. Comprehensive T-matrix reference database: A 2007–2009 update. *J. Quant. Spectrosc. Radiat. Transfer*, **111**(4), 650–658, 2010.

[46] F. W. J. Olver, D. W. Lozier, R. F. Boisvert, and C. W. Clark. *NIST Handbook of mathematical functions*. Cambridge University Press, New York, 2010.

[47] A. Papoulis and S. U. Pillai. *Probability, random variables, and stochastic processes*. McGraw-Hill, Boston, MA, fourth edition, 2002.

[48] B. Peterson and S. Ström. T-matrix for electromagnetic scattering from an arbitrary number of scatterers and representations of E(3). *Phys. Rev. D*, **8**, 3661–3678, 1973.

[49] A. Ramm. Convergence of the T-matrix approach to scattering theory. *J. Math. Phys.*, **23**(6), 1123–1125, 1982.

[50] S. Ström. Introduction to integral representations and integral equations for time-harmonic acoustic, electromagnetic and elastodynamic wave fields. In V. V. Varadan, A. Lakhtakia, and V. K. Varadan, editors, *Field Representations*

70

and Introduction to Scattering, volume 1 of *Handbook on Acoustic, Electromagnetic and Elastic Wave Scattering*, chapter 2, pages 37–141. Elsevier Science Publishers, Amsterdam, 1991.

[51] V. P. Tishkovets. Incoherent and coherent backscattering of light by a layer of densely packed random medium. *J. Quant. Spectrosc. Radiat. Transfer*, **108**(3), 454–463, 2007.

[52] V. Tishkovets, E. Petrova, and M. Mishchenko. Scattering of electromagnetic waves by ensembles of particles and discrete random media. *J. Quant. Spectrosc. Radiat. Transfer*, **112**, 2095–2127, 2011.

[53] L. Tsang and J. A. Kong. *Scattering of Electromagnetic Waves: Advanced Topics*. John Wiley & Sons, New York, NY, 2001.

[54] L. Tsang, J. A. Kong, and K.-H. Ding. *Scattering of Electromagnetic Waves: Theories and Applications*. John Wiley & Sons, New York, NY, 2000.

[55] L. Tsang, J. A. Kong, K.-H. Ding, and C. O. Ao. *Scattering of Electromagnetic Waves: Numerical Simulations*. John Wiley & Sons, New York, NY, 2001.

[56] L. Tsang, C. E. Mandt, and K. H. Ding. Monte carlo simulations of the extinction rate of dense media with randomly distributed dielectric spheres based on solution of Maxwell's equations. *Opt. Lett.*, **17**(5), 314–316, 1992.

[57] V. Twersky. On multiple scattering of waves. *J. Res. Nat. Bur. Standards D*, **64**, 715–730, 1960.

[58] V. Twersky. On propagation in random media of discrete scatterers. In *Proc. Symp. Appl. Math*, volume 16, pages 84–116, 1964.

[59] V. Twersky. Coherent scalar field in pair-correlated random distributions of aligned scatterers. *J. Math. Phys.*, **18**, 2468–2486, 1977.

[60] V. K. Varadan, V. N. Bringi, and V. V. Varadan. Coherent electromagnetic wave propagation through randomly distributed dielectric scatterers. *Phys. Rev. D*, **19**(8), 2480–2489, April 1979.

[61] V. V. Varadan and V. K. Varadan. Multiple scattering of electromagnetic waves by randomly distributed and oriented dielectric scatterers. *Phys. Rev. D*, **21**(2), 388–394, January 1980.

[62] V. Varadan, Y. Ma, and V. Varadan. Propagator model including multipole fields for discrete random media. *JOSA A*, **2**(12), 2195–2201, 1985.

[63] P. C. Waterman. Symmetry, unitarity, and geometry in electromagnetic scattering. *Phys. Rev. D*, **3**(4), 825–839, 1971.

[64] P. C. Waterman and R. Truell. Multiple scattering of waves. *J. Math. Phys.*, **2**, 512–537, 1961.

[65] P. Waterman. Matrix formulation of electromagnetic scattering. *Proc. IEEE*, **53**(8), 805–812, August 1965.

[66] R. West, D. Gibbs, L. Tsang, and A. Fung. Comparison of optical scattering experiments and the quasi-crystalline approximation for dense media. *JOSA A*, **11**(6), 1854–1858, 1994.

[67] N. T. Zakharova, G. Videen, and N. G. Khlebtsov. Comprehensive T-matrix reference database: A 2009–2011 update. *J. Quant. Spectrosc. Radiat. Transfer*, **113**(14), 1844–1852, 2012.